University of Alberta

Froth Structure and Mass Transfer on Distillation Trays

By

Sultana Razia Syeda

A thesis submitted to the Faculty of Graduate Studies and Research in partial fulfillment of the requirements for the degree of Doctor of Philosophy in Chemical Engineering

Department of Chemical and Materials Engineering

Edmonton, Alberta

Spring, 2003

National Library
of Canada

Acquisitions and
Bibliographic Services

395 Wellington Street
Ottawa ON K1A 0N4
Canada

Bibliothèque nationale
du Canada

Acquisisitons et
services bibliographiques

395, rue Wellington
Ottawa ON K1A 0N4
Canada

Your file Votre référence
ISBN: 0-612-82172-2
Our file Notre référence
ISBN: 0-612-82172-2

The author has granted a non-exclusive licence allowing the National Library of Canada to reproduce, loan, distribute or sell copies of this thesis in microform, paper or electronic formats.

The author retains ownership of the copyright in this thesis. Neither the thesis nor substantial extracts from it may be printed or otherwise reproduced without the author's permission.

L'auteur a accordé une licence non exclusive permettant à la Bibliothèque nationale du Canada de reproduire, prêter, distribuer ou vendre des copies de cette thèse sous la forme de microfiche/film, de reproduction sur papier ou sur format électronique.

L'auteur conserve la propriété du droit d'auteur qui protège cette thèse. Ni la thèse ni des extraits substantiels de celle-ci ne doivent être imprimés ou aturement reproduits sans son autorisation.

Canada

University of Alberta

Library Release Form

Name of Author: *Sultana Razia Syeda*

Title of Thesis: *Froth Structure and Mass Transfer on Distillation Trays*

Degree: *Doctor of Philosophy*

Year this Degree Granted: *2003*

Permission is hereby granted to the University of Alberta Library to reproduce single copies of this thesis and to lend or sell such copies for private, scholarly or scientific research purposes only.

The author reserves all other publication and other rights in association with the copyright in the thesis, and except as herein before provided, neither the thesis nor any substantial portion thereof may be printed or otherwise reproduced in any material form whatever without the author's prior written permission.

Syeda Sultana Razia

Department of Chemical Engineering
Bangladesh University of Engineering
and Technology (BUET), Dhaka 1000
Bangladesh

Dated: Jan 21, 2003

University of Alberta

Faculty of Graduate Studies and Research

The undersigned certify that they have read, and recommend to the Faculty of Graduate Studies and Research for acceptance, a thesis entitled **Froth Structure and Mass Transfer on Distillation Trays** submitted by **Sultana Razia Syeda** in partial fulfillment of the requirements for the degree of **Doctor of Philosophy** in Chemical Engineering.

K T Chuang

Dr. Karl T. Chuang (Supervisor)

Dr. Zhenghe Xu

Dr. Biao Huang

Dr. Subir Bhattacharjee

Dr. Adel M. Al Taweel (external examiner)

Date: Jan 7, 2003

ABSTRACT

The knowledge of froth structure on a distillation tray is crucial to estimate the mass transfer efficiency in the froth regime. The physical properties of the gas/liquid system are among the factors whose effect on distillation performance is rather unclear; especially the effect of surface tension gradient on froth structure is one aspect that has not been addressed adequately in the past. Many experimental studies have shown that surface tension gradient developed in surface tension positive systems gives rise to stabilized froth and hence raises tray efficiency. Thus the knowledge of the extent to which the surface tension gradient can cause the froth stabilization is very important to the designers.

In this thesis, a gas hold-up correlation has been proposed, which includes the effect of surface tension gradient on froth structure in binary mixtures. The correlation is validated by the experimental gas hold-up data obtained from a 90 mm diameter shallow bubble column using four binary mixtures. The correlation is able to predict the often-reported enhancement of gas hold-up of surface-active binary mixtures, which has not been accounted for by any other correlation. This correlation is further adopted in developing a point efficiency model based on the efficiency data obtained from an Oldershaw column with six binary mixtures. This is by far the first successful attempt to include surface tension gradient effect in a point efficiency model.

A froth model describing the dispersion structure in froth regime on a large-scale industrial tray has been proposed. The model characterizes the froth as a mixed regime where both bubbling and continuous jetting occur simultaneously. The turbulent break-up theory is applied to determine the bubble size distribution in froth. A fundamental model, based on the proposed froth structure, has been developed to predict the tray efficiency in both froth and spray regimes. This efficiency model includes the volume fraction of gas, bypassing the bubbles in the form of continuous jet, as the determining factor of the regimes and explains the smooth transition between froth and spray regimes. The model has been verified by published experimental efficiency data obtained from large-scale distillation trays.

ACKNOWLEDGMENTS

I am grateful to my supervisor Professor Karl T. Chuang for providing a learning experience throughout this program that helped me to grow as a researcher. I cordially acknowledge the invaluable assistance of Mr. Artin Afacan in experimental work and in proof reading of this thesis. I like to thank Ms. Andree Koenig for her technical assistance and for being a good friend. I also thank Mr. Walter Boddez and Mr. Richard Cooper for their expert advice and help in the experimental work.

I am ever grateful to my parents Nurun Naher Begum and Syed Abu Abbas, my brothers Syed Taslim, Syed Tahmeed and Syed Touhid for being a constant source of encouragement. I thank my husband, Dr. Mahbubur Razzaque, for his patience and for his support in every possible way towards the completion of this work. Finally, I thank my son Omar for bringing in joy and happiness during the completion stage of this dissertation.

TABLE OF CONTENTS

PAGE

CHAPTER 1

INTRODUCTION 1

1.1 INTRODUCTION 1

1.2 TRAY EFFICIENCY MODELS 2

1.3 EFFECT OF PHYSICAL PROPERTIES ON FROTH STRUCTURE AND TRAY EFFICIENCY 3

1.4 PURPOSE AND SCOPE OF THIS STUDY 9

1.4.1 Froth structure and mass transfer on small trays 9

1.4.2 Froth structure and mass transfer on large trays 10

1.5 LITERATURE CITED 13

CHAPTER 2

EFFECT OF SURFACE TENSION GRADIENT ON FROTH STRUCTURE 16

2.1 INTRODUCTION 16

2.2 BACKGROUND 17

2.3 EXPERIMENTAL 19

2.4 MODEL DEVELOPMENT 21

2.4.1 Pure liquids 21

2.4.2 Binary liquids 25

2.4.3 Determination of C_1 and b 29

2.5 RESULTS AND DISCUSSION 31

2.6 CONCLUSIONS 42

2.7 NOMENCLATURE 42

2.8 LITERATURE CITED 44

CHAPTER 3

EFFECT OF SURFACE TENSION GRADIENT ON THE EFFICIENCY OF AN OLDERSHAW COLUMN 50

3.1 INTRODUCTION 50

3.2 EXPERIMENTAL 52

3.3 EFFICIENCY MEASUREMENT 54

3.4 PREDICTION OF POINT EFFICIENCY 57

3.4.1 Estimation of the constants C_1 and C_2 60

3.5 RESULTS AND DISCUSSION 63

3.5.1 Effect of surface tension gradient on point efficiency 70

3.5.2 Effect of surface tension on point efficiency 75

3.5.3 Justification of adopting gas hold-up correlation developed for air/liquid systems in distillation tray efficiency model 78

3.6 CONCLUSIONS 80

3.7 NOMENCLATURE 81

3.8 LITERATURE CITED 84

CHAPTER 4

FROTH STRUCTURE ON A COMMERCIAL SIEVE TRAY: A LITERATURE REVIEW 89

4.1 INTRODUCTION 89

4.2 CHARACTERISTICS OF FROTH 91

4.2.1 Bubble size distribution 91

4.2.2 Bubble rise velocity 96

4.2.3 Fraction of gas bypassing the froth bubbles as gas jets 97

4.2.4 Size of the jets and liquid droplets projected upwards by the jets 97

4.3 EFFECT OF SURFACE TENSION GRADIENT ON FROTH STRUCTURE 97

4.3.1 Bubble size distribution 99

4.3.2 Breakage of foam 100

4.4 CONCLUSIONS 101

4.5 NOMENCLATURE 102

4.6 LITERATURE CITED 103

CHAPTER 5

A FUNDAMENTAL MODEL FOR THE PREDICTION OF SIEVE TRAY EFFICIENCY 108

5.1 INTRODUCTION 108

5.2 MODEL STRUCTURE 110

5.3 THEORY OF MASS TRANSFER 115

5.4 MODEL DEVELOPMENT 116

5.4.1 Bubbling zone 116

5.4.2 Jetting zone 124

5.4.3 Determining the constant *C''* 125

5.5 PREDICTION OF POINT EFFICIENCY 126

5.6 DISCUSSION 135

5.7 CONCLUSIONS 139

5.8 NOMENCLATURE 140

5.9 LITERATURE CITED 143

CHAPTER 6

CONCLUSIONS 148

6.1 INTRODUCTION 148

6.2 EFFECT OF SURFACE TENSION GRADIENT ON GAS HOLD-UP 149

6.3 EFFECT OF SURFACE TENSION GRADIENT ON E_{OG} OF AN OLDERSHAW COLUMN 149

6.4 PREDICTING EFFICIENCY OF COMMERCIAL TRAYS 150

6.5 CONCLUSIONS 151

6.6 RECOMMENDATIONS FOR FUTURE WORK 151

APPENDIX A

OPERATING CONDITIONS AND EXPERIMENTAL RESULTS 153

A1 GAS HOLD-UP DATA IN AIR/LIQUID COLUMN (CHAPTER 2) 153

A2 POINT EFFICIENCY DATA IN OLDERSHAW COLUMN (CHAPTER 3) 154

APPENDIX B

FRI DATA FOR SIEVE TRAY EFFICIENCIES 161

B1 EFFICIENCY DATA FOR CYCLO-HEXANE/N-HEPTANE 161

B2 EFFICIENCY DATA FOR I-BUTANE/N-BUTANE 162

LIST OF TABLES

		PAGE
Table 3.1	Column and tray dimensions	54
Table 3.2	GC column specifications and operating conditions	55
Table 5.1	Reported bubble size distribution on an operating sieve tray	122
Table A1.1	Gas hold-up data for methanol/water and 2-propanol/water systems	153
Table A1.2	Gas hold-up data for ethylene glycol/water and methanol/2-propanol systems	154
Table A2.1	Efficiency data for methanol/water system (u_s=0.25m/s)	155
Table A2.2	Efficiency data for methanol/2-propanol system (u_s=0.25m/s)	156
Table A2.3	Efficiency data for water/acetic acid system (u_s=0.29m/s)	157
Table A2.4	Efficiency data for n-heptane/tolune system (u_s=0.25m/s)	158
Table A2.5	Efficiency data for cyclo-hexane/n-heptane system (u_s=0.29m/s)	159
Table A2.6	Efficiency data for benzene/n-heptane system (u_s=0.29m/s)	160
Table B1.1	Sieve tray efficiencies for cyclo-hexane/n-heptane at 34 kPa operating pressure and open hole area 14% (Yanagi and Sakata, 1982)	161

Table B1.2 Sieve tray efficiencies for cyclo-hexane/n-heptane at 165 kPa operating pressure and open hole area 14% (Yanagi and Sakata, 1982) 162

Table B2.1 Sieve tray efficiencies for i-butane/n-butane at 1138 kPa operating pressure and open hole area 14% (Yanagi and Sakata, 1982) 163

Table B2.2 Sieve tray efficiencies for i-butane/n-butane at 1138 kPa operating pressure and open hole area 8.3% (Sakata and Yanagi, 1979) 163

Table B2.3 Sieve tray efficiencies for i-butane/n-butane at 2068 kPa operating pressure and open hole area 8.3% (Sakata and Yanagi, 1979) 164

Table B2.4 Sieve tray efficiencies for i-butane/n-butane at 2758 kPa operating pressure and open hole area 8.3% (Sakata and Yanagi, 1979) 165

LIST OF FIGURES

		PAGE
Figure 1-1	Marangoni effect in presence of surface active component	6
Figure 1-2	Effect of surface tension gradient on froth stability	8
Figure 1-3	Research outline	12
Figure 2-1	Measurement of the clear liquid height and froth height	20
Figure 2-2	Comparison of the gas hold-up versus composition data in methanol/water (at u_s = 0.32 m/s) with the proposed model	32
Figure 2-3	Comparison of the gas hold-up versus composition data in 2-propanol/water (at u_s = 0.32 m/s) with the proposed model	33
Figure 2-4	Comparison of the gas hold-up versus composition data in ethylene glycol/water (at u_s = 0.32 m/s) with the proposed model	34
Figure 2-5	Comparison of the gas hold-up versus composition data in methanol/ 2-propanol (at u_s = 0.32 m/s) with the proposed model	35
Figure 2-6	Comparison between measured and predicted gas hold-up	38
Figure 2-7(a)	Air bubbles in 2-propanol at u_s = 0.32 m/s	39
Figure 2-7(b)	Air bubbles in 2-propanol/methanol (20 mol% 2-propanol) at u_s = 0.32 m/s	40
Figure 2-7(c)	Air bubbles in 2-propanol/water (15 mol% 2-propanol) at u_s = 0.32 m/s	41

Figure 3-1	Schematic diagram of distillation column	53
Figure 3-2	Comparison of the prediction by the proposed model with the experimental data of point efficiency at different concentration of methanol/water system (u_s = 0.25 m/s)	64
Figure 3-3	Comparison of the prediction by the proposed model with the experimental data of point efficiency at different concentration of n-heptane/toluene system (u_s = 0.25 m/s)	65
Figure 3-4	Comparison of the prediction by the proposed model with the experimental data of point efficiency at different concentration of methanol/2-propanol system (u_s = 0.25 m/s)	66
Figure 3-5	Comparison of the prediction by the proposed model with the experimental data of point efficiency at different concentration of c-hexane/ n-heptane system (u_s = 0.29 m/s)	67
Figure 3-6	Comparison of the prediction by the proposed model with the experimental data of point efficiency at different concentration of water/acetic acid system (u_s = 0.29 m/s)	68
Figure 3-7	Comparison of the prediction by the proposed model with the experimental data of point efficiency at different concentration of benzene/toluene system (u_s = 0.29 m/s)	69
Figure 3-8	Comparison of the point efficiency versus concentration data between a surface tension positive (methanol/water) and a surface tension neutral (methanol/2-propanol) system	74

Figure 3-9 Measured froth height data for aqueous and alcohol systems 76

Figure 3-10 Measured froth height data for hydrocarbon systems 77

Figure 4-1 Fraction of average gas by pass versus superficial F-factor (F_s) for sieve trays and for bubble cup and valve trays (source: Raper et al., (1982)) 98

Figure 5-1 Froth image of pure methanol on a sieve tray in a 0.153 m distillation column 111

Figure 5-2 Froth image of 67wt% methanol/water mixture on a sieve tray in a 0.153 m distillation column 112

Figure 5-3 Schematic representation of froth on an operating sieve tray 113

Figure 5-4 Froth structure model on an operating sieve tray 114

Figure 5-5 Effect of constant C" on the point efficiency; expressed as average absolute error 127

Figure 5-6 Comparison of measured and predicted point efficiencies for the cyclo-hexane/n-heptane system at 34 kPa (Open hole area 14%) 128

Figure 5-7 Comparison of measured and predicted point efficiencies for the cyclo-hexane/n-heptane system at 165 kPa (Open hole area 14%) 129

Figure 5-8 Comparison of measured and predicted point efficiencies for the iso-butane/n-butane system at 1138 kPa (Open hole area 14%) 130

Figure 5-9 Comparison of measured and predicted point efficiencies for the iso-butane/n-butane system at 1138 kPa (Open hole area 8.3%) 131

Figure 5-10 Comparison of measured and predicted point efficiencies for the iso-butane/n-butane system at 2068 kPa (Open hole area 8.3%) 132

Figure 5-11 Comparison of measured and predicted point efficiencies for the iso-butane/n-butane system at 2758 kPa (Open hole area 8.3%) 133

Figure 5-12 Overall comparison of the proposed model with two other existing models 136

CHAPTER 1

INTRODUCTION

1.1 INTRODUCTION

Distillation is by far the most popular separation technology in the chemical process industries. Worldwide about 95% of all separations are accomplished with distillation. The main reasons for such popularity of this process, as mentioned by Kunesh et al. (1995), are as follows;

- Distillation requires lower capital investment than the alternative methods.
- Unlike most other methods it does not require any mass-separating agent .
- Century old technological knowledge of distillation led to a well-developed design method.
- It is well supported by a huge database of vapour/liquid equilibrium (VLE).

Lower capital investment helps distillation retain its distinct economic advantage over other methods at large throughputs. Thus any small improvements in distillation research and design would have a significant impact on overall cash flow because of its massive scale of operation. For example, an estimated amount of two billion dollars were saved in column investments alone by research and development between 1950 and 1970 (Zuiderweg, 1973). In order to maintain this

trend, it is important to improve the applicability and performance of the distillation operation.

1.2 TRAY EFFICIENCY MODELS

The performance of distillation process is generally assessed by the tray efficiency of distillation columns. Although it has been extensively studied over the years, any analytical expression for tray efficiency model could not be achieved due to the complex inter-relationships among the parameters that affect the tray efficiency. All tray efficiency models currently available in literature are empirical or semi-empirical in nature.

The empirical models for estimating tray efficiency are based solely on experimental data. These types of models generally relate efficiency to a few key variables, the most important of which is liquid viscosity. (Drickamer and Bradford, 1943; O'Connell, 1946) The empirical models developed after sixties correlate tray efficiency with dimensionless groups of vapour and liquid properties (English and van Winkle, 1963; MacFarland et al., 1972)

The semi-empirical models, on the other hand, are based on the two-resistance theory of mass transfer and use a sequence to convert the phase resistance into point efficiency. Almost all semi-empirical models have evolved from the AIChE model (1958). Through the years, the AIChE approach has been corrected and

modified. Later versions improved several aspects of the original model and updated its hydrodynamics and mass transfer fundamentals (Zuiderweg, 1983; Chan and Fair 1984; Chen and Chuang, 1993).

None of these models takes into account the structure of gas/liquid dispersion on the sieve tray. To overcome the empirical approach in model development, the knowledge of the dispersion structure in different flow regimes as well as of the extent to which physical properties affect the dispersion is crucial. In distillation the gas phase in the dispersion is in fact the saturated vapour. However, air/liquid test results have been used to estimate different parameters of distillation in the existing literature as well as in the present study. Throughout this study the vapour phase of distillation has been referred to as the gas phase to include the contribution of air/liquid test data except in chapter 3. In chapter 3, the term vapour phase needs to be used to explain the experimental part conveniently.

1.3 EFFECT OF PHYSICAL PROPERTIES ON FROTH STRUCTURE AND TRAY EFFICIENCY

To date the effects of the physical properties of the system on the tray efficiency are not very clear. Most of the tray efficiency correlations generally include system properties such as viscosity, density and diffusivity. However, the effect of surface tension and its gradient have been ignored by most researchers. Previous experimental studies have shown that surface tension and its gradient can

influence the froth structure and hence the tray efficiency. The surface tension of liquids affects the size and stability of bubbles in froth to some extent, which in turn affects the interfacial area of gas/liquid dispersion. Higher surface tension gives rise to larger bubble size, less stable bubbles and thus lower interfacial area and vice versa. Zuiderweg (1983) and Chen and Chuang (1993) included surface tension effect in their efficiency models. However, their analyses ignored the effect of surface tension gradient, which is known to cause froth stabilization in many systems (Zuiderweg and Harmens, 1958; Hoverstreydt, 1963; Hart and Haselden, 1969; Lowry and van Winkle, 1969; and Zuiderweg, 1983). Surface tension gradient develops at gas/liquid interface during distillation when one component of the liquid mixture possesses lower surface tension than the other. Pure liquids or mixtures whose components have similar surface tension does not exhibit surface tension gradient. The mechanism of froth stabilization caused by surface tension gradient is known as Marangoni effect (Marangoni, 1871). This can arise in the following way. The film drainage between bubbles causes the bubble surface to stretch and to thin the film. Since the surface-active component (the component with lower surface tension) of the mixture concentrates at the liquid surface to minimize the free energy of the system, the concentration of this component in the liquid film becomes lower than that in the liquid in contact with other part of the bubble surface. This results in local rise in surface tension in the film. Thus a net surface force develops acting towards the high surface tension region. This causes surface flow of liquid towards the film, which counteracts the

film drainage process and stabilizes the bubbles. This mechanism of froth stabilization is explained by Andrew (1960) as dynamic surface effect. Figure 1-1 illustrates this type of Marangoni effect. The theory of dynamic surface effect has long been the topic of interest in applied surface chemistry, especially in froth flotation process. Jan Leja (1982) covered a wide range of references on this topic.

The first attempt to study the effect of surface tension gradient on the performance of distillation equipment was reported in 1958 by Zuiderweg and Harmens. They classified the distillation systems based on the relative surface tension of the two components that constitute the system:

i) Positive systems, σ^+, where the more volatile component of the mixture has lower surface tension.

ii) Negative systems, σ^-, where the more volatile component of the mixture has higher surface tension.

iii) Neutral systems, σ^0, where both components of the mixture have similar surface tensions.

They also found that surface tension positive systems exhibit higher tray efficiencies than either neutral or negative systems operated in the froth regime. In explaining this phenomenon, they introduced the concept of mass transfer induced Marangoni effect and postulated the following mechanism of froth stabilization (otherwise known as foaming). In the froth regime, a thin liquid film exists between the bubbles. This liquid film is generally rich in less-volatile component

Figure 1-1

Marangoni effect in presence of surface-active component

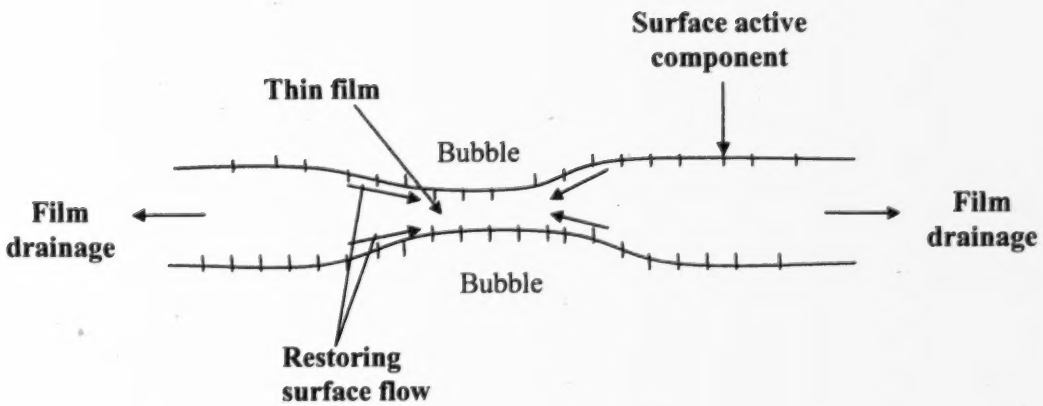

due to the mass transfer in the distillation process. In case of surface tension positive systems, the liquid film in between the bubbles is of higher surface tension than the liquids in contact with other part of the bubble surface. This creates the surface tension gradient along the surface of the bubbles and causes the flow of liquid into the film from other part of the bubble surface. This thickens and locally reinforces thin parts of the film and results in relative slowness in bursting of the bubbles. Thus surface tension positive systems tend to have more stable and uniform bubbles in froth. In surface tension neutral systems, there is no flow of liquid into the film since surface tension gradient does not develop at the interface. For surface tension negative systems, on the other hand, liquid flows out of the film, which leads to film breakage. Therefore, both neutral and negative systems do not exhibit foaming to any significant extent. The froth stabilization by mass transfer induced Marangoni effect is illustrated in Figure 1-2.

After the pioneering work of Zuiderweg and Harmens, many authors have investigated the effect of surface tension gradient on froth stabilization (Hoverstreydt, 1963; Hart and Haselden, 1969; Lowry and van Winkle, 1969; and Zuiderweg, 1983). However, none of the studies were able to quantify the effect of surface tension gradient on froth structure and tray efficiency.

Figure 1-2

Mass transfer induced Marangoni effect

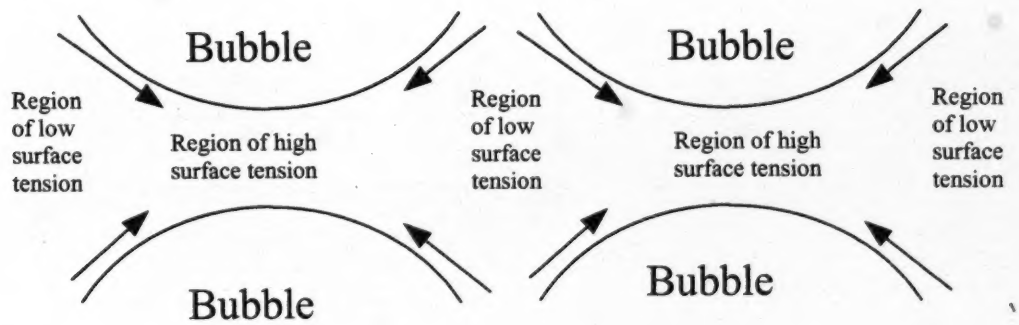

a) Surface tension positive system

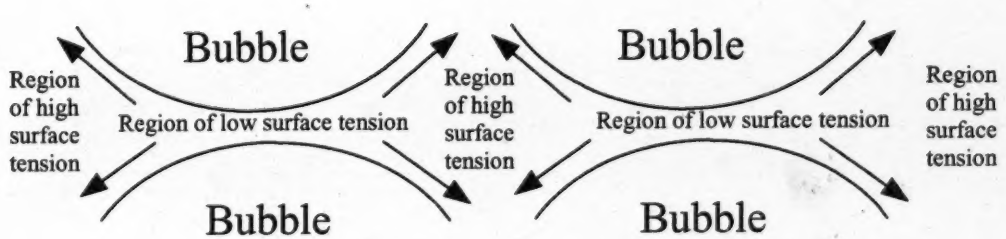

b) Surface tension negative system

1.4 PURPOSE AND SCOPE OF THIS STUDY

Although the nature of dispersion structure on a sieve tray affects the tray efficiency to a great extent, the existing efficiency models in general have ignored this factor. The purpose of the present research is to fill up this gap. The specific goals are two fold,

1. To investigate the nature of the dispersion structure on a sieve tray in froth regime and how it is affected by the physical properties of the system.
2. To incorporate the findings of the investigation in tray efficiency models.

The research has been carried out in two parts. The first part includes the study of froth structure and mass transfer in small-scale laboratory trays. The second part involves analysis of froth structure and mass transfer on large-scale industrial trays. In the following sections the details of the study are described.

1.4.1 Froth structure and mass transfer on small trays

In the first part of this research the effect of surface tension gradient on froth structure was investigated. The froth structure in large columns is complicated due to high gas loads. Thus it is very difficult to detect any effect of surface tension gradient on froth structure in large columns. The investigation, therefore, was carried out in small-scale laboratory columns where the change of froth structure is detectable. Chapters 2 and 3 cover the first part of the research. In chapter 2, the effect of surface tension gradient on froth structure was studied in a 90 mm

diameter shallow bubble column fitted with sieve trays. The column is used to generate comprehensive data of gas hold-up with respect to concentration of four binary systems. A dimensionless correlation of gas hold-up has been proposed, which includes surface tension gradient effect in the form of foamability of binary systems. The correlation was verified by the gas hold-up data obtained from the bubble column. In chapter 3, the effect of surface tension gradient on tray efficiency is studied in a small-scale distillation column, known as Oldershaw column. The gas hold-up correlation, proposed in chapter 2, is adopted in developing a point efficiency model based on the efficiency data of the six binary systems obtained from the Oldershaw column.

1.4.2 Froth structure and mass transfer on large trays

Froth structure on a large industrial tray may vary significantly from that on a small laboratory tray. To estimate the extent to which physical properties affect the tray efficiency of industrial columns, we need to understand and characterize the froth structure on a commercially operated sieve tray. Chapter 4 of this study is a review of the currently available literature that deals with different components of froth. In chapter 5, a froth structure model is proposed where froth is defined and characterized with the help of photographic images taken from a 0.153 m diameter distillation column. Based on the proposed froth structure, a new fundamental model to predict sieve tray efficiency is developed. Turbulent break-up theory is used to explain the nature of bubble size distribution in the

froth. A new method to estimate fraction of small bubble is presented using the rate constant expression proposed by Hesketh et al. (1991). The new efficiency model is tested against distillation data obtained from commercial scale columns published by the Fractionation Research Inc. (FRI) (Sakata and Yanagi, 1979; Yanagi and Sakata, 1982) and is compared with two other current models of Chan and Fair (1984) and Chen and Chuang (1993).

The main body of the text consists of six chapters. Chapter 6 is the conclusion, where the achievements of this study are revisited briefly. Figure 1-3 presents the outline of the research.

Figure 1-3

Research outline

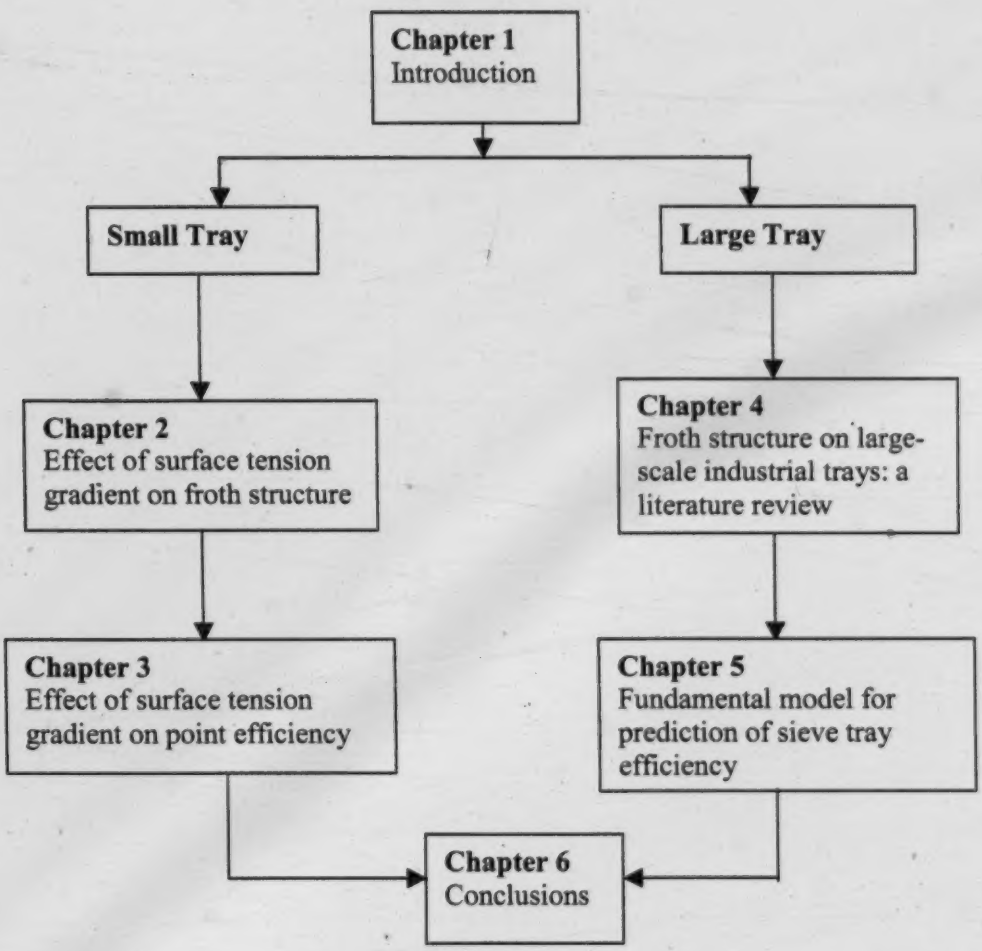

1.5 LITERATURE CITED

Chan, H. and J. R. Fair, "Prediction of Point Efficiencies on Sieve Trays," Ind. Eng. Chem. Process Des. Dev. **23,** 814-819 (1984).

Chen, G. X. and K. T. Chuang, "Prediction of Point Efficiency for Sieve Tray in Distillation," Ind. Eng. Chem. Res., **32**(4), 701-708 (1993).

Drickamer, H. G. and Bradford, J. R., "Overall Plate Efficiency of Commercial Hydrocarbon Fractionating Column as a Function of Viscosity," Trans AIChE, 39, 319 (1943).

English, G. E. and M. van Winkle, "Efficiency of Fractionating Columns," Chem Engng. **70**(23), 241, (1963).

Hart, D. J. and G. G. Haselden, "Influence of Mixture Compositions on Distillation-Plate Efficiency," Int. Chem. Engrs. Symp. Series, **32**, 1:19-1:28, (1969).

Hovestreydt, J., "The Influence of the Surface Tension Difference on the Boiling of Mixtures," Chem. Eng. Sci., **18**, 631-639, (1963).

Hesketh, Robert P., Arthur W. Etchells, and T. W. Fraser Russell, "Experimental Observations of Bubble breakage in Turbulent Flow," Ind. Eng. Chem. Res. **30**, 835-841, (1991).

Kunesh, John G., Henry Z. Kister, Michael J. Lockett and James R. Fair, "Distillation: Still Towering Over Other Options," Chem Eng Prog, (Oct), 43-54, (1995).

Leja, Jan, "Surface Chemistry of Froth Flotation," Plenum Press, New York (1982).

Lockett, M. J., "Distillation Tray Fundamentals," Cambridge University Press (1986).

Lowry, R. P. and M. van Winkle, "Foaming and Frothing Related to System Physical Properties in a Small Perforated Plate Distillation Column," AIChE J. **15**(5), 665-670, (1969).

MacFarland, S. A., P. M. Sigmund, and M. van Winkle, "Predict Distillation Efficiency," Hydrocarbon Proc., **7**, 111. (1972).

O'Connell, H. E., " Plate Efficiency of Fractionating Columns and Absorbers," Trans AIChE, **42**, 741 (1946).

Sakata, M. and Y. Yanagi, "Performance of a Commercial-Scale Sieve Tray," Inst. Chem. Eng. Symp. Ser. No.56, 3.2/21 (1979).

Yanagi, Y. and M. Sakata, "Performance of a Commercial-Scale 14% Hole Area Sieve Tray," Ind. Eng. Chem Process Des. Dev. **21**(4) 712-717 (1982).

Zuiderweg, F. J., "Distillation: Science and Business," The Chem. Eng. (Sept), 404- 410, (1973).

Zuiderweg, F. J., "Marangoni Effect in Distillation of Alcohol-water Mixtures," Chem. Eng. Res. Des. **61**, 388-390, (1983).

Zuiderweg, F. J. and A. Harmens, "The Influence of Surface Phenomena on the Performance of Distillation Columns," Chem Eng Sci **9**, 89-108, (1958).

Zuiderweg, F. J., P. A. M. Hofius and J. Kuzniear, "Flow Regimes on Sieve Trays: the Significance of the Emulsion Flow Regime," Chem. Eng. Res. Des., **62,** 39-48, (1984).

CHAPTER 2

EFFECT OF SURFACE TENSION GRADIENT ON FROTH STRUCTURE

2.1 INTRODUCTION

Estimation of gas hold-up in two-phase mixture is one way to quantify the dispersion structure on a sieve tray. Thus the effect of physical properties on dispersion structure can be determined by estimating the effect on gas hold-up. The present research deals with froth regime with a special focus on the effect of surface tension gradient on froth structure and on tray efficiency in distillation. This chapter is dedicated to the study of the surface tension gradient effect on gas hold-up on a sieve tray operating in froth regime.

Testing of distillation tray with air/water is a common practice in developing distillation equipment. All existing correlations for gas hold-up, clear liquid height, and pressure drop are based on air/water and air/liquid test data on sieve trays in simulator columns. The main reason behind such practice lies in the difficulties that arise in controlling different operating parameters, such as, gas/liquid flow rates, liquid height etc in the distillation column. In air/liquid columns these parameters can be controlled with a little effort. A large number of data covering wide range of operating conditions can be obtained conveniently in

---

A version of this chapter has been published in Can J Chem Eng 80 (1): 44-50 Feb 2002

such columns. This fact has made the air/liquid testing results popular in developing correlations for distillation column. The same approach has been adopted in present study. A shallow bubble column fitted with sieve trays was used as a simulator column. Gas hold-up data of different air/liquid mixtures were obtained from this column to carry out the study. A semi-empirical correlation for gas hold-up in pure liquids as well as in binary mixtures has been developed. Surface tension gradient effect, causing froth stabilization in binary mixtures, has been included in the proposed gas hold-up correlation.

In literature, the term 'stabilized froth' is used to refer foam. In the rest of this study the terms foam and foamability are used in place of stabilized froth and froth stability, respectively, for the convenience of writing.

2.2 BACKGROUND

Most of the works dealing with gas hold-up measurement and prediction are based on deep liquid pool in bubble column (Hughmark, 1967; Akita and Yoshida, 1973; Kumar et al., 1976; Hikita et al., 1980; Kelkar et al. 1983; Chaudhari and Hofmann, 1994). Relatively less work has been done on distillation trays (Gilbert, 1959; Colwell, 1981; Bennett et al., 1983) or shallow bubble columns (Miyahara et al., 1989) where liquid height is rather small. Among the work done on gas hold-up or froth density, particularly for distillation trays, Colwell's (1981) froth

flow model in combination with the Francis weir formula is the most commonly recommended for industrial applications (Kister, 1992).

Researchers often report higher gas hold-up for aqueous alcohol systems in bubble columns (Schugerl et al., 1977; Oels et al., 1978; Hikita et al., 1980; Kelkar et al., 1983; Chaudhari and Hofmann, 1994). The surface tension gradient that develops at the interface of this type of systems gives rise to foaming tendency or coalescence hindering nature in bubbles and is identified as the main factor for higher gas hold-up. Kelkar et al. (1983) and Chaudhari and Hofmann (1994) made attempts to predict effects of alcohol solutes on gas hold-up in aqueous solutions. Both of their semi-empirical models were based on data obtained from only one composition of a particular mixture. Therefore, the models may not be able to predict the trend of gas hold-up over a range of concentration. According to Tunier et al. (1996) the foamability of an aqueous alcohol solution is maximum at an alcohol concentration that does not depend on the gas flow rate; at higher alcohol concentrations, the foamability decreases strongly with increasing alcohol content. Nevertheless, no studies have correlated gas hold-up with the foamability, caused by surface tension gradient, of binary systems.

2.3 EXPERIMENTAL

For the experimental study, two stainless steel sieve plates were mounted in a Perspex column of 90 mm inside diameter and 610 mm height. The bottom plate, just above the gas inlet, contained 25 holes of 5 mm diameter. It ensured uniform gas flow over the column cross-section. The second sieve plate, with 75 holes of 3 mm diameter, was mounted 280 mm above the first plate. This plate was used for the experimental measurement of clear liquid height and froth heights. Air was supplied through the gas inlet at a fixed flow rate. One end of a differential pressure transducer (DP /cell) was connected to the bottom of the upper sieve plate and the other end was open to the atmosphere (Figure 2-1). The clear liquid height h_L is obtained from the DP/cell reading, which was calibrated against static liquid height prior to the experiment. The average froth height, h_f, was measured visually with a scale mounted on the wall of the column. The gas hold-up was then calculated with the following equation

$$\varepsilon = 1 - \frac{h_L}{h_f} \tag{2.1}$$

The froth level fluctuated mostly due to the collapse of the surface bubbles. The uncertainty in froth height measurement was minimized by taking 15 to 20 sets of readings of h_f and h_L at a particular concentration. The average gas hold-up, ε, calculated from h_f and h_L was then plotted against the concentration. This procedure is repeated for every concentration of the mixtures shown in the Figures 2-2 to 2-5. The standard deviation of the gas hold up data is maximum for pure

Figure 2-1

Measurement of the clear liquid height and froth height

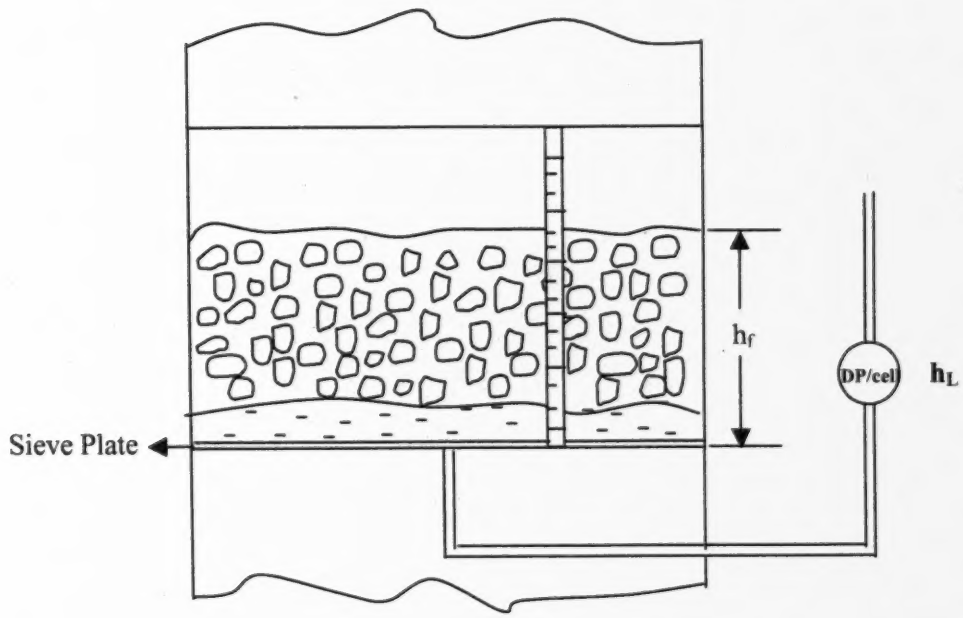

liquids and minimum for mixtures at the composition where foaming is the highest.

2.4 MODEL DEVELOPMENT

2.4.1 Pure liquids

Gas hold-up is greatly affected by the bubble stability in liquids. Both break up and coalescence control the evolution of bubble sizes in a gas/liquid contactor. In froth regime, at low gas flow rate, with more than 50% gas hold-up bubble break up is unlikely. Thus the bubble stability mostly depends on bubble coalescence i.e. the rate of liquid drainage between bubbles. With more stable bubbles the gas hold-up is much higher than that with the less stable ones. The stability of gas bubbles may vary from pure liquids to binary mixtures. Therefore, any gas hold-up model, either for deep pool bubble column or for shallow distillation tray, needs to include a bubble stability i.e. liquid drainage criterion for a better prediction of gas hold-up in different liquids and liquid mixtures. Despite the above facts none of the existing gas hold-up correlations considered bubble stability as a variable. The factors most commonly used are superficial velocity u_s, the gas and liquid densities ρ_G and ρ_L, the gas and liquid viscosities μ_G and μ_L, the surface tension σ and the gravitational constant g. A number of gas-hold up correlations for pure liquids are available in the literature. A summary of these correlations is given by Hikita et al. (1980). Among the correlations, the one proposed by Hikita et al. (1980) is unique for its simplicity and direct relationship

with the physical properties as well as the comprehensiveness in terms of correlation factors. This correlation has been used later as a basis for other correlations such as those by Grover et al. (1986) and by Chaudhari and Hofmann (1994). However, this model has the common limitation as others i.e. the model has been mainly derived from pure liquid data and is not able to predict high gas hold-up value of some aqueous alcohol mixtures.

In this chapter, our target is to develop a correlation that takes into account the effect of surface tension gradient on gas hold-up. We will use stability of bubbles as one of the factors that influence the gas hold-up behaviour of different liquids.

In absence of bubble break up probability of coalescence of gas bubbles in liquids provides a rough estimation of bubble stability in the froth regime. Coalescence between two bubbles consists of three sub-processes: collision, film drainage and rupture. The first consideration that gives the basis for a preliminary estimate of the probability is the ratio of drainage time to interaction time, t_c/t_i. Coalescence occurs if the interaction time, t_i, exceeds the drainage time, t_c, required for drainage to reach the critical film thickness h_c (Chesters, 1991).

The coalescence probability, given by Ross et al. (1978), is

$$P = \exp\left(-\frac{t_c}{t_i}\right) \tag{2.2}$$

For large values of t_c/t_i, P tends to be zero and for small values of t_c/t_i, P tends to be unity. In the froth regime, the bubble Reynolds number is much larger than unity. Therefore, the coalescence model for turbulent flow is considered here. For turbulent flow, the drainage model based on full interfacial mobility and inertia control is applicable provided the shear stress exerted by the gas is truly negligible. The interaction time t_i, from the onset of flattening up to the point at which the particle motion is arrested, is given by (Chesters, 1991):

$$t_i \cong \left[\left(\frac{4\rho_G}{3\rho_L}+1\right)\frac{\rho_L r_{eq}^3}{2\sigma}\right]^{\frac{1}{2}} \tag{2.3}$$

The drainage time, t_c, can be calculated as

$$t_c \approx \frac{0.5\rho_L U r_{eq}^2}{\sigma} \tag{2.4}$$

Thus from equations (2.3) and (2.4) and assuming $\frac{\rho_G}{\rho_L}=0$, the coalescence criterion can be expressed as

$$\frac{t_c}{t_i} \approx \left(\frac{We}{2}\right)^{\frac{1}{2}} \tag{2.5}$$

Here the Weber number is calculated in terms of relative bubble velocity and equivalent bubble radius

$$WE = \left(\frac{\rho_L U^2 r_{eq}}{\sigma}\right) \tag{2.6}$$

Combining equations (2.2), (2.5) and (2.6) the probability of coalescence can be expressed as;

$$P \approx \exp\left[-\left(\frac{WE}{2}\right)^{\frac{1}{2}}\right] \tag{2.7}$$

or

$$P \cong \exp\left[-c_1\left(\frac{WE}{2}\right)^{\frac{1}{2}}\right] \tag{2.8}$$

where c_1 is a constant of order unity. Thus the term $\left(\frac{WE}{2}\right)^{\frac{1}{2}}$ gives an estimation of bubble stability in pure liquids and will be used in the new correlation.

Hikita et al (1980) applied dimensional analysis and least square method to the experimental data to obtain the gas hold-up correlation. They used four dimensionless groups, namely, $\left(\frac{u_s\mu_L}{\sigma}\right)$, $\left(\frac{\mu_L^4 g}{\rho_L\sigma^3}\right)$, $\left(\frac{\rho_G}{\rho_L}\right)$, and $\left(\frac{\mu_G}{\mu_L}\right)$ to correlate the gas hold-up with the factors influencing the gas hold-up. Despite the limitation of their model the same dimensionless groups and the exponents have been adopted in the new correlation to avoid the repetition of regression and dimensional analysis of the experimental data that have been done numerous times in the past. Hence, the new gas hold-up correlation for pure liquids, which includes the probability factor from equation (2.8) as bubble stability criterion, is given by,

$$\varepsilon = C_1\left(\left(\frac{WE}{2}\right)^{1/2}\right)^b\left(\frac{u_s\mu_L}{\sigma}\right)^{0.578}\left(\frac{\mu_L^4 g}{\rho_L\sigma^3}\right)^{-0.131}\left(\frac{\rho_G}{\rho_L}\right)^{0.062}\left(\frac{\mu_G}{\mu_L}\right)^{0.107} \tag{2.9}$$

The constant C_1 and the exponent b will be determined experimentally in combination with the model proposed for binary mixtures.

2.4.2 Binary liquids

For binary mixtures, especially for dilute aqueous solutions of aliphatic alcohols, foaming ability is another important factor that affects gas hold up of a particular gas/liquid mixture system. Thinning and rupturing of liquid film between bubbles in binary mixtures may differ from that of the pure liquids depending on the nature of the solute. For solutes with moderate and weak surface activity, two models, one proposed by Andrew (1960) and the other by Marucci (1969), have been used to predict film thinning rates. Marucci's liquid phase diffusion model is found to give satisfactory result for salt solutions (Marucci et al., 1969) but becomes unrealistic for dilute solutions of n-alcohols (Sagert et al., 1976). On the other hand, Andrew's dynamic surface tension model has been used to predict coalescence times for bubbles in dilute solutions of n-alcohols by Sagert et al. (1976) and is preferred to Marucci's model.

The present study is concerned with organic mixtures, mainly those involving n-alcohols. Therefore, the discussion on coalescence theory will be limited to Andrew's model. The model, derived from the concept of surface elasticity, proposed a quantitative method of predicting the maximum foaming composition of two component mixtures. In this model, it is considered that the rapid

stretching of froth laminae in a two component liquid mixture provides a stabilizing influence by causing a dynamic rise in surface tension. This rise in surface tension above the static value is a result of the slowness of migration of the molecules of the component with the lower surface tension into the adsorption layer at the interface.

The simplified equation for dynamic rise of surface tension for a stretching rate S, as a result of slow diffusion to the surface, is given by (Andrew, 1960)

$$\Delta\sigma = \frac{1}{CRT}\sqrt{\frac{\pi S}{2D}}\theta(x)\left(\frac{d\sigma}{dx}\right)^2 \tag{2.10}$$

where

$$\theta(x) = \frac{x(1-x)}{\left(1-x+\frac{V_1}{V_2}x\right)} \tag{2.10a}$$

and C, D and V_i are molar density, diffusion coefficient and molar volume, respectively. In equation (2.10), the variations of the term $\theta(x)\left(\frac{d\sigma}{dx}\right)^2$ among different mixtures are the most important for a given expansion rate S. The most stable bubbles form at a composition for which the rise in surface tension is the highest, provided that the rise in surface tension is the primary stabilizing factor for bubble growth. Therefore, maximum foamability occurs at the composition at which $\theta(x)\left(\frac{d\sigma}{dx}\right)^2$ is a maximum.

When the total volume of the liquid in the film is conserved, the stretching rate S is given as (Marucci, 1969)

$$S = \frac{1}{a_D}\left[\frac{da_D}{dt}\right] = -\frac{1}{h}\frac{dh}{dt} \tag{2.11}$$

For a film thickness h, the overall force balance is given by

$$h\Delta p = 2\Delta\sigma \tag{2.12}$$

The total pressure Δp resulting from capillary pressure and van der Waals forces is

$$\Delta p = \frac{2\sigma}{r} + \frac{A}{6\pi h^3} \tag{2.13}$$

where A is the Hamaker constant.

Substitution of equations (2.10), (2.11) and (2.13) into equation (2.12) gives the time t'_c, required to stretch a film from infinite thickness to a final thickness h'_c (Sagert and Quinn, 1978).

$$t'_c = \frac{\pi}{2Dk}\left(\frac{crk^2}{\sigma}\right)^2 \int_{\infty}^{h'_c} \frac{h^3k^3}{\left(1+h^3k^3\right)} dh \tag{2.14}$$

where

$$c = 2\Delta\sigma\left(\frac{\pi S}{2D}\right)^{-\frac{1}{2}} = \frac{2}{CRT}\theta(x)\left(\frac{d\sigma}{dx}\right)^2 \tag{2.15}$$

and

$$k = \left(\frac{12\pi\sigma}{Ar}\right)^{\frac{1}{3}} \tag{2.16}$$

The dimensionless parameter $\frac{crk^2}{\sigma}$ in equation (2.14), first proposed in the theory of Marucci (1969), is of extreme importance in terms of understanding the mobility of thin films. Whenever this parameter is less than about 2, coalescence occurs very rapidly, as in the cases of pure liquids or very dilute solutions. In contrast, for $\frac{crk^2}{\sigma} > 25$ the coalescence is suppressed due to electrostatic double layer repulsion forces as suggested by Sagert and Quinn (1978). Thus $\frac{crk^2}{\sigma}$ provides a measure of froth stability i.e. foamability of a binary mixture. However, when x approaches either 0 or 1, as in case of pure liquids, $\theta(x)$ approaches zero, i.e. foamability becomes zero. In absence of foaming, bubble stability of the pure liquid comes into play and contributes to the fractional gas hold-up as we proposed in equation (2.9). Thus, the stability of bubbles in pure liquids and the stability of foam in binary mixtures are algebraically complementary. Hence, the new gas hold-up model proposed for the whole range of composition of binary mixtures is given by,

$$\varepsilon = C_1\left[x\left(\frac{WE_1}{2}\right)^{1/2} + \left(\frac{crk^2}{\sigma}\right) + (1-x)\left(\frac{WE_2}{2}\right)^{1/2}\right]\left(\frac{u_s\mu_L}{\sigma}\right)^{0.578}\left(\frac{\mu_L^4 g}{\rho_L\sigma^3}\right)^{-0.131}\left(\frac{\rho_G}{\rho_L}\right)^{0.062}\left(\frac{\mu_G}{\mu_L}\right)^{0.107} \tag{2.17}$$

Here WE_1 and WE_2 represent the Weber numbers of the pure liquids with lower and higher surface tension respectively in the binary mixtures. At x = 0 or 1,

equation (2.17) coincides with the model suggested for pure liquids (i.e. equation (2.9)).

2.4.3 Determination of C_1 and b

By comparing equation (2.17) to experimental gas hold-up, ε, data for four pure liquids and four organic binary mixtures, the values of C_1 and b have been found to be 1.334 and 0.032, respectively. Getting accurate physical property data particularly surface tension data of the mixtures with respect to concentration is crucial while predicting the gas hold-up. Surface tension of aqueous alcohol mixtures, such as, methanol/water, 2-propanol/water etc shows 'exponential decay' behaviour when plotted against alcohol concentration. As bubble stabilization depends mainly on surface tension gradients any minor error in surface tension versus concentration profile would affect both the trend and magnitude of the predicted gas hold-up. However, surface tension of mixtures with similar components, such as, methanol/2-propanol remains almost constant and insensitive to the concentration of the mixture. To minimize the error in physical property data, reported experimental values (Timmermans, Jean, 1960; D'Aprano et al., 1979;Vazquez et al., 1995; Tsierkezos and Molinou, 1998; Slusher, 2000) have been used in this study rather than predictions from different existing models.

The Weber number used in equation (2.9) and (2.17) is derived strictly for pure liquids. Any change in bubble size and bubble mobility that might affect gas hold-up of the mixtures is included in foaming parameter $\frac{crk^2}{\sigma}$. The velocity term, U, in the Weber number, as derived from the coalescence theory, is the relative velocity of the two approaching bubbles and the radius, r_{eq}, is their equivalent radius. The exact estimation of *WE* requires knowledge of bubble size distribution in the froth along with their velocity profiles. Due to the complexity that arises in measurement of bubble diameter and velocity beyond the column wall, no definitive information is available in existing literature. For present study an approximate estimation of *WE* is done from the available knowledge of bubble dynamics.

The velocity of bubbles in froth on a sieve tray is estimated by the following equation (Burgess and Calderbank, 1975; Nicklin, 1962),

$$U_i = U_{i\infty} + \frac{G}{A} \tag{2.18}$$

where A is the dispersion gas flow area, G is the gas flow rate and $U_{i\infty}$ is the isolated spherical cap bubble rise velocity described by Davis and Taylor (1950),

$$U_{i\infty} = 25 v_i^{1/6} \tag{2.19}$$

where v_i is the bubble volume. The equations (2.18) and (2.19) show that the relative velocity U ($=U_1-U_2$) of two approaching bubbles is directly related to their volumes i.e. the bubble size. In this study the observed diameters of two

coalescing bubbles differed approximately from 0-10 mm. For this range of size differences, the estimated relative bubble velocity obtained from equations (2.18) and (2.19) ranges from 0 to 100 mm/sec. An approximate value of 50 mm/sec is used in Weber number estimation. Within the observed range, the effect of U on the ultimate gas hold-up estimation is less than 5%.

For binary mixtures the bubble size may vary with the concentration and nature of the components. The drainage of foam also depends on the bubble size distribution as drainage proceeds more slowly when bubbles are smaller. However, surface tension gradients are reported to be more important for the foaming behaviour than possible bubble size effects (Tunier et. al., 1996). The observed bubble diameter for different mixtures varied from 5 mm to 10 mm. The calculated value of the parameter $\frac{crk^2}{\sigma}$ is found to be insensitive to any value of r within this range. An average value of $r = 4$ mm has been used to calculate the parameter $\frac{crk^2}{\sigma}$.

2.5 RESULTS AND DISCUSSION

Figures 2-2 to 2-5 present the experimental data of gas hold-up along with the values estimated by using equation (2.17). The dotted line represents the predicted values from equation (2.9) proposed for pure liquids, where the surface tension

Figure 2-2

Comparison of the gas hold-up versus composition data in methanol/water (at $u_s = 0.32$ m/s) with the proposed model

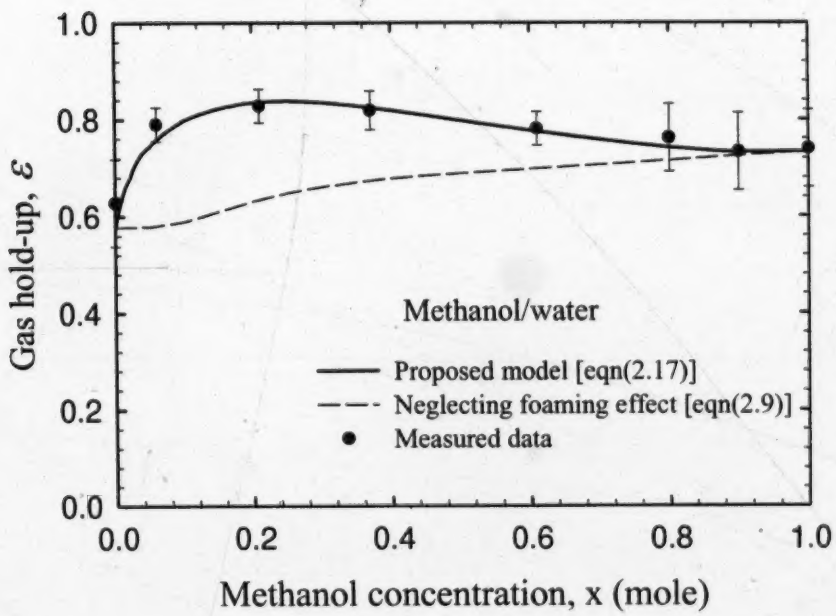

Figure 2-3

Comparison of the gas hold-up versus composition data in 2-propanol/water (at u_s = 0.32 m/s) with the proposed model

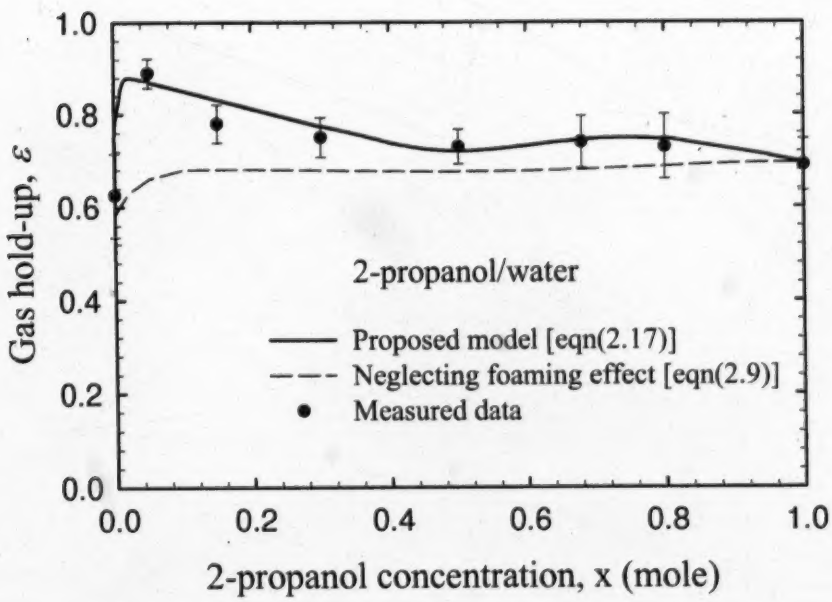

Figure 2-4

Comparison of the gas hold-up versus composition data in ethylene glycol/water (at u_s = 0.32 m/s) with the proposed model

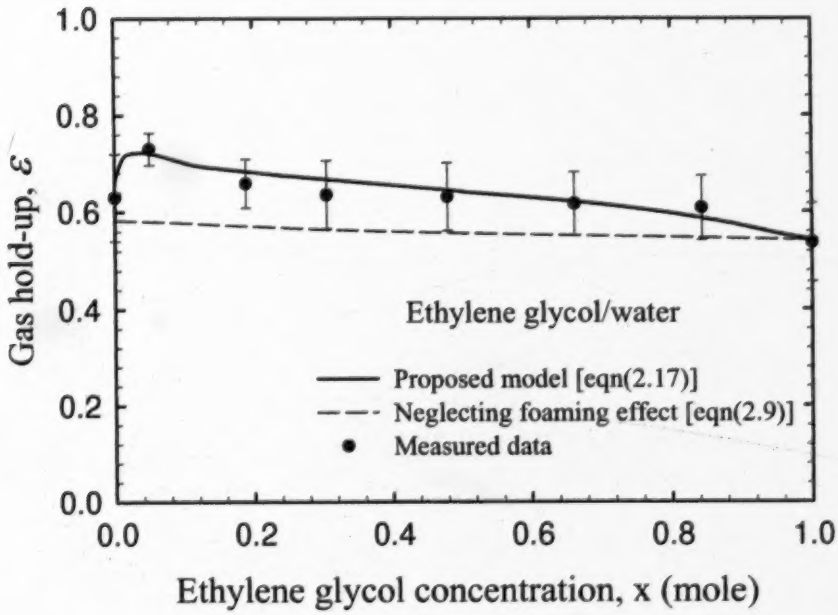

Figure 2-5

Comparison of the gas hold-up versus composition data in methanol/ 2-propanol (at u_s = 0.32 m/s) with the proposed model

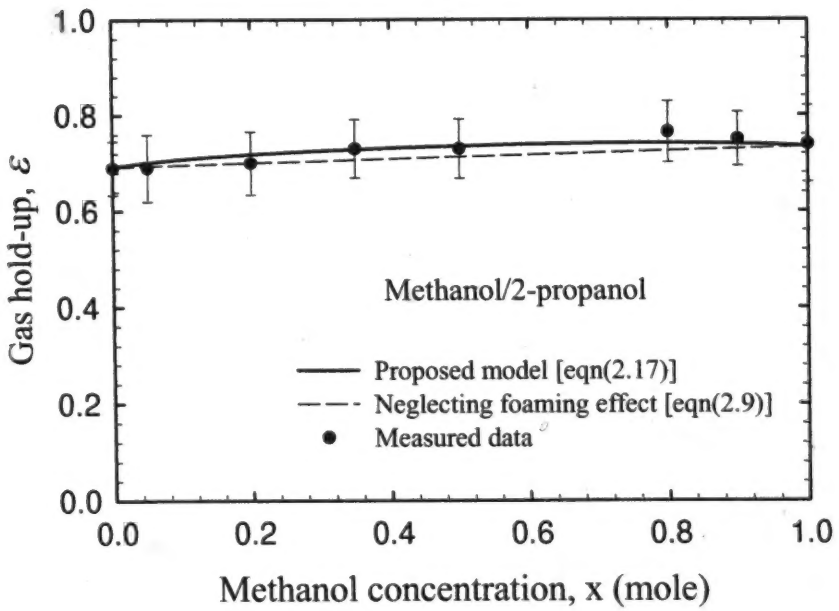

gradient effect (i.e. the foamability of mixture) has been neglected. The frequently reported higher gas hold-up for aqueous alcohol solution is observed for methanol/water and 2-propanol/water systems at the low concentration of the more volatile component (Figures 2-2 and 2-3). For the ethylene glycol/water system the enhancement of ε is rather insignificant (Figure 2-4). Methanol/2-propanol system gives almost constant ε with respect to concentration (Figure 2-5). The figures also show that the proposed correlation, equation (2.17), is able to predict all the different trends of ε observed for these mixtures. The force term c in the parameter $\frac{crk^2}{\sigma}$ (equation (2.15)) contains the surface tension gradient term $\theta(x)\left(\frac{d\sigma}{dx}\right)^2$, which quantifies the magnitude of enhancement of ε and the corresponding alcohol concentration of different mixtures. Thus, inclusion of the dimensionless parameter $\frac{crk^2}{\sigma}$ in equation (2.17) makes it possible to predict the magnitude and location of the gas hold–up peak value at a particular concentration as shown in Figures 2-2 and 2-3. However, for pure liquids and for binary mixtures whose components have similar surface tension, such as methanol/2-propanol, the term $\theta(x)\left(\frac{d\sigma}{dx}\right)^2$ approaches zero and the coalescence behaviour of the bubbles is dominated by the criterion given in equation (2.8). Thus, the Weber number gives estimation of gas hold-up in absence of foaming. An algebraic

combination of these two factors i.e. $\frac{crk^2}{\sigma}$ and $\left(\frac{WE}{2}\right)^{1/2}$, included in gas hold-up correlation, is found to predict the trend and magnitude within ±7% (Figure 2-6) of the gas hold-up for both pure liquids and binary mixtures successfully. If the foamability of the mixtures is neglected i.e. the correlation proposed for pure liquids (equation (2.9)) is applied for binary mixtures the predicted gas hold-up would follow the dashed lines in the graphs. Therefore, using the correlation based on gas hold-up data from pure liquids, such as those existing in literature, to predict gas hold-up of binary mixtures can lead to an error as high as 50%.

Figure 2-7 (a), (b) and (c) are the photographs of air bubbles taken in pure 2-propanol, 2-propanol/methanol mixtures (20mol% 2-propanol) and 2-propanol/water mixtures (15mol% 2-propanol), respectively. The bubble size and froth structure are almost same for pure 2-proapnol and 20mol% 2-propanol/methanol mixtures. However, 15mol% 2-propanol/water mixture gives distinct froth structure with more uniform smaller bubbles. This confirms that bubble size and froth structure of pure liquids may or may not differ from that of binary mixtures depending on the foamability of its components. Any correlation that does not include foamability i.e. surface tension gradient effect is inadequate to account for the diversified froth structures of different binary systems. Equations (2.9) and (2.17) are tested and validated only for the froth regime. The liquid height range is within 10 mm to 20 mm.

Figure 2-6

Comparison between measured and predicted gas hold-up

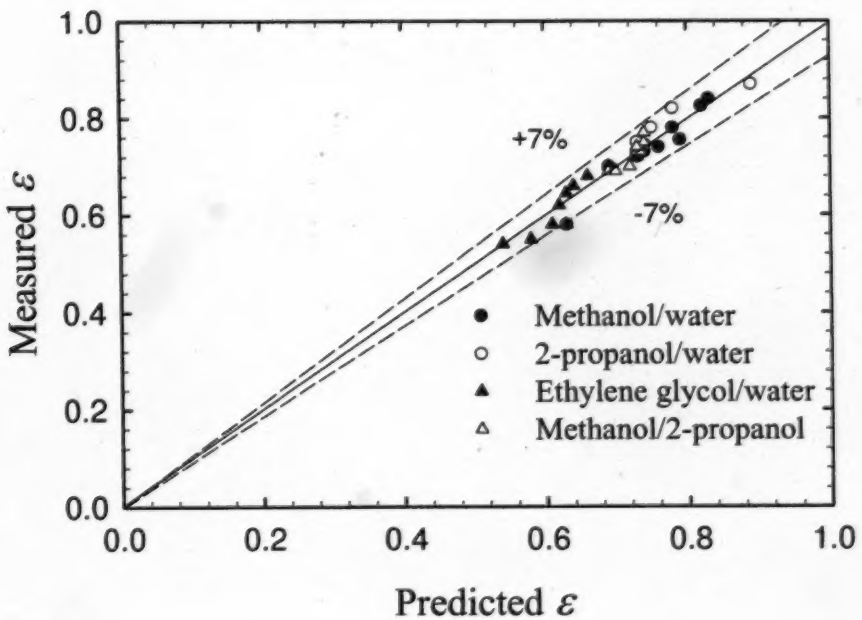

Figure 2-7(a)

Air bubbles in 2-propanol at $u_s = 0.32$ m/s

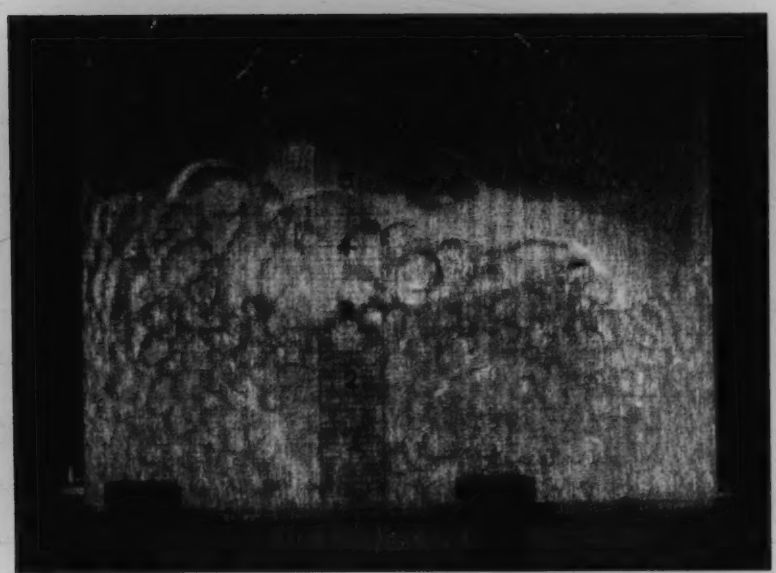

Figure 2-7(b)

Air bubbles in 2-propanol/methanol (20 mol% 2-propanol) at $u_s = 0.32$ m/s

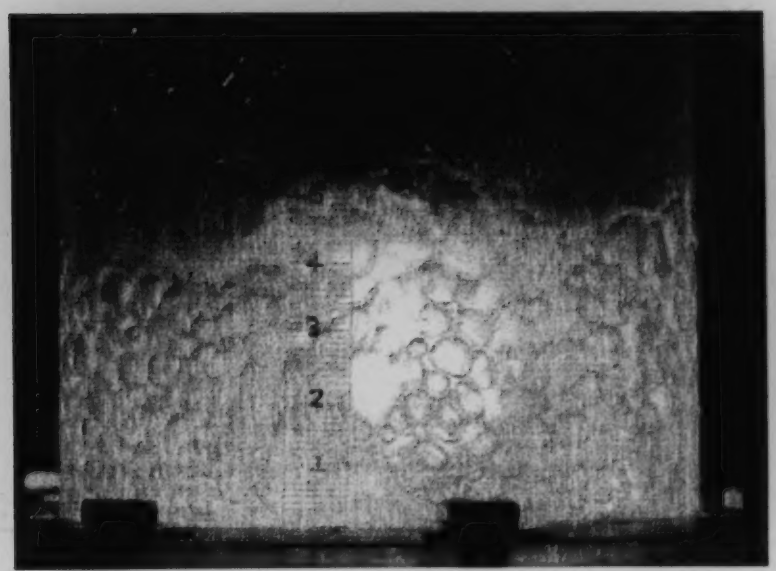

Figure 2-7(c)

Air bubbles in 2-propanol/water (15 mol% 2-propanol) at $u_s = 0.32$ m/s

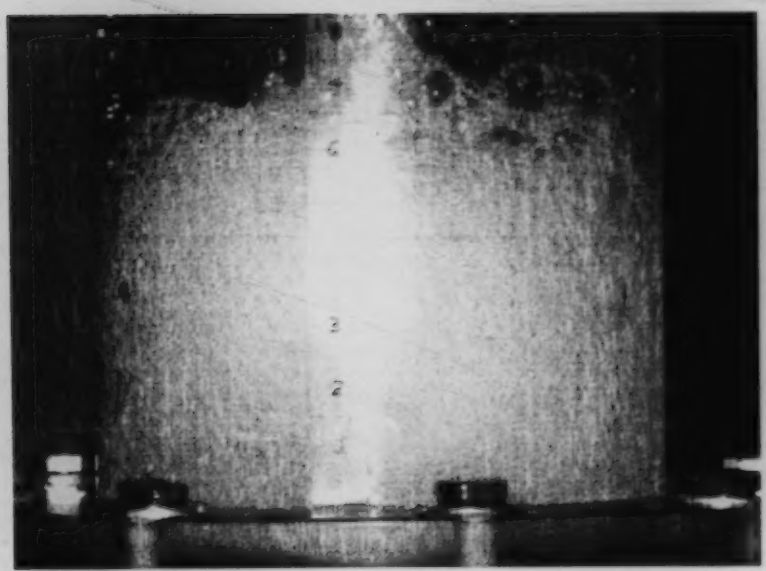

2.6 CONCLUSIONS

A gas hold-up correlation has been proposed that includes bubble coalescence criteria in pure and binary liquids. This correlation is the first attempt ever to include the effect of surface tension gradient on the gas hold-up of binary mixtures. The correlation is able to predict the often-reported enhancement of gas hold-up in surface-active binary liquids, which has not been accounted for by any other models.

For the first time comprehensive gas hold-up data for binary mixtures have been presented with respect to concentration. Predicted values are in good agreement (within ± 7%) with the measured values.

2.7 NOMENCLATURE

a_D	area of disc shaped liquid film, m^2
A	Hamaker- London constant for water, 3.5×10^{-20} J
b	experimentally determined exponent in equations (2.9) and (2.17)
c	force defined by equation (2.15), N.
c_1	dimensionless constant in equation (2.8)
C	molar density of the mixture, mol/m^3
C_1	experimentally determined constant in equations (2.9) and (2.17)
D	diffusion coefficient, m^2/s

g	gravity constant, m/s^2
h	film thickness, m
h_c	critical film rupture thickness, m
h_f	froth height, m
h_L	clear liquid height, m
k	defined by equation (2.16), m^{-1}
p	pressure, Pa
P	coalescence probability
r	bubble radius, m
R	gas constant, J/ (K-mol)
r_{eq}	equivalent radius of two coalescing bubbles, m
Re_d	bubble Reynolds number, $\left(\frac{U\rho_L d}{\mu_L}\right)$
S	normalized stretching rate, s^{-1}
t_c	time required for drainage to the critical rupture thickness, s
t'_c	time required to stretch a film from infinite thickness to a final thickness in a foam, s
t_i	interaction time of colliding particle, s
T	temperature in K.
u_s	superficial gas velocity based on column diameter, m/s
U	relative bubble rise velocity, m/ s
U_i	bubble rise velocity, cm/ s

U_i bubble rise velocity, cm/ s

v_i volume of bubbles, cm^3

V_1, V_2 molar volumes of solute and solvent, m^3 /mol

WE Weber number, $\left(\frac{\rho_L U^2 r_{eq}}{\sigma}\right)$

x mole fraction component with lower surface tension

Greek letters

ε gas hold-up

μ_G gas viscosity, Pa s

μ_L liquid viscosity, Pa s

ρ_G gas density, kg/m^3

ρ_L liquid density, kg/m^3

$\Delta\rho$ $(\rho_L-\rho_G)$, kg/m^3

σ surface tension, N/m

$\theta(x)$ function of x and V_i defined by equation (2.10a)

2.8 LITERATURE CITED

Akita, K., and F. Yoshida, "Gas Holdup and Volumetric Mass Transfer Coefficient in Bubble Columns," Ind. Eng. Chem. Process Des. Dev., **12**, 76-80 (1973).

Akita, K., and F. Yoshida, "Bubble size, Interfacial Area, and Liquid-Phase Mass Transfer Coefficient in Bubble Columns," Ind. Eng. Chem. Process Des. Dev., **13**, 84-90 (1974).

Andrew, S.P.S., "Frothing in Two-Component Liquid Mixtures," Int. Symp. On Distillation IChemE, 73-78 (1960).

Bennett, D. L., Rakesh Agarwal and P. J. Cook, "New Pressure Drop Correlation for Sieve Tray Columns," AIChE J, **29**, 434-442 (1983).

Burgess, J. M. and P.H. Calderbank, "The Measurement of Bubble Parameters in Two-Phase Dispersion-II," Chem. Eng. Sci. **30**, 1107-1121, (1975).

Chaudhari, R. V., and Hofmann, H., "Coalescence of Gas Bubbles in Liquids," Rev. Chem. Eng, **10**,134-190 (1994).

Chesters, A.K., "The Modelling of Coalescence Processes in Fluid-Liquid Dispersions: A Review of Current Understanding," Trans IChemE, **19,** 259-270 (1991).

Colwell, Charles J., "Clear Liquid Height and Froth Density on Sieve Trays," Ind. Eng. Chem. Process Des. Dev., **20**, 298-307 (1981).

D'Aprano, Alessandro, Ines Dorina Donato, Eugenio Caponetti, and Valeria Agrigento, "Viscosity Studies of Solutions of Water in n-Aliphatic Alcohols at Various Temperatures," J. Solution Chemistry, **8**, 793-800 (1979).

Davies, R. M., and G. I. Taylor, "The Mechanics of Large Bubbles Rising through Extended Liquids and through Liquids in Tubes," Proc. Roy. Soc., **A200,** 375-390 (1950).

Gilbert, T.J, "Liquid Mixing on Bubble–cap and Sieve Plates," Chem Eng Sci, **10**, 243-253 (1959).

Grover, G. S., C. V. Rode, and R. V. Chaudhari, "Effect of Temperature on Flow Regimes and Gas Hold-up in a Bubble Column," Can J Chem Eng, **64,** 501-504 (1986).

Hikita, M.S. Asai, K. Tanigawa, K. Segawa, and M. Kitao, "Gas Holdup in Bubble Column," Chem Eng J., **20**, 59-67 (1980).

Hughmark, G. A., "Hold up and Mass Transfer in Bubble Columns," Ind. Eng. Chem. Process Des. Dev., **6**, 218-220 (1967).

Kelkar, B. G., S. P. Godbole, M. F. Honath, Y. T. Shah, N. L. Carr, and W.-D. Deckwer, "Effect of Addition of Alcohols on Gas Holdup and Back mixing in Bubble Columns," AIChE J, **29,** 361-369 (1983).

Kister, H. Z., Distillation Design, McGraw-Hill, New York, 1992.

Kumar, A., T. T. Dagaleesan, G. S. Laddha, and H. E. Hoelscher, "Bubble Swarm Characteristics in Bubble Columns," Can J Chem Eng, **54**, 503-508 (1976).

Marucci, G., "Theory of Coalescence," Chem Eng Sci, **24,** 975-985 (1969).

Marucci, G., L. Nicodemo, and D. Acierno, Co-Current Gas-Liquid Flow, Plenum Press, 95-150 (1969).

Miyahara, Toshiro, Masahiko Tsuzaki, Toshiaki Saito, Yorishige Matsuba, and Teruo Takahashi, "Froth Characteristics of Shallow Bubble Columns with Sieve Plates," Chem Eng J, **40,** 21-29 (1989).

Nicklin, D. J., "Two-Phase Bubble Flow," Chem. Eng. Sci. **17,** 693-702, (1962).

Oels, U., J. Lucke, R. Buchholz, and K. Schugerl, "Influence of Gas Distributor Type and Composition of Liquid on the Behavior of a Bubble Column Bioreactor," Ger. Chem. Eng.,**1,** 115-129 (1978).

Ross, Saymour L., Francis H. Verhoff, and Rane L. Curl, "Droplet Breakage and Coalescence Processes in an Agitated Dispersion, 2. Measurement and Interpretation of Mixing Experiments," Ind Eng Chem Fund., **17,** 101-108 (1978).

Sagert, N. H., M. J. Quinn, S. C. Cribbs, and E. L. J. Rosinger, "Foams," Academy Press, 147-162 (1975).

Sagert, N. H., and M. J. Quinn, "The Coalescence of Gas Bubbles in Dilute Aqueous Solutions," Chem Eng Sci, **33**, 1087-1095 (1978).

Schugerl, K., J. Lucke, and U. Oels, "Bubble Column Bioreactors," Adv. Biochem. Eng., **7,** 1-84 (1977).

Slusher, Joseph T., "Shear Viscosity and Dielectric Constant in Aqueous Isopropanol and Aqueous Acetonitrile," Molecular Physics, **98**, 287-293 (2000).

Timmermans, Jean, The Physical-Chemical Constants of Binary Systems in Concentrated Solutions, Vol 4, Interscience Publishers, Inc (1960).

Tsierkezos, Nikos G., and Ioanna E. Molinou, "Thermodynamic Properties of Water+Ethylene Glycol at 283.15, 293.15, 303.15 and 313.15k," J. Chem. Eng. Data, **43**, 989-993 (1998).

Tunier, Remco, Chris G. J. Bisperink, Cor van den Berg and Albert Prins, "Transient Foaming Behavior of Aqueous Alcohol Solutions as Related to Their Dilational Surface Properties," J. Colloid and Int. Sci., **179**, 327-334 (1996).

Vazquez, Gonzalo, Estrella Alverez, and Jose M. Navaza, "Surface Tension of Alcohol + Water from 20 and 50° C," J. Chem. Eng. Data, **40**, 611-614 (1995)

CHAPTER 3

EFFECT OF SURFACE TENSION GRADIENT ON TRAY EFFICIENCY OF AN OLDERSHAW COLUMN

3.1 INTRODUCTION

The Oldershaw column is a small-scale distillation column (Oldershaw, 1941), which has been widely used in laboratories for conducting basic research on distillation. The study of Zuiderweg and Harmens (1958) shows that froth stabilization caused by surface tension gradient is strong in Odershaw column and has significant effect on both froth height and tray efficiency. Thus, in this chapter, Oldershaw column has been used to study the effect of surface tension gradient on tray efficiency.

Previous studies show that both surface tension and its gradient have significant influence on tray efficiency. There are efficiency models (Stichlmair, 1979; Zuiderweg, 1982; Chen and Chuang, 1993), where the effect of surface tension on tray efficiency is considered based on the theoretical analysis of two-phase dispersions. Chen et al. (1994) experimentally studied the effect of surface tension on point efficiency and determined the dependency of interfacial area on surface tension. The effect of surface tension gradient on distillation efficiency, however, needs to be investigated further. After the pioneering study of Zuiderweg and Harmens (1958) on the effect of surface tension gradient on froth structure,

several attempts have been made to quantify this effect on mass transfer efficiency (Hoverstreydt, 1963; Hart and Haselden, 1969; Lowry and van Winkle, 1969; and Zuiderweg, 1983). The general conclusion of these studies was that the positive systems exhibit higher efficiency than the negative or neutral systems in the middle concentration range and show a more pronounced decrease in efficiency at both high and low ends. However, none of these attempts were successful in quantifying surface tension gradient effect on point efficiency.

Tray efficiency depends on a number of factors namely, tray dimension, operating condition and physical properties. Thus it is difficult to single out the effect of one factor from the others. The general practice in developing the existing tray efficiency models was to estimate combined mass transfer coefficient and interfacial area. In this study, the interfacial area has been treated separately from the mass transfer coefficients. The main purpose of the present study is to investigate and quantify the effect of surface tension gradient on tray efficiency. With this goal in mind, tray efficiency of an Oldershaw column has been measured with respect to composition for six binary systems. These systems can be classified into positive, negative and neutral groups according to the definitions provided by Zuiderweg and Harmens (1958). The systems are methanol/water and n-heptane/toluene (positive systems), cyclo-hexane/n-heptane and methanol/iso-propanol (neutral systems) and acetic acid/water and benzene/n-heptane (negative systems). An expression for interfacial area has been developed, which takes into

account the surface tension gradient effect on gas/liquid dispersion in froth regime. The gas hold-up correlation proposed in chapter 2 is adopted in developing this interfacial area expression. Finally, a tray efficiency model is proposed by combining the interfacial area with mass transfer coefficient, which is able to predict both magnitude and trend of the measured point efficiency as a function of composition of the more volatile component.

3.2 EXPERIMENTAL

A schematic diagram of the experimental set-up is presented in Figure 3-1. An Oldershaw column with inner diameter 74.3 mm was used. The column and trays were made of Pyrex glass and contained five identical sieve trays. The second, third and fourth trays from the top were chosen as the test trays, where end-effects were minimal. Each test tray was equipped with liquid sampling point. The whole test loop was instrumented for continuous unattended operation at the steady state. Detailed dimensions of the column and the trays are given in Table 3.1.

The experiments were conducted at total reflux under atmospheric pressure and at a fixed superficial vapour velocity. The column was operated in froth regime. Once steady state was achieved, the liquid samples from second, third and fourth tray, vapour condensate flow rate and froth heights were measured. The liquid samples taken from each tray were analyzed using gas chromatograph (GC). For

Figure 3-1

Schematic diagram of the distillation column

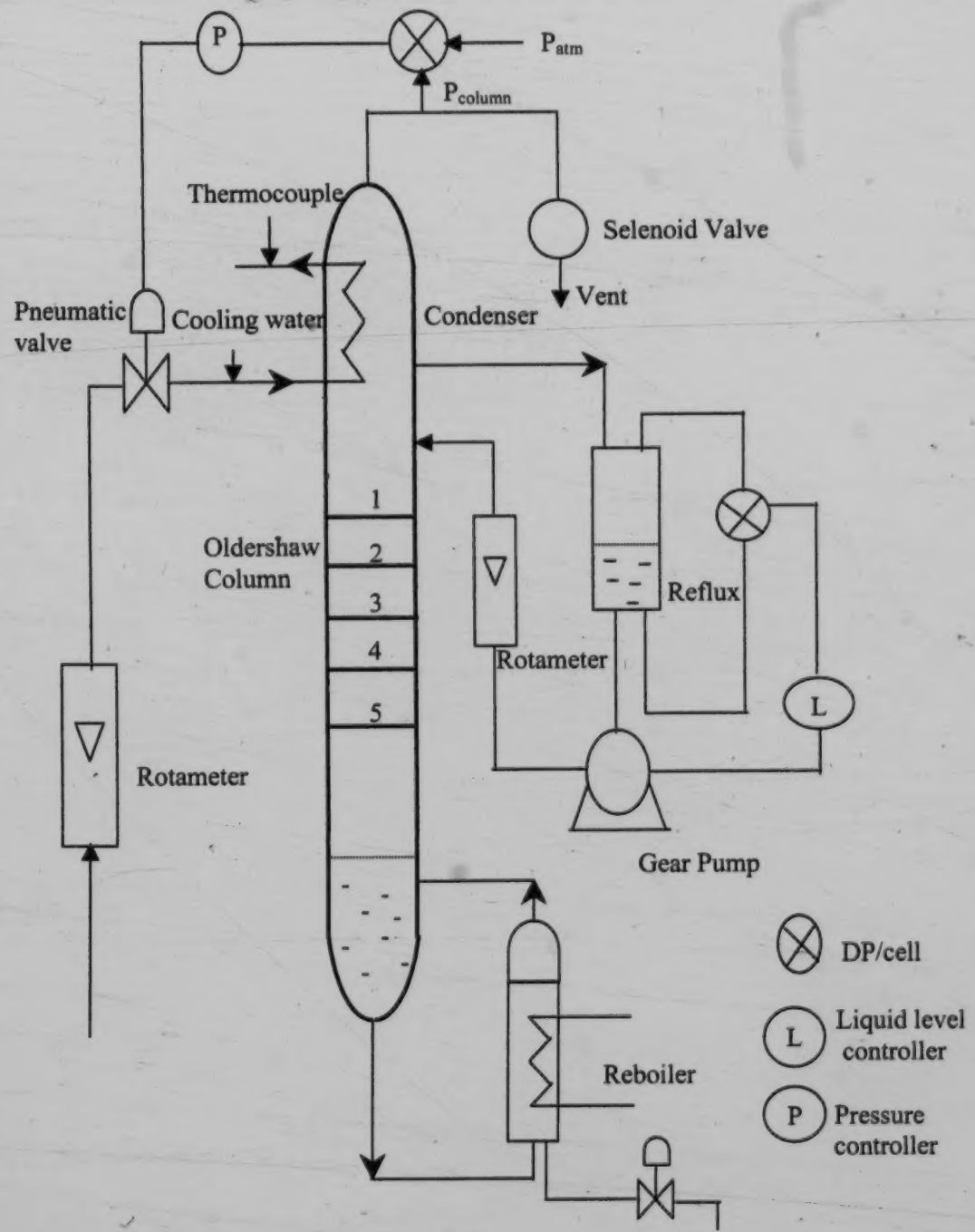

Table 3.1 Column and tray dimensions

Column diameter (mm)	74.3
Total column cross-sectional area (mm^2)	4333
Bubbling area (mm^2)	3840
Down comer area (mm^2)	494.5
Hole diameter (mm)	0.889
Open hole area (mm^2)	317
Tray thickness (mm)	25.4
Outlet weir height (mm)	2
Weir length (mm)	26.3
Tray spacing (mm)	50

alcohol and aqueous systems gas GC HP 5790A equipped with thermal conductivity detector (TCD) was used. GC HP 5890 Series-II with flame ionisation detector (FID) was used for hydrocarbon systems. Table 3.2 gives the details of the operating conditions and column specifications of the GC used for each system.

3.3 EFFICIENCY MEASUREMENT

Several definitions of tray efficiency exist in literature. Among them, the two definitions of Murphree efficiencies (Murphree, 1925) are mostly used. The first

Table 3.2 GC column specifications and operating conditions

System	GC	Detector	Column	Operating Condition	
				Temperatures	He flow rate
Methanol/ water	HP 5790A	TCD	6.6% CBX 20m 80/100 Carbopark 6' R21044	Injector : 250°C Detector : 200°C Oven: 88°C	300ml /min
Methanol/ 2-propanol	HP 5790A	TCD	3% Aprezon L on W 36" 1/8 ss column	Injector: 250°C Detector: 200°C Oven: 88°C	300ml /min
acetic acid/ water	HP 5790A	TCD	3% Aprezon L on W 36" 1/8 ss column	Injector: 250°C Detector: 200°C Oven: 100°C	300ml /min
Methanol/ 2-propanol	HP 5890 Series-II	FID	Fused silica capillary column 30m × 0.32 mm ID	Injector: 200°C Detector: 200°C Oven: 90°C	Detector outlet: 42ml/min Split out let: 27 ml/min
Cyclohexane/n-heptane	HP 5890 Series-II	FID	Fused silica capillary column 30m × 0.32 mm ID	Injector: 220°C Detector: 220°C Oven: 60°C	Detector outlet: 42ml/min Split out let: 27 ml/min
Benzene/n-heptane	HP 5890 Series-II	FID	Fused silica capillary column 30m × 0.32 mm ID	Injector: 220°C Detector: 220°C Oven: 70°C	Detector outlet 42ml/min Split out let: 27 ml/min

one is Murphree vapour phase point efficiency E_{OG}, expressed as the ratio of the change of vapour composition at a point to the change that would occur if equilibrium were reached:

$$E_{OG} = \left(\frac{y_n - y_{n-1}}{y_n^* - y_{n-1}} \right)_{point} \tag{3.1}$$

Another type of Murphree efficiency is Murphree vapour phase tray efficiency, which is defined as the ratio of the change of vapour composition across the tray to the change that would occur on an ideal tray.

$$E_{MV} = \left(\frac{y_n - y_{n-1}}{y_n^* - y_{n-1}} \right)_{tray} \tag{3.2}$$

At total reflux, it follows from a simple component balance that the value of y_n is equal to the composition of the liquid entering the tray, i.e., $y_n = x_{n-1}$ and similarly $y_{n+1} = x_n$. Therefore, the Murphree vapour tray efficiency can be expressed as

$$E_{MV} = \left(\frac{x_{n-1} - x_n}{y_n^* - x_n} \right)_{tray} \tag{3.2a}$$

The Murphree tray efficiency, E_{MV}, of the Oldershaw column was calculated by analysing the liquid samples taken from above every tray. If perfectly mixed, the liquid and vapour composition on the tray can be considered uniform. The Murphree tray efficiency, E_{MV}, is then equal to the point efficiency, E_{OG}, at any point on the tray (Lewis, 1936). In an Oldershaw column, where the diameter of the column is small, it is assumed that the vapour and liquid on each tray are

perfectly mixed and the Murphree tray efficiency, E_{MV} is equal to the point efficiency, E_{OG}.

3.4 PREDICTION OF POINT EFFICIENCY

The overall number of mass transfer units, N_{OG}, can be related to the point efficiency, E_{OG}. by:

$$E_{OG} = 1 - \exp(-N_{OG}) \tag{3.3}$$

The following relation between mass transfer units is obtained from two-film theory:

$$\frac{1}{N_{OG}} = \frac{1}{N_G} + \frac{\lambda}{N_L} \tag{3.4}$$

where,

$$N_{OG} = aK_{OG}t_G \tag{3.5}$$

$$N_G = ak_G t_G \tag{3.6}$$

$$N_L = ak_L t_L \tag{3.7}$$

and

$$\lambda = \frac{mG_m}{L_m} \tag{3.8}$$

Based on Higbie penetration theory (Higbie, 1935) and several other studies (Lockett et al. 1979; Mehta and Sharma, 1966; and Chen and Chuang, 1992) the following equations for mass transfer coefficients are postulated,

$$k_G = C_1\left(\frac{D_G}{t_G}\right)^{0.5} \tag{3.9}$$

and

$$k_L = C_2\left(\frac{D_L}{t'_L}\right)^{0.5} \tag{3.10}$$

Substituting equations (3.9) and (3.10) into equations (3.6) and (3.7), respectively, we get

$$N_G = C_1 a\left(D_G t_G\right)^{0.5} \tag{3.11}$$

$$N_L = C_2 a\left(D_L t'_L\right)^{0.5}\left(\frac{M_G G_m}{M_L L_m}\right) \tag{3.12}$$

Here, the vapour residence time in the two-phase dispersion is expressed as

$$t_G = \frac{h_f \varepsilon}{u_s} \tag{3.13}$$

Similarly, liquid residence time is

$$t_L = t'_L\left(\frac{M_G G_m}{M_L L_m}\right) \tag{3.14}$$

where,

$$t'_L = t_G \frac{\rho_L}{\rho_G} \tag{3.14a}$$

The interfacial area in froth regime is generally estimated in terms of gas hold-up, ε and Sauter mean bubble diameter, d_{32};

$$a = \frac{6\varepsilon}{d_{32}} \tag{3.15}$$

Due to small liquid height and low gas load, in the Oldershaw column, bubbles departed from orifice coalesce before forming secondary bubbles. Therefore, the

bubbles in froth are essentially the departure bubbles from the holes of the sieve tray. Bennet et al. (1983) proposed the following equation for the departure bubble diameter from hole in sieve trays.

$$D_B = 1.27\left(\frac{D_H \sigma}{g(\rho_L - \rho_G)}\right)^{1/3} \tag{3.16}$$

Equation (3.16) has been used to estimate Sauter mean bubble diameter, d_{32}, throughout this chapter.

The gas hold-up correlation proposed in chapter 2 (equation 2.17) is based on the measured data of a shallow bubble column where the column diameter and the gas flow rates are comparable with those of the Oldershaw column used in this study. The correlation also includes bubble coalescence criteria that accounts for the froth stabilization caused by the surface tension gradient. This correlation of gas hold-up for surface tension positive systems, reproduced below as equation (3.17), has been used to develop the present model for Oldershaw column,

$$\varepsilon = 1.334\left[x\left(\frac{WE_1}{2}\right)^{1/2} + (1-x)\left(\frac{WE_2}{2}\right)^{1/2} + \left(\frac{crk^2}{\sigma}\right)\right]^{0.032}\left(\frac{u_s^{0.6}\mu_G^{0.11}\rho_G^{0.062}\rho_L^{0.07}}{\sigma^{0.2}\mu_L^{0.03}g^{0.13}}\right) \tag{3.17}$$

where,

$$c = \frac{2}{CRT}\theta(x)\left(\frac{d\sigma}{dx}\right)^2 \tag{3.18}$$

$$\theta(x) = \frac{x(1-x)}{\left(1 - x + \frac{V_1}{V_2}x\right)} \tag{3.19}$$

and $$k = \left(\frac{12\pi\sigma}{Ar}\right)^{\frac{1}{3}} \tag{3.20}$$

WE_1 and WE_2 represent the Weber numbers of the bubbles in pure liquids with low and high surface tensions, respectively. Both surface tension negative and neutral systems are non-foaming mixtures and their gas hold-ups are assumed not to be affected by the surface tension gradient. Thus equation (2.9) is used for negative and neutral systems,

$$\varepsilon = 1.334\left(\left(\frac{WE}{2}\right)^{1/2}\right)^{0.032}\left(\frac{u_s^{0.6}\mu_G^{0.11}\rho_G^{0.062}\rho_L^{0.07}}{\sigma^{0.2}\mu_L^{0.03}g^{0.13}}\right) \tag{3.21}$$

Equation (2.6) gives the expression for the Weber number,

$$WE = \frac{\rho_L U^2\left(d_{eq}/2\right)}{\sigma} \tag{3.22}$$

Finally, by combining equations (3.3), (3.11) and (3.12), we get the expression for the over all mass transfer unit,

$$N_{OG} = \frac{N_G}{1+\lambda\dfrac{N_G}{N_L}} = \frac{C_1 a\left(D_G t_G\right)^{0.5}}{1+\lambda\dfrac{C_1}{C_2}\left(\dfrac{M_L L_m}{M_G G_m}\right)\left(\dfrac{D_G\rho_G}{D_L\rho_L}\right)^{0.5}} \tag{3.23}$$

3.4.1 Estimation of the constants C_1 and C_2

The gas hold-up, ε, is first calculated from equations (3.17) and (3.21). The term $(WE/2)^{1/2}$ in gas hold-up correlations is in fact the ratio of drainage time to

interaction time, t_c/t_i, as shown in equation (2.5). Since it is very difficult to estimate the exact value of Weber number of the bubbles in froth, an approximate value of Weber number is estimated in this model.

In Odershaw column, the observed froth structure in pure liquids was in the form of small spray bed. This observation is in agreement with that described by Zuiderweg and Harmens (1958). Such spray bed is formed by the instant coalescence of bubbles formed at the orifice. In earlier studies Chesters and Hoffman (1982) and Chesters (1991) proposed the following equation for coalescence time between two fully formed approaching bubbles

$$t_c = \frac{\rho_L U (d_{eq}/2)^2}{\sigma} \tag{3.24}$$

Their estimated t_c is of the order of 10^{-4} to 10^{-2} sec for pure liquids. If the coalescence happens while the bubbles are forming, the coalescence time is almost 10^{-1} to 10^{-2} times less than that for the fully formed bubbles (Kirkpatrick and Lockett, 1974). Since, in this study, the bubbles originated from the sieve tray holes coalesce upon formation, we approximately estimated $t_c \cong 10^{-5}$ sec. This gives approach velocity, U, of 10^{-5} m/sec. This value of U has been used to estimate Weber number in equation (3.22). The exponent to U is very small i.e. 0.032, in gas hold-up equations (2.9) and (2.17). Thus the predicted value of E_{OG} is rather insensitive to the exact value of U. Ten times decrease or increase in U leads to approximately ± 5% change in the final predicted value of E_{OG}.

The coalescence time $t_c \cong 10^{-5}$ sec implies that bubbles practically do not exist in the froth of pure liquids. Small gas jets at the orifice and drops formed by coalescing bubbles constitute the froth structure. Due to the difficulty that arises in estimating the interfacial area in small spray bed in pure liquids, in present study it is considered that both interfacial area and bubble size equations (equations (3.15) and (3.16)) are applicable to the whole concentration range of the mixtures including the pure liquids.

Thus the interfacial area, a, is estimated from equations (3.15) and (3.16). Equations (3.13) and (3.14a) are used to estimate the residence times t_G and t'_L from the measured froth height data. From equation (3.3) the experimental value of N_{OG} is obtained from measured E_{OG} data. Finally, by fitting equation (3.23) to the experimental N_{OG} data at different concentration for the six binary systems the constants C_1 and C_2 have been determined to be 3 and 2.5, respectively.

Froth stabilization force, c, in parameter $\frac{crk^2}{\sigma}$ is sensitive to surface tension of the mixtures with respect to concentration. Due to lack of experimental data at boiling point we used correlations to estimate surface tension of the binary mixtures. For aqueous solutions of various alcohols Vazquez et al. (1995) proposed the following equation

$$\sigma(mN/m) = K_1 - K_2 t(^o c) \tag{3.25}$$

where K_1 and K_2 are experimentally measured values. The surface tension of the organic binaries are estimated by using the following equation (Meissner and Michaels, 1947), according to the procedure mentioned by Yang and Maa (1983);

$$\sigma^{1/4} = \left(\frac{P_{mix}}{R_{mix}}\right)\left(\frac{n_{mix}^2 - 1}{n_{mix}^2 + 2}\right) \qquad (3.26)$$

In this equation n_{mix}, P_{mix} and R_{mix} are the refractive index, parachor and molar refraction of the mixtures respectively.

3.5 RESULTS AND DISCUSSION

The point efficiency measured in the Oldershaw column and predicted by the proposed model are shown in Figures 3-2 to 3-7 for the six systems as a function of composition of the more volatile component at constant superficial velocity, u_s. of the vapour. Surface tension positive systems, i.e., methanol/water and n-heptane/toluene (Figures 3-2 and 3-3) exhibit much higher point efficiency in the middle range of the efficiency versus composition curve. A pronounced decrease in efficiency is observed in the regions of high and low concentration of the more volatile component. This is consistent with those reported in the literature (Van Wijk and Thijssen, 1954; Zuiderweg and Harmens, 1958; Ellis and Biddulph, 1967; Ruckenstein and Smilgelschi, 1967). For neutral (Figures 3-4 and 3-5) and negative systems (Figures 3-6 and 3-7) the change in efficiency with composition is not as significant as that for positive systems.

Figure 3-2

Comparison of the prediction by the proposed model with the experimental data of point efficiency at different concentrations of methanol/water system (u_s = 0.25 m/s)

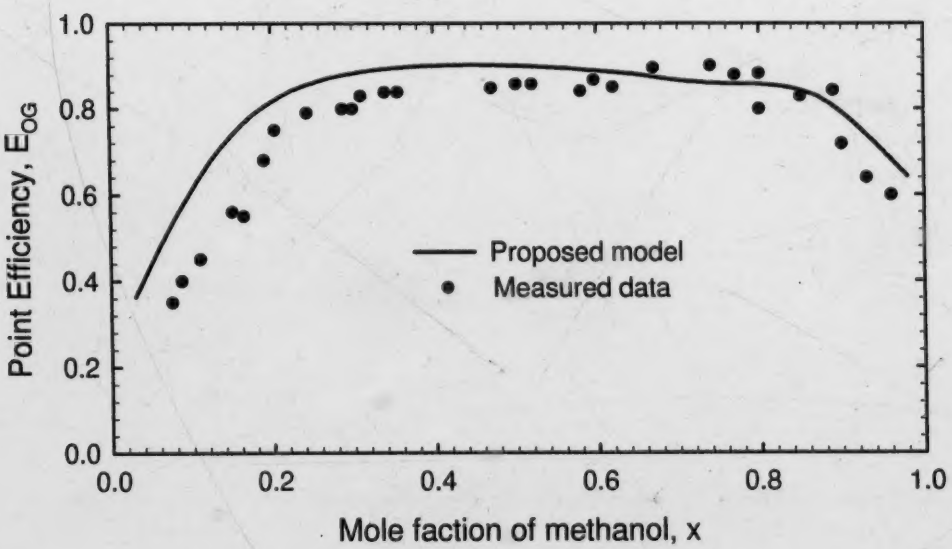

Figure 3-3

Comparison of the prediction by the proposed model with the experimental data of point efficiency at different concentrations of n-heptane/toluene system (u_s = 0.25 m/s)

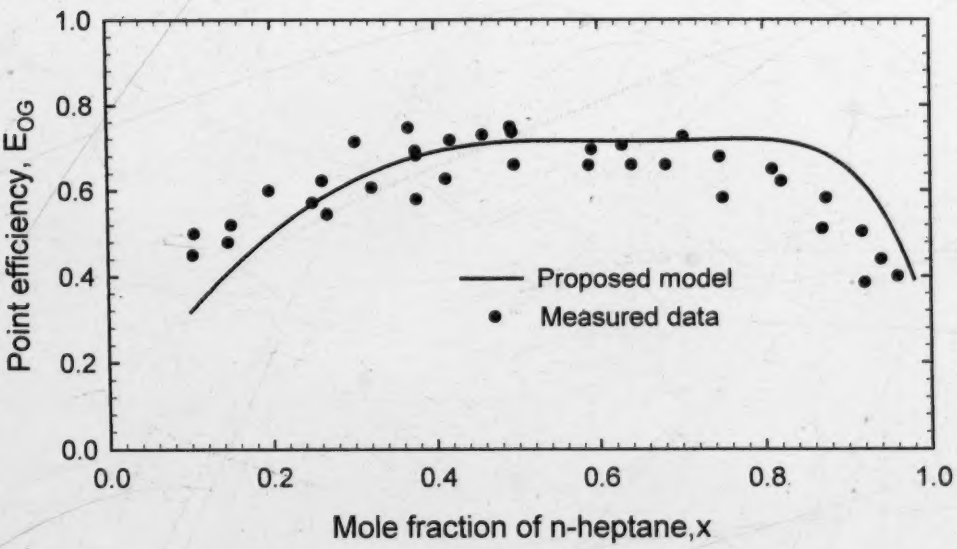

Figure 3-4

Comparison of the prediction by the proposed model with the experimental data of point efficiency at different concentrations of methanol/2-propanol system (u_s = 0.25 m/s)

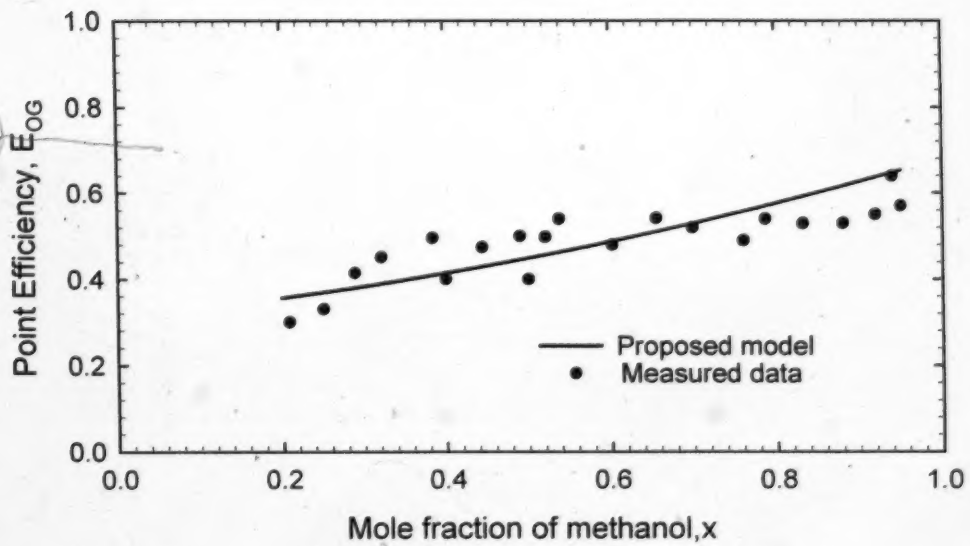

Figure 3-5

Comparison of the prediction by the proposed model with the experimental data of point efficiency at different concentrations of c-hexane/ n-heptane system (u_s = 0.29 m/s)

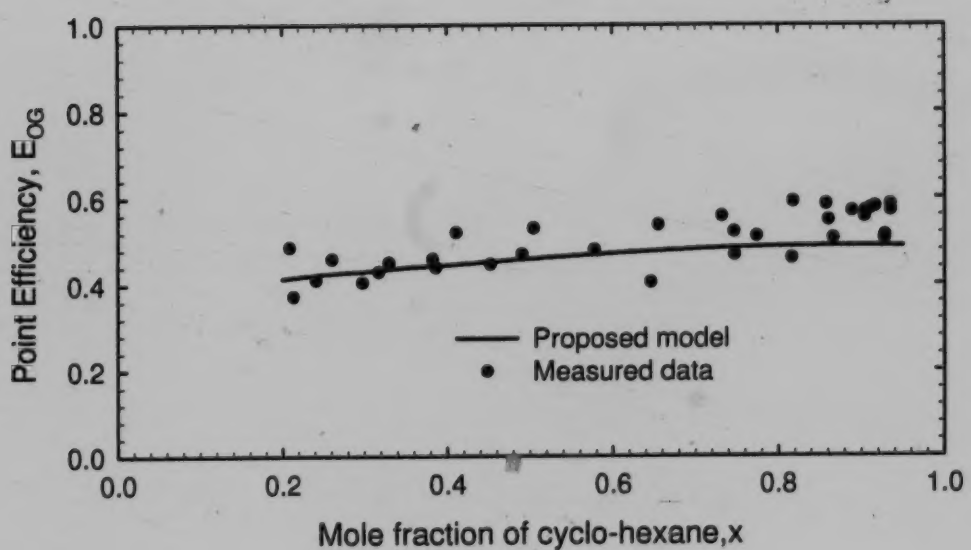

Figure 3-6

Comparison of the prediction by the proposed model with the experimental data of point efficiency at different concentrations of water/acetic acid system (u_s = 0.29 m/s)

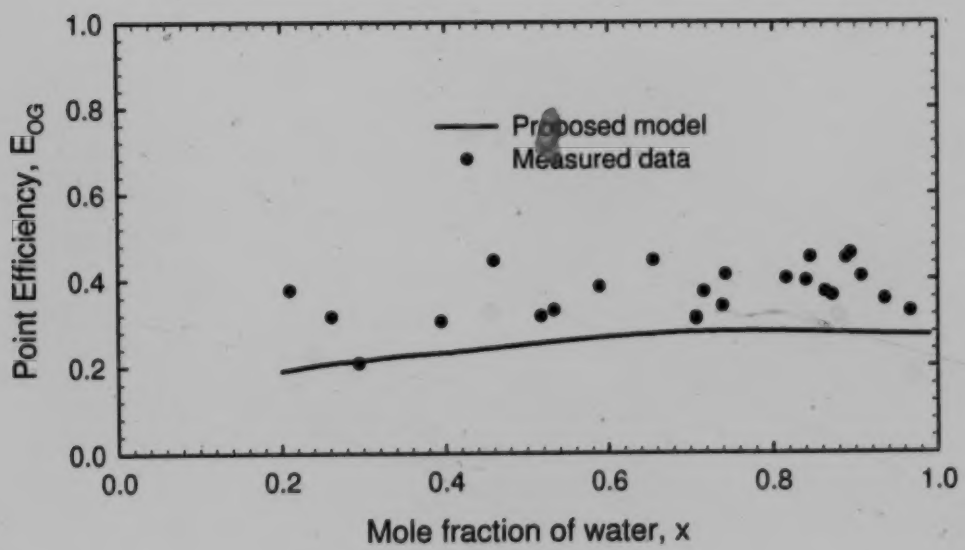

Figure 3-7

Comparison of the prediction by the proposed model with the experimental data of point efficiency at different concentrations of benzene/toluene system (u_s = 0.29 m/s)

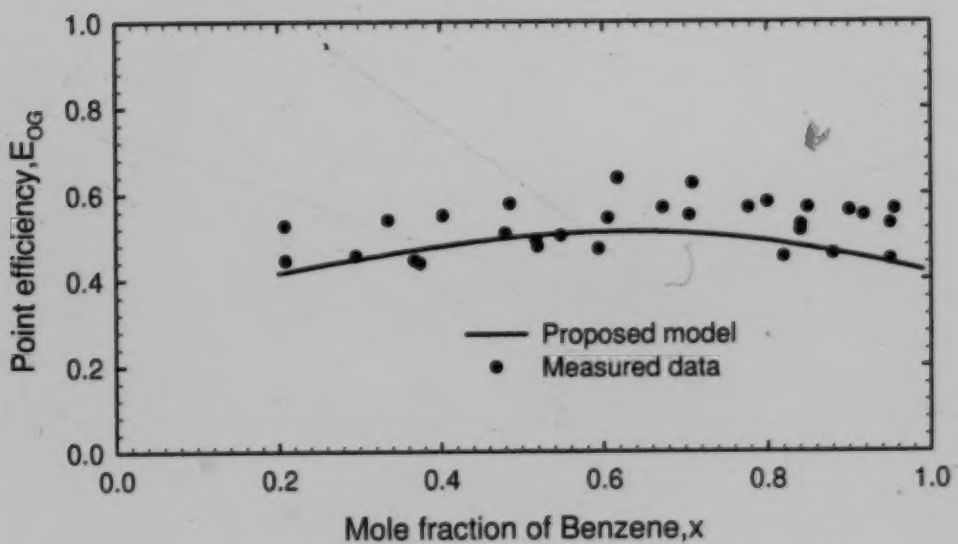

3.5.1 Effect of surface tension gradient on point efficiency

It is evident from Figures 3-2 to 3-7 that the proposed model (equation (3.23)) adequately predicted both magnitude and trend of the point efficiency obtained for the six different mixtures except for the acetic acid/water system. The agreement between the measured and predicted values is particularly significant for surface tension positive systems, as the model can predict the enhanced efficiency in the middle range and the drop off of efficiency at both ends of the efficiency versus concentration curves. The enhancement of point efficiency accompanied by a sharp drop off at high concentration end is a well-established phenomenon for surface tension positive systems. Such phenomenon cannot be quantified by the existing models as the commonly considered parameters, such as, flow parameters, tray geometry and physical properties to quantify gas/liquid dispersions in pure liquids are not always adequate to explain the froth structure in binary systems. For example, some binary systems exhibit phenomenon like foaming, which is not thermodynamically plausible in pure liquids (Ross 1967). Presence of surface-active impurities or solutes in mixtures prevents liquid drainage between bubbles, thus enabling bubbles to resist coalescence. Resistance to coalescence stabilizes the froth and leads to foaming. Surface tension gradient developed at the interface of the gas/liquid dispersion plays the key role in such stabilizing process.

The mechanism of froth stabilization is generally explained in terms of Marangoni effect (Zuiderweg and Harmens, 1958; Andrew, 1960). Surface tension positive systems have surface-active solutes and form stable and uniform froth, which leads to increased interfacial area and consequently to high point efficiency. However, froth stabilizing force in positive systems diminishes as the mol fraction of the more volatile component (mvc) approaches zero and unity. This causes significant decrease in interfacial area in these regions and resulting in lower point efficiency.

In the proposed efficiency model for positive systems, term c in the parameter $\frac{crk^2}{\sigma}$ in equation (3.17) accounts for the surface tension gradient effect, which is responsible for the change in interfacial area due to froth stabilization. Equations (3.18) and (3.19) show that $\frac{crk^2}{\sigma}$ approaches zero as the mol fraction of mvc approaches either zero or unity. Thus at the both ends of the efficiency versus concentration curve, the proposed model interprets the diminishing effect of surface tension gradient. This makes $(WE/2)^{1/2}$, the bubble coalescence criterion in pure liquids, the only contributor to the interfacial area. The estimated interfacial area of the proposed model, thus, changes with the change of froth stability. This unique characteristic of this model enables it to predict the trend of the experimental point efficiency of surface tension positive systems with the change of concentration as shown in Figures 3-2 and 3-3.

For methanol/water system, the $\frac{crk^2}{\sigma}$ value is highest around 15-20mol% of methanol. However, in Figure 3-2, the point efficiency starts going down at a methanol concentration $x \leq 0.25$. The slope of equilibrium curve, m, contributes to this decrease in efficiency, since the estimated $\frac{1}{N_G} << \frac{\lambda}{N_L}$ in equation (3.4).

For n-heptane/toluene system, $\frac{crk^2}{\sigma}$ is highest around 60mol% and the slope of equilibrium curve does not change significantly with respect to concentration.

Froth stabilizing force is absent in surface tension neutral systems. In surface tension negative systems, surface tension gradient develops in the reverse direction of that of the positive systems and destabilizes the froth. Thus, for both neutral and negative systems the froth stabilization parameter, $\frac{crk^2}{\sigma}$, has been ignored in the proposed model and equation (3.21) is used for gas hold-up estimation. The model predicted the efficiency of neutral systems satisfactorily (Figures 3-4 and 3-5). However, for negative systems the predictions are somewhat lower than the measured data (Figures 3-6 and 3-7). This can result from drop stabilization caused by the reverse surface tension gradient effect at the interface of drops in negative systems. The froth on Oldershaw trays mainly consists of bubbles. The froth also contains liquid drops formed during the bursting of bubbles at the interface. The contribution of drops to the net interfacial

area is insignificant in positive and neutral systems. It can, however, become significant in negative systems where stabilization of drop occurs (Fane and Sawistowski, 1968). The scope of the present study is limited to the effect of surface tension gradient on bubble stability. The proposed efficiency model does not include contribution of drop stabilization to the interfacial area. Therefore, for negative systems the interfacial area estimated by the model can be lower than the effective interfacial area. This explains the lower predictions of the model than the experimental data for surface tension negative systems. The difference in surface tension between the components of acetic acid/water is higher than that between the components of benzene/n-heptane. This results in higher drop stabilization in acetic acid/water than that in benzene/n-heptane, which justifies the under prediction of efficiency for acetic/water system than that for benzene/n-heptane system.

Figure 3-8 compares the point efficiencies between a surface tension positive and a surface tension neutral system; both contain a common more volatile component (mvc) methanol. In the middle concentration range methanol/water shows higher efficiency than methanol/2-propoanol. However, at the right end of the graph, where both systems reduce to pure methanol, the point efficiency curve of methanol/water goes down and meets the methanol/2-propanol curve. Similar phenomenon is observed in froth height versus concentration graphs for different

Figure 3-8

Comparison of the point efficiency versus concentration data between a surface tension positive (methanol/water) and a surface tension neutral (methanol/2-propanol) system

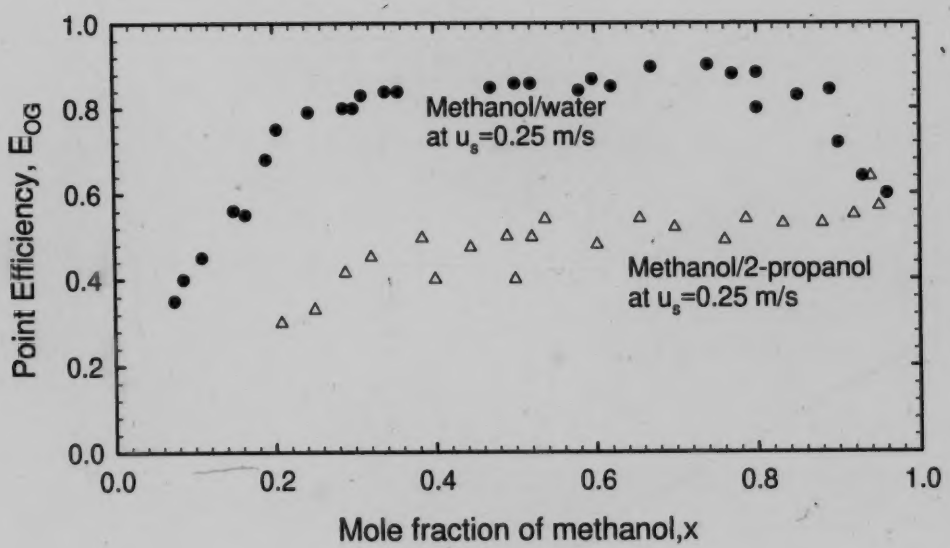

systems shown in Figures 3-9 and 3-10. In positive systems, stabilized bubbles give rise to higher froth height in the middle concentration range. As the concentration approaches both ends, the froth heights of the positive systems decrease and coincide with those of negative and neutral systems, confirming the decrease in bubble stabilization. Thus the often reported enhanced point efficiency for positive systems are due to the presence of stable bubbles in froth caused by the surface tension gradient, whereas the decline of efficiency at the high ends are due to the less stable bubbles caused by the diminished surface tension gradient effect. The negative and neutral systems give constant froth height through out the whole concentration range, even where the systems become pure liquids. This confirms the absence of bubble stabilization in these systems.

3.5.2 Effect of surface tension on point efficiency

The proposed model includes the effect of surface tension on tray efficiency besides the surface tension gradient effect. Leaving aside the effect of properties other than surface tension, we get following expressions for diameter and gas hold-up from equations (3.16) and (3.17) or (3.21),

$$d_{32} \propto \sigma^{0.333} \tag{3.27}$$

$$\varepsilon \propto \sigma^{-0.216} \tag{3.28}$$

The change in composition results in a change of surface tension as well as the slope of equilibrium line (m). In order to separate the effect surface tension from the effect of m, the expressions for N_G and N_L are used to determine the effect of

Figure 3-9

Measured froth height for aqueous and alcohol systems

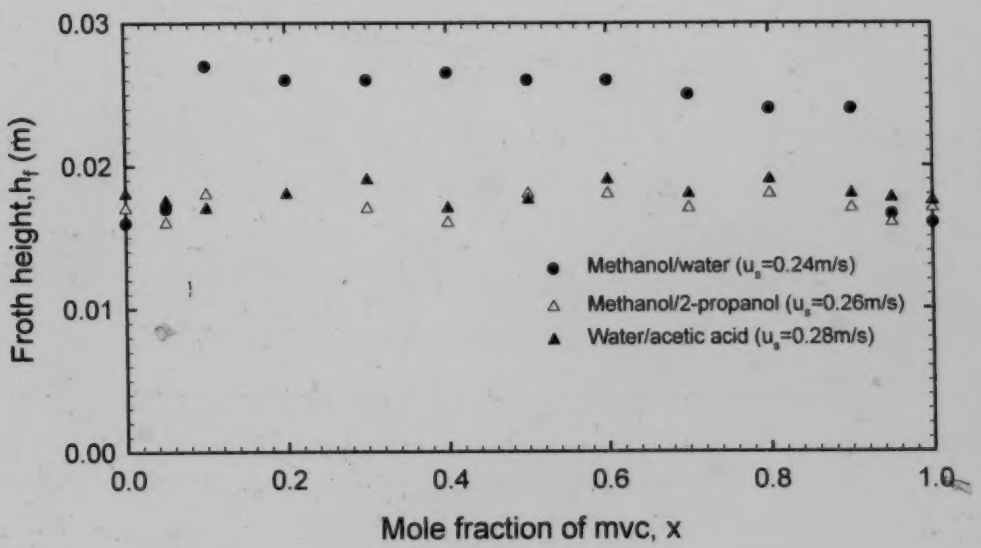

Figure 3-10

Measured froth height for hydrocarbon systems

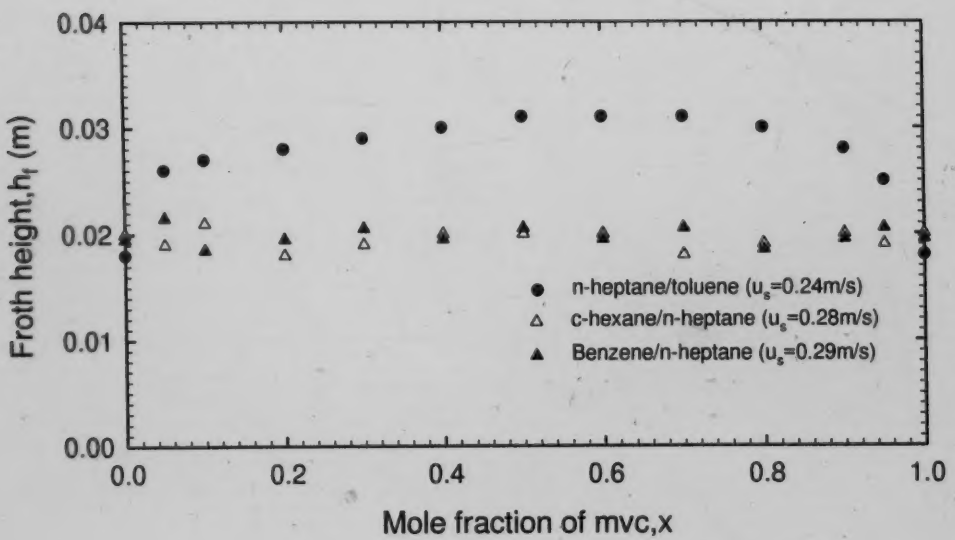

surface tension on point efficiency. From the proposed mass transfer model, i.e. equations (3.11) and (3.12), we get the following expressions for the gas and the liquid mass transfer units,

$$N_G \propto \frac{\varepsilon^{1.5}}{d_{32}} \propto \sigma^{-0.657} \tag{3.28}$$

$$N_L \propto \frac{\varepsilon^{1.5}}{d_{32}} \propto \sigma^{-0.657} \tag{3.29}$$

Equations (3.28) and (3.29) show the dependency of mass transfer units on surface tension as determined from the proposed model. These expressions are in good agreement with those proposed by Chen and Chuang (1993) and Zuiderweg (1982) and obtained by Chen et al. (1994) based on experimental observations. They reported that mass transfer units are proportional to $\sigma^{-0.667}$, $\sigma^{-0.53}$ and $\sigma^{-0.663}$, respectively.

3.5.3 Justification of adopting gas hold-up correlation developed for air/liquid system in distillation tray efficiency model

In distillation, froth stabilization is considered to be induced by mass transfer phenomenon (section 1.3). Although discussed numerous times in literature, mass transfer induced froth stabilization, however, is still a hypothesis. No quantifying factor is available to assess its contribution to froth stabilization.

One study of Yang (1990) shows that the dynamic surface effect (Andrew, 1960) plays an important role in the boiling process of aqueous solution. This implies

that the froth stabilization in distillation is not solely a mass transfer induced phenomenon. Dynamic surface effect also contributes substantially to this process. Another study (Yang and Maa, 1984) suggested that dynamic surface effect could be dominant over mass transfer effect in stabilizing froth in distillation process. An interesting observation in air/liquid column, described below, in fact supports this suggestion. It is generally considered that no mass transfer between gas/liquid phases takes place in air/methanol-water and air/2-propanol-water systems at ambient condition. However, in reality both methanol and 2-propanol diffuses into air to some extent due to their highly volatile nature. Despite this fact the gas hold-up of these systems were adequately predicted with the help of dynamic surface theory in chapter 2. Thus in this chapter the same gas hold-up correlation based on the data in air/liquid system is used to develop the point efficiency model in distillation.

Using air/liquid test data in distillation design is a well-established practice. All existing correlations for gas hold-up are based on the air/liquid test data from simulator columns. Therefore, by using the gas hold-up correlation based on air/liquid data from a simulator bubble column the new model in fact follows the established trend in distillation research. Furthermore, the agreement between the measured and predicted point efficiencies in Figures 3-2 and 3-3 proves the validity of this approach.

3.6 CONCLUSIONS

In this study we have analyzed surface tension gradient effects on point efficiency in an Oldershaw column. A point efficiency model, supported by measured data from six binary systems, has been proposed. The gas hold-up correlation proposed in chapter 2 is introduced in the interfacial area expression of the point efficiency model. Thus the model inherits the froth stabilizing factor caused by surface tension gradient from the gas hold-up correlation. This is the first successful attempt to include froth stabilizing effect in a point efficiency model. The major contribution of this model is its ability to predict the point efficiency enhancement, caused by Marangoni effect, in the middle concentration range of positive systems. The predictions are satisfactory for neutral systems.

The comprehensive experimental study of point efficiency undertaken by this study allows one to compare the efficiency behaviour of different mixtures with wide range of physical properties under the same tray geometry and similar flow conditions.

The proposed tray efficiency model is developed for the laboratory scale small column. This model may not be directly applicable to large industrial columns as both tray geometry and flow conditions in large columns may vary significantly from those in the Oldershaw column and can have major impact on froth structure. Additional investigation is required to understand the froth structure on

large-scale industrial trays. In the following chapters, froth structure on industrial tray will be analysed.

3.7 NOMENCLATURE

a	Interfacial area, m^2
A	Hamaker- London constant for water, $3.5x10^{-20}$ J
c	froth stabilizing force defined by equation (3.18), N
C	molar density of the mixture, mol/m^3
C_1, C_2	experimentally determined constants in equations (3.11) and (3.12)
d_{32}	sauter mean bubble diameter, m
d_{eq}	equivalent diameter of two coalescing bubbles, m
D_B	bubble departure diameter from orifice, m
D_H	orifice diameter, m
D_L	liquid phase diffusivity, m^2/s
D_G	gas phase diffusivity, m^2/s
E_{OG}	Point efficiency
E_{MV}	Murphree vapor tray efficiency
E_{ML}	Murphree liquid tray efficiency
G_m	vapour flow rate kmol/sec
h	thickness of liquid film, m
h_f	froth height, m
k	defined by equation (3.20), m^{-1}

k_G	gas film mass transfer coefficient, m/s
k_L	liquid film mass transfer coefficient, m/s
K_1, K_2	constants in equation (3.25)
K_{OG}	overall mass transfer coefficient, m/s
L_m	liquid flow rate, kmol/s
m	slope of equilibrium curve
M_G	vapour phase molecular weight, kg/kmol
M_L	liquid phase molecular weight, kg/kmol
n_{mix}	refractive index of mixtures
N_G	number of gas phase mass transfer units
N_L	number of liquid phase mass transfer units
N_{OG}	number of overall gas phase mass transfer units
P_{mix}	parachor of mixtures
R	gas constant, 8.31 J /K-mol
R_{mix}	molar refraction of mixtures
S	normalized stretching rate, s^{-1}
t_G	gas residence time, s
t_L	liquid residence time, s
t'_L	liquid residence time defined by equations (3.14) and (3.14a), s
T	temperature, K
u_s	superficial gas velocity based active area, m/ s
U	bubble approach velocity, m/s

V_1, V_2 molar volumes of solute and solvent, m^3/mol

WE Weber number, $\left(\frac{\rho_L U^2 d_{eq}/2}{\sigma}\right)$

x mole fraction of mvc in liquid

y mole fraction of mvc in vapour

x_n liquid composition leaving the tray

x_{n-1} liquid composition entering the tray

x_n^* liquid composition at equilibrium

y_n vapour composition leaving the tray

y_{n-1} vapour composition entering the tray

y_n^* vapour composition at equilibrium

Greek letters

ε gas hold-up

λ stripping factor, mG_m/L_m

μ_G gas viscosity, Pa s

μ_L liquid viscosity, Pa s

ρ_G gas density, kg/m^3

ρ_L liquid density, kg/m^3

σ surface tension, N/ m

$\theta(x)$ function of x and V_i defined by equation (3.19)

3.8 LITERATURE CITED

Andrew, S.P.S., "Frothing in Two-Component Liquid Mixtures," Int. Symp. On Distillation IChemE, 73-78 (1960).

Bennett, D. L., R. Agarwal and P. J. Cook, "New Pressure Drop Correlation for Sieve Tray Distillation Columns," AIChE J **29** (3), 434-442, (1983).

Chan, H., and J. R. Fair, "Prediction of Point Efficiencies on Sieve Trays," Ind. Eng. Chem. Proc. Des. Dev. **23**, 814-819, (1984).

Chen, G. X., and K. T. Chuang, "Predicting Point Efficiencies for Sieve Trays in Distillation," Ind. Eng. Chem. Res. **32**, 701-708, (1993).

Chen, Guang X., A. Afacan and K. T. Chuang, "Effects of Surface Tension on Tray Point Efficiencies," Can J Chem Eng, **72**, 614-621, (1994)

Chesters, A.K., "The Modeling of Coalescence Processes in Fluid-Liquid Dispersions: A Review of Current Understanding," Trans IChemE, **19,** 259-270 (1991).

Chesters, A.K. and G. Hoffman, "Bubble Coalescence in Pure Liquids," Appl. Sci. Res. **38**, 353-361, (1982).

Colwell, C. J., "Clear Liquid Height and Froth Density on Sieve Trays," Ind. Eng. Chem. Proc. Des. Dev. **20** (2), 298-307, (1979).

Ellis, S. R. M. and M. W. Biddulph, "The Effect of Surface Tension Characteristics on Plate Efficiencies," Trans. Inst. Chem. Engrs. **45**, T223-T228, (1967).

Fair, J. R., H. R. Null and W. L. Boles, "Scale-Up of Plate Efficiency from Laboratory Oldershaw Data," Ind. Eng. Chem. Proc. Des. Dev. **22**, 53-58, (1983)

Fane, A. G. and H. Sawistowski, "Surface Tension Effects in Sieve-Plate Distillation," Chem. Eng. Sci. **23**, 943-945, (1968).

Hart, D. J. and G. G. Haselden, "Influence of Mixture Compositions on Distillation-Plate Efficiency," Int. Chem. Engrs. Symp. Series **32**, 1:19-1:28, (1969).

Higbie, R., "The Rate of Absorption of a Pure Gas into a Still Liquid During Short Periods of Exposure," Trans. Am. Inst. Chem. Engrs. **31**, 365-388, (1935).

Hovestreydt, J., "The Influence of the Surface Tension Difference on the Boiling of Mixtures," Chem. Eng. Sci. **18**, 631-639, (1963).

Jamialahmadi, M. and H. Muller-Steinhagen, "Effect of Alcohol, Organic Acid and Potassium Chloride Concentration on Bubble Size, Bubble Rise Velocity and Gas Hold-up in Bubble Columns," Chem Engng J. **50**, 47-56, (1992).

Kirkpatrick, R. D. and M. J. Lockett, "The Influence of Approach Velocity on Bubble Coalescence," Chem Engng Sci. **29**, 2363-2373, (1974).

Lewis, W. K. Jr., "Rectification of Binary Mixtures," Ind. Eng. Chem., **28** (1), 399-413, (1936).

Lockett, M. J., R. D. Kirkpatrick and M. S. Uddin, "Froth Regime Point Efficiency for Gas-Film Controlled Mass Transfer on a Two-Dimensional Sieve Tray," Trans. IChemE **57**, 25-34, (1979).

Lowry, R. P. and M. van Winkle, "Foaming and Frothing Related to System Physical Properties in a Small Perforated Plate Distillation Column," AIChE J. **15**(5), 665-670, (1969).

Marangoni, C. "Spreading of Droplets of a Liquid on the Surface of Another," Ann. Phys. Lpz. **143** (7), 337-350, (1871).

Mehta, V. D. and M. M. Sharma, "Effect of Diffusivity on Gas-Side Mass Transfer Coefficient," Chem. Eng. Sci. **21**, 361-365, (1966).

Meissner, H. P. and A. S. Michaels, "Surface Tensions of Pure Liquids and Liquid Mixtures," Ind. Eng. Chem. **41**(12), 2782-2787, (1949).

Murphree, E. V., "Rectifying Column Calculations with Particular Reference to N-Component Mixtures," Ind. Eng. Chem. Res. **17**(7), 747-757, (1925).

Oldershaw, C. F., "Perforated Plate Columns for Analytical Batch Distillations," Ind. Eng. Chem. **13**, 265-269, (1941).

Ross, S., "Mechanism of Foam Stabilization and Antifoaming Action," Chem Engng Prog. **63** (9), 41-47, (1967).

Ruckenstein, E., and O. Smigelschi, "The Thermal Theory and Plate Efficiency," Can J Chem Eng **45**, 334-340, (1967).

Stichlmair, J. "Die Grundlagen des Ga-Flussig-Kontaktapparates Bodenkolonne", Verlag Chemie: Weinheim, 1978.

van Wijk, W. R., and H. A. C. Thijssen, "Concentration and Plate Efficiency in Distillation Columns," Chem. Eng. Sci. **3**, 153-160, (1954).

Vazquez, Gonzalo, Estrella Alverez, and Jose M. Navaza, "Surface Tension of Alcohol+Water from 20 and 50° C," J. Chem. Eng. Data **40**, 611-614, (1995).

Yang, Yu Min, "Dynamic Surface Effect on Boiling of Aqueous Surfactant Solutions," Int. Comm. Heat Mass Transfer, **17**, 711-727, (1990).

Yang, Yu Min and Jer Ru Maa, "Dynamic Surface Effect on the Boiling of Mixtures," Chem Eng. Commun., **25**, 47-62, (1984)

Zuiderweg, F. and A. Harmens, "The Influence of Surface Phenomena on the Performance of Distillation Columns," Chem Eng Sci, **9**, 89-108, (1958).

Zuiderweg, F., J. "Sieve Trays: A View on the State of the Art," Chem Eng Sci, **37**, 1441-1464, (1982)

Zuiderweg, F. J., "Marangoni Effect in Distillation of Alcohol-water Mixtures," Chem. Eng. Res. Des. **61**, 388-390, (1983).

CHAPTER 4

FROTH STRUCTURE ON INDUSTRIAL SIEVE TRAYS: A LITERATURE REVIEW

4.1 INTRODUCTION

The froth structure described in chapters 2 and 3 consists of bubbles closely packed in liquid continuous phase (Figures 2.7 (a), (b) and (c)). The low gas flow rate and geometry of laboratory trays, studied in these chapters, give rise to a flow field favourable for bubble coalescence. Thus gas hold-up and bubble size distribution in the froth of such trays are mainly governed by coalescence process. The froth structure on large-scale industrial trays, however, may vary from what was observed on small trays. To understand the mass transfer phenomenon in large scale industrial operation, the knowledge of froth structure on large trays is important.

The dispersion structure on a sieve tray is directly related to the flow regime. Numerous studies on flow regime have been done to understand the hydrodynamic behaviour of an operating sieve tray. Most of these studies are mainly focussed on the transition of froth regime to spray regime. Nevertheless, the definition of froth itself is very vague in the literature. In the froth regime, the presence of pulsating jets, bubbles, liquid splashes and droplets give rise to a highly complex dispersion structure. The traditional approach of defining froth as

a mixture of uniform bubbles in a continuous liquid phase undermines the real situation and can lead to major error in estimation of the effective interfacial area. This situation was elaborated by Lockett and Plaka (1983). They showed that the small bubbles stay longer in the froth and contribute only marginally to the overall concentration change in the gas phase. As a result the effective interfacial area is much lower than the total available interfacial area.

Froth is usually defined as a liquid continuous phase through which the gas passes as jets and bubbles. Previous studies by Ashley and Haselden (1972) and Calderbank and Rennie (1962) reported the presence of continuous gas jets along with the gas bubbles in the froth regime. Lockett et al. (1979) studied froth structure in a two-dimensional sieve tray. They observed pulsating jets issued from the holes and a range of bubble size within the bulk of the froth. A comprehensive study by Raper et al. (1982) with electronic probe and gamma-ray density-meter showed that bubbles and jets coexist in froth regime. A wide range of bubble size was observed and some of the jets formed at the orifice were found to break the surface of the froth and thus bypasses the bubbles. Zuiderweg (1982) defined froth regime as a transition region between spray and emulsion/bubbling regime where jetting action generates both bubbles and droplets in the two-phase mixture.

Although majority of the industrial trays are reported to operate in the spray regime (Fell and Pinczewski, 1977), froth regime operation has distinct advantages in high-pressure distillation where liquid rates are high (Lockett et al, 1979). In this chapter, an attempt has been made to understand the complex dispersion structure that exists in froth regime. In the following sections, we will explore the existing literature dealing with experimental and theoretical studies of different components of the froth, i.e., bubble size distribution, bubble rise velocity, jetting etc. To keep the study simple, neutral system has been considered first where surface tension gradient is absent. Later, the effect of surface tension gradient on froth structure has been discussed.

4.2 CHARACTERISTICS OF FROTH

In order to characterize the froth, information is required on the following parameters:

- Bubble size distribution
- Bubble rise velocity
- Fraction of gas bypassing the froth bubbles as gas jets
- Size of the jets and the liquid droplets projected upwards by the jets

4.2.1 Bubble size distribution

The fundamental understanding of the hydrodynamics and the rate process that governs bubble size distribution in a gas/liquid contactor is required to develop a

theoretical expression to estimate the bubble size distribution. Bubble size in any process depends on a balance of coalescence and break-up rates within the system. For break-up to occur the available intertial force due to kinetic energy of the turbulent flow needs to overcome the surface tension. A bubble would break-up if the ratio of the inertial and surface tension forces exceed a critical value (Hinze, 1955). The ratio can be presented in the form of Weber number,

$$We = \frac{\rho_L \overline{u}^2 d}{\sigma} \tag{4.1}$$

and the critical Weber number is given by,

$$We_{cr} = \frac{\rho_L \overline{u}^2 d_{\max}}{\sigma} \tag{4.2}$$

where d_{max} is the maximum bubble diameter that is stable against break-up by turbulence and $\overline{u}^2$ is the mean square velocity variation over a distance equal to d_{max},

$$\overline{u}^2 = 2(\omega d_{\max})^{2/3} \tag{4.3}$$

Here ω is the rate of energy dissipation per unit mass. Ideally the value of We_{cr} is close to unity (Hinze, 1955; Sevik and Park, 1973). However, depending on how ω is estimated, We_{cr} can be different from unity. In many cases the estimated ω gives the average energy dissipation of the system rather than the energy dissipated by the turbulent field. The We_{cr} obtained by using such expression of ω can be larger than unity (Lewis and Davidson, 1982).

The rate of bubble coalescence, on the other hand, may accelerate or slow down by the turbulent flow field. The frequency of bubble coalescence is dependent upon the frequency of collision and the fraction of collision that results in coalescence. Lee et al. (1987) proposed theoretical models for the rate processes of both bubble break-up and coalescence. Their study suggests that bubble coalescence is almost absent in distillation since the approach velocities of the bubbles are high in the dispersion. This finding is in agreement with the experiments conducted by Kirkpatrick and Lockett (1974). In industrial distillation trays, Weber number in the froth regime is high enough to consider the break-up to be the main process that governs the bubble size distribution. The study of Calderbank and Moo Young (1960) supports the turbulent break up of bubbles in froth. Two recent tray efficiency models by Chen and Chuang (1992) and Garcia and Fair (2000) used turbulent break-up theory to estimate the bubble size distribution in froth.

Most of the experimentally reported bubble size distribution data are for air/water systems measured by photographic technique (Hofer, 1983; Ashely and Haselden, 1972; Kaltenbacher, 1982: Lockett et al, 1979). These studies suggest bimodal distribution of bubble sizes in the froth regime. The bimodal distribution of bubble size emphasizes on the existence of either an incomplete process or two simultaneous processes within the froth. Considering break-up to be the only process that determines bubble size in froth, an incomplete break-up of formation

bubbles into secondary bubbles would give rise to this bimodal distribution, where large bubbles represent the formation bubbles and small bubbles represent the secondary bubbles.

To characterize the froth, bubble size of both types needs to be estimated. As bulk of the froth contains both formation and secondary bubbles, any information on formation bubbles must be obtained at the formation zone. The only comprehensive study of this type is done by Prado and Fair (1987). The authors used small-wired probes to measure bubble size distribution just above the sieve tray holes. They observed a considerable amount of gas jetting and large gas bubbling at the formation zone with a negligible amount of small bubbles. The Sauter mean diameter of the large bubbles was found to vary with the changing gas hole velocity and different hole diameters and was correlated with the following equation:

$$d_{32L} = 0.887 D_H^{0.846} u_H^{0.21} \tag{4.4}$$

Turbulent theory of bubble break-up is generally used to estimate the size of secondary bubble. Most of the models used to predict bubble size in turbulent flow are based on the work of Kolmogoroff (1949) and Hinze (1955). Chen and Chuang (1992) proposed the following equation to predict the maximum stable bubble diameter in sieve tray dispersion,

$$d_{\max} \propto \frac{\sigma^{0.6}\mu_L^{0.1}}{\left(\rho_L^2\rho_G\right)^{0.2}\left(u_s g\right)^{0.4}} \tag{4.5}$$

The Sauter mean diameter of the secondary bubble is proportional to the maximum stable bubble diameter, i.e.

$$d_{32S} \propto d_{\max} = C_1 d_{\max} = C_1 \frac{\sigma^{0.6}\mu_L^{0.1}}{\left(\rho_L^2\rho_G\right)^{0.2}\left(u_s g\right)^{0.4}} \tag{4.6}$$

The proportional constant C_1 needs to be determined experimentally. Measured data are available only for air/water system. Garcia and Fair (2000) used a value of 3.34 for C_1 for air/water system. Further experimental study of bubble size in different systems is required for a more universal value of the constant C_1.

The maximum stable bubble size mentioned above is only achieved if the bubble remains in the turbulent flow field for a sufficient period of time. The bubble residence time in distillation is often inadequate to complete the break-up of all formation bubbles. Thus both formation and secondary bubbles, as mentioned earlier, coexist in the froth. The fraction of secondary i.e. small bubbles, *FSB*, is yet another unknown factor that needs to be estimated to quantify the froth structure. Kaltenbacher (1982) observed bimodal bubble size distribution on small hole diameter sieve trays and reported values of fraction of small bubbles ranging from 0.2 to 0.4 for 1.5 mm holes and 0 to 0.2 for the 2.5 mm hole diameter trays. Lockett el al. (1979) estimated a value around 0.45 from photographic image of a rectangular sieve tray. However, no study is done on systematic measurement of

fraction of small bubbles in froth. Prado and Fair (1990) found that a value of 0.532 for FSB best fitted both liquid and gas phase efficiency models for air/water systems at atmospheric pressure. Garcia and Fair (2000) correlated this factor with a parameter called stability parameter ratio, which was introduced by the authors in light of turbulent break-up theory. The correlation is lacking in sound theoretical base and at the same time there is not enough experimental data available to verify its applicability.

4.2.2 Bubble rise velocity

Ashley and Haselden (1972) determined experimentally that the small bubbles rise at a velocity equal to their terminal velocity. However, it is generally considered that the small bubbles remain trapped in froth long enough to become saturated. Thus the exact residence time of small bubbles in froth is of less interest in developing tray efficiency models.

The rise velocity of large bubbles is much higher than the terminal velocity. Burgess and Calderbank (1975) measured the velocity of large bubbles in froth and found that the mean velocity of large bubbles on a sieve tray could be estimated by the following equation proposed by Nicklin (1962),

$$U_{LB} = U_{\infty} + \frac{G}{A} \tag{4.7}$$

where A is the dispersion gas flow area, G is the gas flow rate and U_{∞} is the isolated spherical cap bubble rise velocity described by Davis and Taylor (1950),

$$U_c = 25V^{1/6} \qquad (4.8)$$

4.2.3 Fraction of gas bypassing the froth bubbles as gas jets

Raper et al. (1982) did the most comprehensive study of gas bypassing in froth. Any fraction of total gas, passing through the froth and undetected by bubble probe, is considered to bypass the froth as gas jets. With higher gas load, greater proportion of gas entering the tray was found to pass through the froth as jets. Figure 4-1 gives the average value of the fraction of jetting plotted against F-factor, reported by Raper et al. (1982).

4.2.4 Size of the jets and the liquid droplets projected upwards by the jets

The jetting zone consists of orifice jets, which intermittently break the surface of the froth and project liquid splashes and drops above. There is no definitive information available in the literature regarding the size of the jets and the projected drops in the froth regime.

4.3 EFFECT OF SURFACE TENSION GRADIENT ON FROTH STRUCTURE

The froth structure described above is based on the theory and measurements related to the gas/liquid systems that do not develop surface tension gradient at the interface. Systems with surface-active solutes i.e. the surface tension positive systems develop surface tension gradient at the interface. The presence of surface tension gradient in these systems can have significant impact on different

Figure 4-1

Fraction of average gas bypass versus superficial F-factor (F_s) for sieve trays and for bubble cup and valve trays (source: Raper et al., 1982)

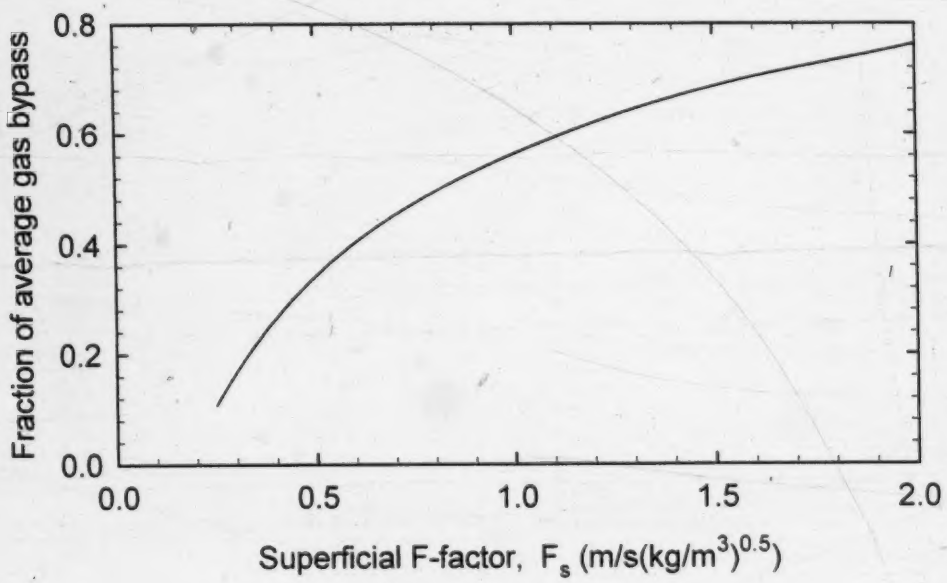

components of froth. In the following sections the effect of surface tension gradient on some of the froth components is discussed.

4.3.1 Bubble size distribution

When surface tension gradient causes foaming in surface tension positive systems the bubbles remain closely packed in the foam at low gas flow rates. At higher gas flow rate both large voids and small bubbles are formed by bubble coalescence and bubble break-up process. As the flow rate increases only break-up dominates and eventually foam breaks down into froth. Bubble diameter in foam depends on the foamability of the mixture, and on clear liquid height as well as on the initial bubble size (Darton and Sun, 1999). Steiner et al. (1977) observed that the bubble diameter is not constant along the foam height as bubble in the foam may coalesce any time independently of others of the same generation. This observation led them to adopt statistical approach to estimate bubble size in foam. The size of the secondary bubbles, formed by turbulent break-up in surface tension positive systems, is affected by the nature of the surfactants. Walter and Blanch (1985) found out that for the short-chained surfactants the maximum stable bubble size can be predicted by turbulence theory. However, for the long chained surfactants the maximum stable bubble is much larger than the prediction. The authors modified the turbulent break-up theory and included the surface tension gradient effect in the form of surface elasticity in order to estimate the maximum stable bubble size for the long chained surfactants;

$$d_{max} = \frac{1.12(E+\sigma)^{0.6}}{\omega^{0.4}\rho^{0.2}}\left[\frac{\mu_c}{\mu_G}\right]^{0.1} \tag{4.9}$$

Here E is the surface elasticity and can be described by Gibb's equation

$$E = \frac{\partial\sigma}{\partial \ln a} = -RT\frac{\partial\Gamma}{\partial \ln a} \tag{4.10}$$

where Γ is the surface excess and is a measure of the surfactant concentration at the interface.

$$\Gamma = -RT\frac{\partial\sigma}{\partial \ln C_S} \tag{4.11}$$

The main drawback of this equation, as mentioned by the authors, is lack of information about the surface elasticity.

4.3.2 Breakage of foam

Breakage of foam on a sieve tray depends on the operating conditions, surfactant type and tray geometry. It is expected that the pulsating jets formed on commercial trays at high vapour loads breaks down the foam to some extent. With the increase of gas load the foam breaks down into froth and eventually forms spray. In order to estimate the surface tension gradient effect in large-scale operation the knowledge of foamability of the liquid mixture as well as the extent to which the breakage of foam occurs at different gas flow rate is crucial.

Although the transition of froth to spray has been the subject of frequent studies, breakage of foam to froth has not drawn enough attention of the researchers. A

rather rare attempt to study this subject is made by Darton and Sun (1999). The systems they used were aqueous solutions of diethanolamine (DEA). The transition from foam to froth is marked by the break in gas hold-up versus gas flow rate curve, at $u_s > 0.3$ m/sec. Further investigation is required to get more comprehensive estimate of foam breakage at different flow condition.

4.4 CONCLUSIONS

In this study, an attempt is made to understand the froth structure on industrial trays. The existing literature is analysed in order to get the right information to characterize the froth structure. The study leads to the conclusion that the froth regime is truly a mixed regime where both bubbling and uninterrupted jetting occur simultaneously. There are a number of studies dealing with bubble size distribution in froth regime. However, no information is available on continuous gas jets mainly due to the difficulties in separating them from the bubbles in froth.

The literature dealing with surface tension gradient effect on different parameters of froth is also discussed. On commercial tray, the stabilized froth caused by surface tension gradient breaks down to some extent due to high gas load. The bubble size distribution in froth is also affected by the surface tension gradient. Further research is recommended to understand the surface tension gradient effect on the froth structure on industrial trays.

4.5 NOMENCLATURE

a	surface area, m^2
A	dispersion gas flow area, m^2
C_1	proportional constant defined by equation (4.6)
C_S	surfactant concentration in bulk, kg-mol/m^3
d	bubble diameter, m
d_{32L}	sauter mean diameter of large (formation) bubbles, m
d_{32S}	sauter mean diameter of small (secondary) bubbles, m
D_H	hole diameter, m
d_{max}	maximum stable bubble diameter in turbulent flow field, m
E	surface elasticity
FSB	fraction of small (secondary) bubbles
g	gravitational constant, 9.8 m/s^2
G	gas flow rate, m^3/s
R	Universal gas constant
T	absolute temperature, K
u_H	hole velocity, m/s
u_s	superficial gas velocity based on net area conditions, m/s
U_{LB}	rise velocity of large (formation) bubbles, m/s
U_∞	the isolated spherical cap bubble rise velocity described by the equation (4.8)
We	Weber number defined by equation (4.1)

Greek letters

μ_G shear viscosity, kg/(m-s)

μ_L liquid viscosity

ρ_G gas density, kg/m^3

ρ_L liquid density, kg/m^3

σ surface tension, N/m

ω local energy dissipation rate per unit mass, $\omega = u_s g$, W/kg

Γ surface excess, $kg\text{-}mol/m^3$

4.5 LITERATURE CITED

Ashley, M.J., and G. G. Haselden, "Effectiveness of Vapor-Liquid Contacting on a Sieve Plate," Trans. Inst. Chem. Eng. **50,** 119-124, (1972).

Burgess, J. M. and P.H. Calderbank, "The Measurement of Bubble Parameters in Two-Phase Dispersion-II," Chem. Eng. Sci. **30**, 1107-1121, (1975).

Calderbank, P. H. and J. Rennie, "The Physical Properties of Foams and Froths Formed on Sieve Plates," Trans. Inst. Chem. Engrs **40**, 3-12, (1962).

Calderbank, P. H. and M. B. Moo-Young, "The Mass transfer Efficiency of Distillation and Gas-Absorption in Plate Columns, Part II: Liquid-Phase Mass

Transfer Coefficients in Sieve-Plate Columns," International Symposium on Distillation, Inst. Chem. Engrs, 61-72, (1960).

Chen, G. X. and K. T. Chuang, "Prediction of Point Efficiency for Sieve Tray in Distillation," Ind. Eng. Chem. Res. **32**(4), 701-708, (1993).

Chesters, A. K., "The Modelling of Coalescence Processes in Fluid-Liquid Dispersions: A Review of Current Understanding," Trans IChemE **69**, 259-270, (1991).

Darton, R.C. and K. H. Sun, "The effect of Surfactant on Foam and Froth Properties," Trans IChemE, **77**, 535-542, (1999).

Davies, R. M. and G. I. Taylor, "The Mechanics of Large Bubbles Rising through Extended Liquids and through Liquids in Tubes," Proc. Roy. Soc. **A200**, 375-390, (1950).

Fell, C. J. D., and W. V. Pinczewski, "New Considerations in the Design and Operation of High-Capacity Sieve Trays," The Chemical Engineers, 45-49, (1977).

Garcia, J. Antonio and James, R. Fair, "A fundamental Model for the Prediction of Distillation Sieve Tray Efficiency. 2. Model Development and Validation," Ind. Eng. Chem. Res. **39**, 1818-1825, (2000).

Hinze, J. O., "Fundamentals of the Hydrodynamics Mechanism of Splitting in Dispersion Processes," AIChE J **1**(3), 289-295, (1955).

Hófer, H., "Influence of Gas-Phase Dispersion on Plate Column Efficiency," Ger. Chem. Eng. **6,** 113-118, (1983).

Kaltenbacher, E., "On the Effect of the Bubble Size Distribution and the Gas-Phase Diffusion on the Selectivity of Sieve Trays," Chem. Eng. Fund. **1**(1), 47-68, (1982).

Kirkpatrick, R. D. and Lockett, M. J., "The Influence of Approach velocity on Bubble Coalescence," Chem. Eng. Sci. **29**, 2363-2373, (1974).

Kolmogoroff, A. N., "On the Breaking of Drops in Turbulent Flow," Doklady Akad. Nauk. SSSR, **66**, 825-828, (1949).

Lee, Chung-Hur, L. E. Erickson and L. A. Glasgow, "Bubble Break-up and Coalescence in Turbulent Gas-Liquid Dispersions," Chem. Eng. Comm. **59**, 65-84, (1987).

Lewis, D. A. and J. F. Davidson, "Bubble Splitting in Shear Flow," Trans I Chem Eng., **60**, 283-291, (1982)

Lockett, M. J., "Distillation Tray Fundamentals," Cambridge University Press (1986).

Lockett, M. J., R. D. Kirkpatrick and M. S. Uddin, "Froth Regime Point Efficiency for Gas-Film Controlled Mass Transfer on a Two-Dimensional Sieve Tray," Trans IChemE, **57**, 25-34, (1979).

Lockett, M. J. and T. Plàka, "Effect on Non-Uniform Bubbles in the Froth on the Correlation and Prediction of Point Efficiencies," Chem. Eng. Res. Des. **61**, 119-124, (1983).

Nicklin, D. J., "Two-Phase Bubble Flow," Chem. Eng. Sci. **17**, 693-702, (1962).

Pinczewski, W. V. and C. J. D. Fell, "Droplet Sizes on Sieve Plates Operating in the Spray Regime," Trans. Inst. Chem. Engrs. **55**, 46, (1977).

Prado, Miguel, Kim L. Johnson, and James R. Fair, "Bubble-to-Spray Transition on Sieve Trays," Chem. Eng. Prog. **83**(3), 32-40, (1987).

Raper, J. A., M. S. Kearney, J. M. Burgess and C. J. D. Fell, "The Structure of Industrial Sieve Tray Froths," Chem, Eng. Sci. **37**(4), 501-506, (1982).

Sevik, M. and S. H. Park, "The Splitting of Drops and Bubbles by Turbulent Fluid Flow," J Fluids Eng 53-60, (1973).

Steiner, L., R. Hunkeler and S. Hartland, "Behaviour of Dynamic Cellular Foams," Trans IChemE **55**, 153-163, (1977).

Walter, James, and Harvey W. Blanch, "Bubble Break-up in Gas-Liquid Bioreactor: Break-up in Turbulent Flows," Chem. Eng. J. **32,** B7-B17, (1986).

Zuiderweg, F. J., "Sieve Trays: A View on the State of the Art," Chem. Eng. Sci. **37**(10), 1441-1464, (1982).

Zuiderweg, F. J., "Marangoni Effect in Distillation of Alcohol-water Mixtures," Chem. Eng. Res. Des., **61**, 388-390, (1983).

CHAPTER 5

A FUNDAMENTAL MODEL FOR PREDICTION OF SIEVE TRAY EFFICIENCY

5.1 INTRODUCTION

Mass transfer efficiency in distillation is associated with the fluid dynamics on a sieve tray that determines the dispersion structure or the contact area between the gas and liquid phases. Dispersion structures on sieve trays may vary depending on the flow regimes. For example, in spray regime, where the gas/liquid ratio is high, a gas continuous dispersion occurs. On the other hand, in froth regime, where the gas/liquid ratio is low, a liquid continuous dispersion prevails. The mechanism of the froth to spray transition has been the topic of research since the early seventies. The traditionally perceived picture of the froth regime consists of bubbles in a liquid continuous phase and that of the spray regime consists of droplets in a gas continuous phase. These definitions of froth and spray regime suggest a sudden change in the nature of two-phase mixture in the transition zone and ask for two separate expressions of interfacial area to predict the tray efficiency in these two regimes. Zuiderweg (1982) and Stichlmair (1978) developed their tray efficiency models based on this approach.

The FRI efficiency data of commercial sieve trays, on the other hand, show smooth transition of tray efficiency from the weeping to flooding point. This

compelled many researchers to resort to a single efficiency model for both froth and spray regimes. Most of the existing tray efficiency models (AIChE, 1958; Chan and fair, 1984; Chen and Chuang, 1993) are of this type.

None of these above-mentioned models took into account the structure of the two-phase mixture that is generated on the tray in different regimes. The single major attempt that considers the dispersion structure in the froth regime was made by Prado and Fair (1990) for air/water system. Later Garcia and Fair (2000) extended this model to other systems. Their model was shown to agree with a wide range of data favourably. However, too many adjustable parameters introduced at different stages of the model emphasize on its mechanistic nature.

The literature describing the froth structure on a sieve tray has been explored in chapter 4. In this chapter, the froth is modelled based on the analysis of froth images taken in a 0.153 m diameter distillation column. The model describes the froth as a combination of bubbles and continuous jets. At higher gas load, the jetting fraction dominates and gives rise to the spray regime. This froth model is further adopted to develop a fundamental model for predicting sieve tray efficiency. The efficiency model takes into account the contribution of both bubbles and jets to the net mass transfer. The model, however, does not consider the effect of surface tension gradient on froth structure and is limited to the surface tension neutral systems.

5.2 MODEL STRUCTURE

Froth images taken in a 0.153 m diameter distillation column are shown in Figures 5-1 and 5-2. Based on a careful study of these kind of froth images froth structure has been schematically presented in Figure 5-3, where froth is shown as a combination of jets, bubbles and liquid splashes. The images show that the liquid droplets and splashes constitute a major part of the froth. Part of the droplets is formed when bubbles break out of the surface of the froth. However, the presence of liquid splashes confirms that some of the gas jets manage to penetrate through the froth without forming bubbles and generates liquid splashes at the end of liquid continuous zone. Figure 5-4 shows the detail of the froth model; divided into jetting and bubbling zones. The jetting zone elaborates how some of the gas jets, formed at the sieve tray holes, cross the froth uninterrupted and throw liquid splashes above by tearing down the liquid surface. The bubbling zone shows the process of large and small bubbles formation in the froth. Both zones remain intimately mixed with each other in real froth. At relatively low liquid flow rate, no jetting can be achieved. This regime is called bubbling regime, which occurs close to the weeping limit and is of limited significance for commercial sieve tray operation. As the gas load is increased, an increasingly greater proportion of gas passes the dispersion in the form of jets. When all gas jets, formed at the orifice, reach the liquid surface uninterrupted and project the liquid up to form small drops the spray regime occurs. Unlike in froth regime, where bubbles form a

Figure 5-1

Froth image of pure methanol on a sieve tray in a 0.153 m distillation column

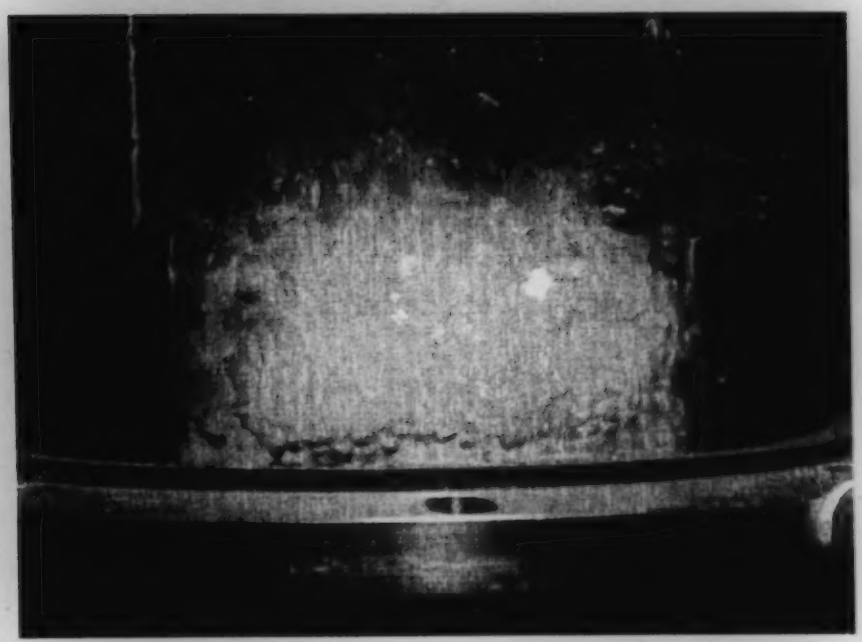

Figure 5-2

Froth image of 67wt% methanol/water mixture on a sieve tray in a 0.153 m distillation column

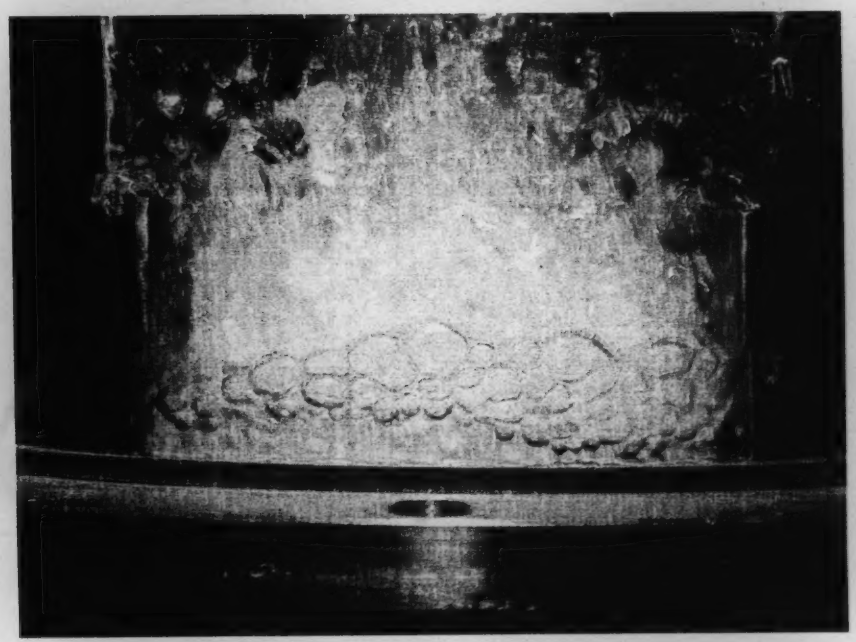

Figure 5-3

Schematic representation of froth on an operating sieve tray

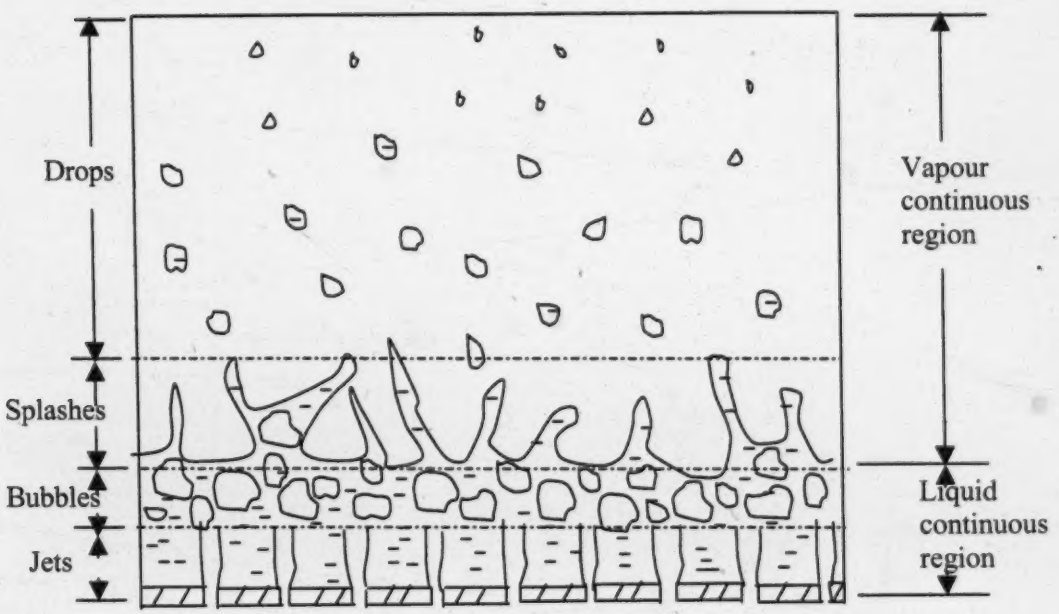

Figure 5-4

Forth structure model on an operating sieve tray

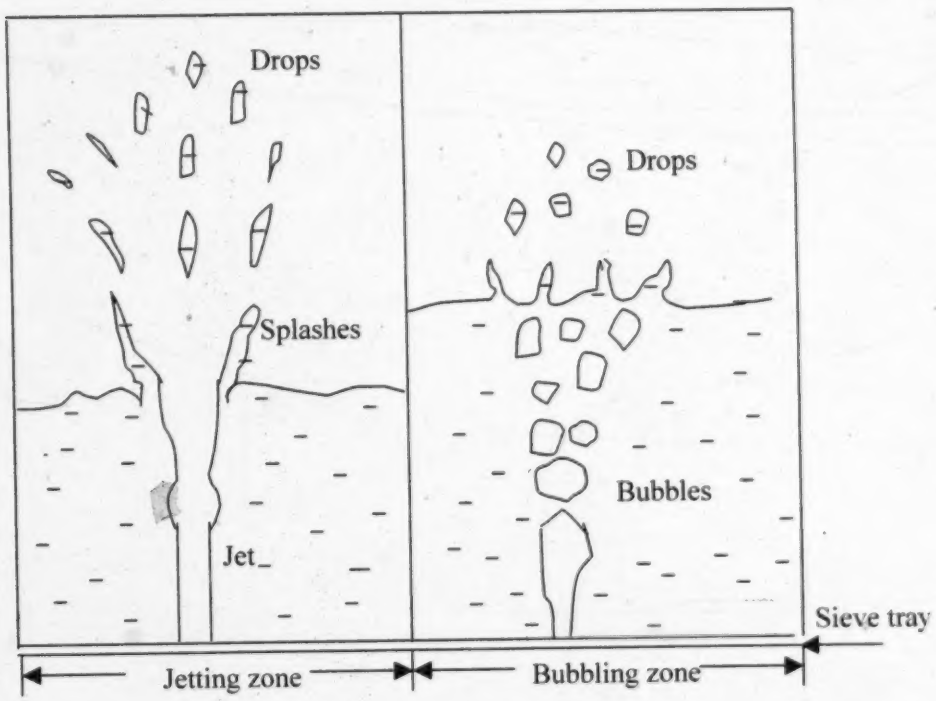

major part of the interfacial area, in spray regime drops are the only contributor to the interfacial area.

The point efficiency in froth regime is estimated by combining the contributions from both bubbling and jetting zones that exist on a tray.

$$E_{OG} = (1 - f_j)E_B + f_j E_j \tag{5.1}$$

where f_j is the volume fraction of the gas that bypasses the bubbles as continuous jets, E_B and E_j are contributions of bubbling and jetting zone, respectively, to the net point efficiency. Due to incomplete break up of the large (formation) bubbles both large (formation) and small (secondary) bubbles coexist in bubbling zone. Thus E_B has contributions from both large and small bubbles,

$$E_B = (1 - FSB)E_{LB} + FSB * E_{SB} \tag{5.2}$$

where FSB is the fraction of small bubbles.

5.3 THEORY OF MASS TRANSFER

Following expressions can be obtained from two-film theory,

$$N_G = a' k_G t_G \tag{5.3}$$

$$N_L = a * k_L t_L \tag{5.4}$$

where,

$$a * t_L = \frac{\rho_L G_f}{\rho_G L_f} a' t_G \tag{5.5}$$

Here a' and a^* are the geometrical interfacial area per unit volume of gas and liquid, respectively. Assuming that the liquid composition does not change vertically and vapour passes as plug flow without mixing, the overall mass transfer unit can be related to point efficiency as follows,

$$E_{OG} = 1 - \exp(-N_{OG}) \tag{5.6}$$

In the present study, E_{OG} is obtained from the measured Murphree efficiency, E_{mv}, as outlined by Garcia and Fair (2000).

5.4 MODEL DEVELOPMENT

In the following sections a method to estimate point efficiency E_{OG} from equations (5.1) and (5.2) has been discussed. The steps to estimate E_{SB}, E_{LB} and FSB in equation (5.2) are described in section 5.4.1. E_f and f_f in equation (5.1) are dealt in section 5.4.2.

5.4.1 Bubbling zone

Bubbling zone is considered to have bimodal size distribution of bubbles as reported in many studies (Porter et al., 1967; Ashley and Haselden, 1972; Lockett et al., 1979; Kaltenbacher, 1982; Hofer, 1983; Klugh and Vogelpohl, 1983). The small bubbles are the secondary bubbles formed by the turbulent break-up of formation bubbles originated from the orifice. The large bubbles are the unbroken formation bubbles that remain in the froth due to incomplete break-up.

The specific interfacial area and residence time for the large i.e. the formation bubbles in froth can be estimated from the following equations, respectively:

$$a = \frac{6}{d_{32L}} \tag{5.7}$$

$$t_{GLB} = \frac{h_f}{U_{LB}} \tag{5.8}$$

Due to complex nature of the process, analytical expressions for any design parameter is rare in distillation. The general trend is to use correlations, which are supported by reliable experimental data. The following equations are used to estimate the diameter and rise velocity of the initial bubbles formed at the orifice, respectively.

$$d_{32L} = 0.887 D_H^{0.846} u_H^{0.21} \qquad \text{(Prado and Fair, 1987)} \quad (5.9)$$

$$U_{LB} = 25 V^{1/6} + \frac{G}{A} \qquad \text{(Nicklin, 1962)} \quad (5.10)$$

Equation (5.9) was derived from the bubble size data measured by electronic probes just above the sieve tray (Prado and Fair, 1997). Thus the equation estimates the unbroken formation bubbles in froth. Three different liquid systems with nine different tray geometries were used to generate the bubble size data. This is by far the only correlation for formation bubbles on a sieve tray. Equation (5.10) was originally developed for estimating rise velocity of bubble swarms through a porous bed (Nicklin, 1962). Later Burgess and Calderbank (1975) showed that this equation adequately predicts rise velocity of large bubbles in froth on sieve trays. This is again the only study done on this topic.

The mass transfer coefficient for the liquid phase, k_{LLB}, is modelled with Higbie penetration theory (Higbie, 1935),

$$k_{LLB} = 1.13\left(\frac{D_L}{t_G}\right)^{0.5} \tag{5.11}$$

This is a well-established model used previously by numerous studies. The mass transfer coefficient for gas phase, k_{GLB}, of the large bubbles is estimated from the numerical solution presented by Zaritzky and Calvelo (1979). This solution was developed for mass transport models in distillation. It was tested against experimental data and was applied in efficiency models such as those by Prado and Fair (1990) and Garcia and Fair (2000). The solution is presented as a plot of Peclet number (Pe_G) of the gas phase versus the asymptotic Sherwood number (Sh_∞). Within the range $40 < Pe_G < 200$ the following polynomial provides an excellent fit (Prado and Fair, 1990) for the plot,

$$Sh_\infty = -11.878 + 25.879(\log Pe_G) - 5.64(\log Pe_G)^2 \tag{5.12}$$

For the range $Pe_G > 200$,

$$Sh_\infty = 17.9 \tag{5.13}$$

Froth height, h_f, is estimated from Bennett et al's (1983) correlation for effective froth height,

$$h_f = h_w + C\left(\frac{Q_L}{W\alpha_e}\right)^{0.67} \tag{5.14}$$

where,
$$\alpha_e = \exp\left[-12.55\left(u_s\left(\frac{\rho_G}{\rho_L - \rho_G}\right)^{0.5}\right)^{0.91}\right] \quad (5.14a)$$

and
$$C = 0.5 + 0.438\exp(-137.8h_w) \quad (5.14b)$$

There are a number of correlations available in literature to estimate the froth height on a sieve tray. The unique characteristic of equation (5.14), proposed by Bennett et al. (1983), is that unlike any other correlations it gives effective froth height i.e. the height of the liquid continuous region. Since in the present model, froth height is used to estimate the residence time of bubbles in froth, the height of liquid continuous region calculated by equation (5.14) gives the right estimation. Other correlations, which give total froth height i.e. the combined height of liquid and vapour continuous region, would over estimate the residence time of bubbles as they include the vapour continuous region of the froth where bubbles cannot survive.

Using the above information, N_{GLB} and N_{LLB} can be calculated from equations (5.3) and (5.4). Equation (3.4) is then used to get the overall mass transfer unit, N_{OGLB}, from which the contribution of the large bubbles, E_{LB}, to the net efficiency is obtained by using the equation (5.6).

The small bubbles in froth are considered to reach equilibrium when mass transfer rate is high (Lockett and Plaka, 1983). Kaltenbacher (1982) also suggested that the small bubbles get trapped in the froth and leave the froth practically saturated.

Considering that the equilibrium prevails between the vapour and the liquid phase of small bubbles, the efficiency of small bubbles becomes unity, i.e.,

$$E_{SB} = 1 \tag{5.15}$$

In order to estimate the contribution of small bubbles to the total efficiency, we need to determine the fraction of small bubbles, *FSB*, in froth. Due to lack of experimental data and reliable method to estimate this parameter, expression for *FSB* has been derived from turbulent break-up theory of bubbles.

In any flow field, the *FSB* is governed by the bubble breakage rate and the bubble residence time in turbulent zone. Previous theoretical studies (Valentas et al., 1966; Valentas and Amundson, 1966) dealing with drop size distribution assumed that the breakage rate of a drop is of first order with respect to the number of drops. Later Hesketh et al. (1991) used this concept for bubble break-up in pipelines. The same approach is applied here for sieve tray analysis, where a first order bubble breakage rate is assumed. The breakage rate of large bubbles in froth is given by,

$$\frac{dN}{dt} = -kN \tag{5.16}$$

Here k is the breakage rate constant and N is the number of large bubbles. Two additional assumptions are made to keep the calculation simple.

i) All large bubbles are bigger than the maximum stable bubble size and are equally susceptible to break-up.

ii) The number of large and small bubbles at any particular cross section of the froth is constant.

Let us consider that the number of large bubbles entering the froth at $t = 0$ *is* N_i. Due to turbulent break-up, N_i reduces to N_f at $t = \Delta t$. Here Δt is the residence time of large bubbles in the flow field. Therefore, by integrating equation (5.17) from N_i at $t = 0$ to N_f at $t = \Delta t$, the following expression is obtained,

$$N_f = N_i e^{-k\Delta t} \tag{5.17}$$

Let us consider that the fractions of large and small bubbles at $t = \overline{\Delta t}$ represent the average fraction of large and small bubbles in the froth. The number of unbroken large bubbles at $t = \overline{\Delta t}$ is given by,

$$\overline{N_f} = N_i e^{-k\overline{\Delta t}} \tag{5.18}$$

For binary breakage,

$$\overline{N_s} = 2\left(N_i - \overline{N_f}\right) \tag{5.19}$$

where $\overline{N_s}$ is the number of small bubbles formed at $t = \overline{\Delta t}$. Thus the volume fraction of small bubbles in froth can be estimated as follows:

$$FSB = \frac{\overline{N_s} V_s}{\overline{N_s} V_s + \overline{N_f} V_L} = \frac{2\left(N_i - \overline{N_f}\right)}{2\left(N_i - \overline{N_f}\right) + \overline{N_f} \frac{V_L}{V_s}} \tag{5.20}$$

Here V_S and V_L are the volumes of small and large bubbles respectively. Assuming spherical shape for the bubbles, we get the following expression for *FSB* from equations (5.18) and (5.20),

$$FSB = \frac{2\left(1 - e^{-k\bar{\Delta t}}\right)}{2\left(1 - e^{-k\bar{\Delta t}}\right) + \left(\frac{d_{32L}}{d_{32S}}\right)^3 e^{-k\bar{\Delta t}}} \tag{5.21}$$

The ratio of large bubble diameter to small bubble diameter, d_{32L}/d_{32S}, is obtained from the existing literature. The reported diameter ratios are summarized in Table 5.1.

Table 5.1 Reported bubble size distribution on an operating sieve tray

Source	Small bubble	Large bubble	Ratio
Hofer (1983)	5 mm	25 mm	5
Ashley & Haselden (1982)	5-10 mm	40-80 mm	8
Kaltenbacher (1967)	4 mm	25 mm	6
Porter et al. (1967)	5 mm	20 mm	4
Lockett et al. (1979)	5 mm	25 mm	5

From the above table, we find that the most probable value of the ratio d_{32L}/d_{32S} is 5.

The breakage rate constant k is a function of the turbulent flow field and the fluid physical properties. Hesketh et al. (1991) showed that the measured deformation

times and breakage time of bubbles can be characterized by the natural mode of oscillation of a sphere given by Lamb (1932) and proposed the following functionality of the rate constant k,

$$k = \left(\frac{3.8}{We_{cr}^{0.9}}\right)\frac{\rho_L^{0.1}\rho_G^{0.3}\omega^{0.6}}{\sigma^{0.4}} \tag{5.22}$$

In distillation, $\omega = u_s g$ (Kawase and Moo-Young, 1990); thus the rate constant becomes,

$$k = \left(\frac{3.8}{We_{cr}^{0.9}}\right)\frac{\rho_L^{0.1}\rho_G^{0.3}}{\sigma^{0.4}}(u_s g)^{0.6} \tag{5.23}$$

The breakage time $\overline{\Delta t}$ can be expressed as

$$\overline{\Delta t} = nt_{GLR} \qquad (0< n <1) \tag{5.24}$$

Since both n and We_{cr} are contants, we can combine them into single constant,

$$C''' = \frac{n}{We_{cr}^{0.9}} \tag{5.25}$$

By multiplying equations (5.23) and (5.24) we get,

$$k\overline{\Delta t} = C'''\left(\frac{3.8\rho_L^{0.1}\rho_G^{0.3}}{\sigma^{0.4}}\right)(u_s g)^{0.6} \tag{5.26}$$

The constant C'' will be estimated by comparing the model with the measured efficiency data.

5.4.2 Jetting Zone

In froth regime, it is difficult to investigate jetting zone separately as jets are intimately mixed with bubbles. No information is available in literature on the size of jets or droplets present in froth. In this study, we will treat the jetting zone as spray and use the correlations of spray regime to estimate the contribution of jets in froth regime. Although numerous studies have been done to determine the onset of spray, very few studies have been focussed exclusively on mass transfer efficiency in this regime. Fane et al. (1973) achieved some success in predicting efficiency in spray regime on a small tray by using free trajectory model. However, Raper et al. (1979) showed that Fane et al.'s model under predicts the tray efficiency when applied for industrial tray. Another important attempt to predict mass transfer efficiency in spray regime was made by Zuiderweg (1983). His semi-empirical model is based on the FRI experimental data. This is the only model so far that is not case sensitive and is readily applicable for spray regime. In this study, we have chosen Zuiderweg's spray regime model (equations (5.27) to (5.32)) to estimate the contribution of jetting zone to the total mass transfer efficiency in froth regime;

$$k_{Gj} = \frac{0.13}{\rho_G} - \frac{0.065}{\rho_G^2} \qquad (1<\rho_G<80\ \text{kg/m}^3) \qquad (5.27)$$

$$k_{Lj} = \frac{2.6\times10^{-5}}{\mu_L^{0.25}} \qquad (5.28)$$

$$E_j = 1 - \exp\left(-\frac{a h_f K_{OGj}}{u_s}\right) \qquad (5.29)$$

$$ah_f = \frac{40}{F^{0.3}}\left(\frac{F_{bbo}^2 h_L FP}{\sigma}\right)^{0.37} \tag{5.30}$$

Here,
$$h_L = 0.6h_w\left(\frac{p}{b}FP\right)^{0.25} \tag{5.31}$$

and at total reflux
$$FP = \left(\frac{\rho_G}{\rho_L}\right)^{.5} \tag{5.32}$$

We need to know the volume fraction of gas that bypasses the bubbles as jets, f_j, to estimate the net contribution of jetting zone. The experimentally measured data of Raper et al. (1982) are used for this purpose. Following equation gives an excellent fit for the average value of jetting fraction, f_j, as a function of F-factor, F_{bbo}. (Figure 4-1)

$$f_j = -0.1786 + 0.9857\left(1 - e^{-1.43F_{bbo}}\right) \tag{5.33}$$

5.4.3 Determining constant C"

Constant C'' is determined by comparing the model with six sets of FRI data (Sakata and Yanagi, 1979; Yanagi and Sakata, 1982). These data sets cover two hydrocarbon systems, cyclo-hexane/n-heptane and i-butane/n-butane, at five different pressures in two different tray geometries. The cyclo-hexane/n-heptane system is widely used for testing distillation tray performance. The properties of this system are representative of many hydrocarbon systems operated at 400kPa pressure or below. The data sets for this system are taken at two different pressures, 34 kPa and 165 kPa. The data sets for i-butane/n-butane cover three

different pressure levels. The measured efficiencies at high pressures (2068 kPa and 2758 kPa) have been corrected for vapour entrainment with the down flow liquid (Hoek and Zuiderweg, 1983). Figure 5-5 presents the effect of different values of constant C'' on the estimated point efficiency for the six sets of FRI data. The average absolute error was calculated by the following equation,

$$Error\% = \frac{\sum \frac{|Estimated - Experimental|}{Experimental}}{N} \tag{5.34}$$

The minimum error was obtained at C''= 0.16. This value has been adopted in the proposed model to predict the large tray point efficiency. The implication of the constant C'' = 0.16 is that for a suggested value of $\overline{\Delta t} = 0.5 t_{GLB}$ the critical Weber number We_{cr} will be 3.6.

5.5 PREDICTION OF POINT EFFICIENCY

The present model suggests a new method to estimate sieve tray efficiency based on a froth structure that describes the hydrodynamics of an operating sieve tray. The predicted point efficiencies, E_{OG}, from the proposed model are compared with the FRI data in Figures 5-6 to 5-11. In all cases, predictions from two earlier models of Chan and Fair (1984) and Chen and Chuang (1993) are also compared with the proposed model. The unique characteristics of the new model is that unlike the two other models it predicts the trend of efficiency change from weeping to flooding point more closely (Figures 5-7, 5-8 and 5-9). The steady

Figure 5-5

Effect of constant *C''* on point efficiency; expressed as average absolute error

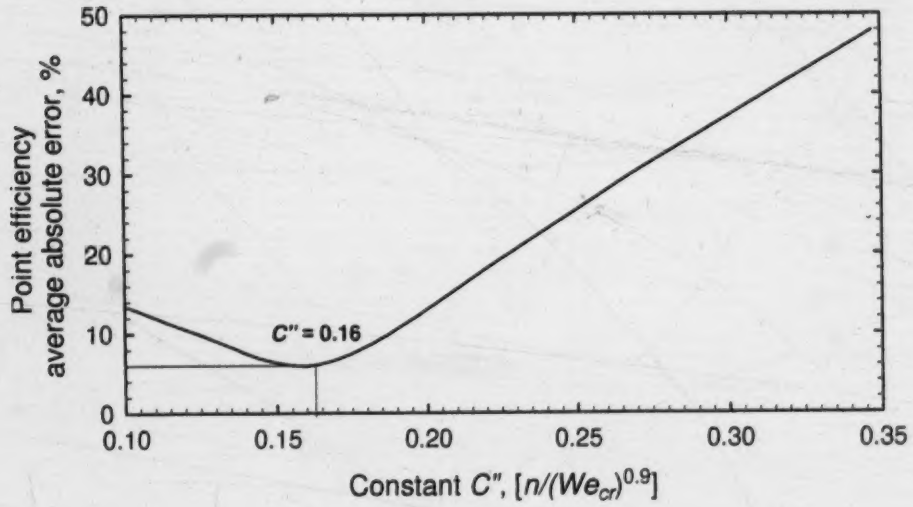

Figure 5-6

Comparison of measured and predicted point efficiencies for the cyclo-hexane/n-heptane system at 34 kPa (Open hole area 14%)

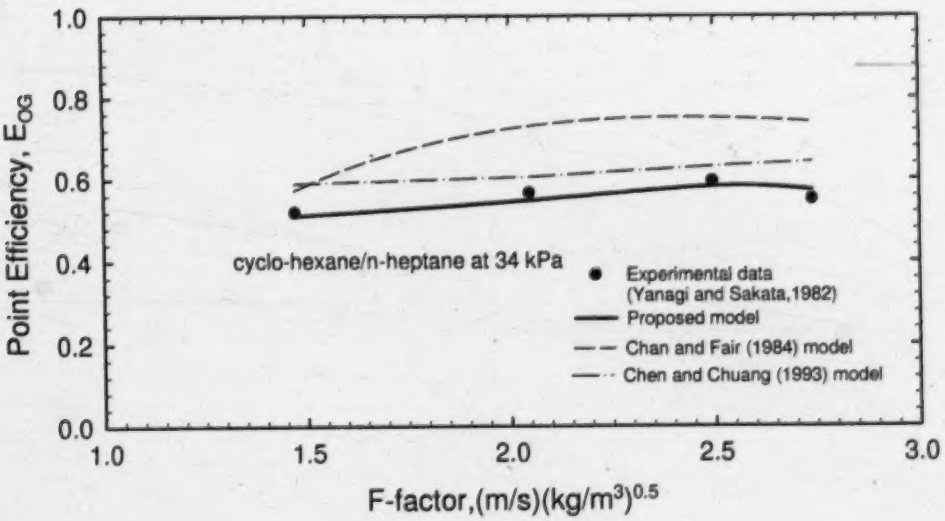

Figure 5-7

Comparison of measured and predicted point efficiencies for the cyclo-hexane/n-heptane system at 165 kPa (Open hole area 14%)

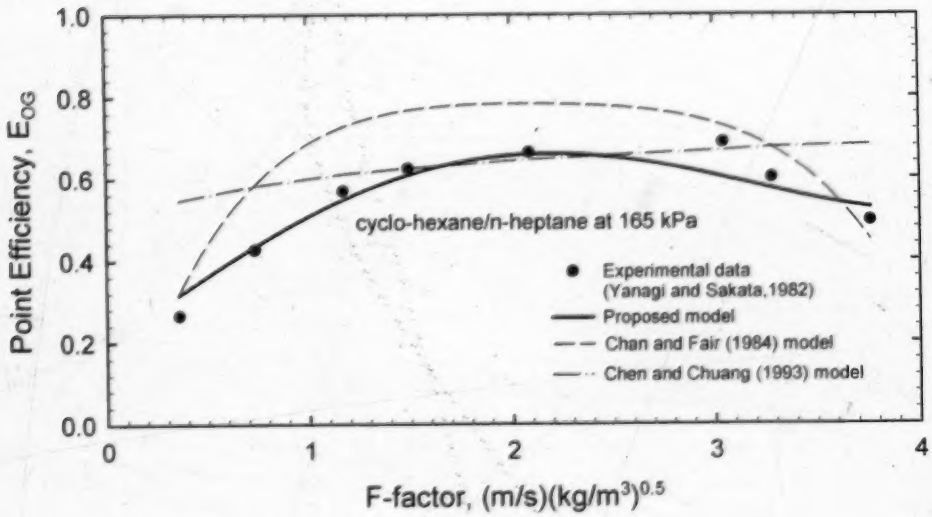

Figure 5-8

Comparison of measured and predicted point efficiencies for the iso-butane/n-butane system at 1138 kPa (Open hole area 14%)

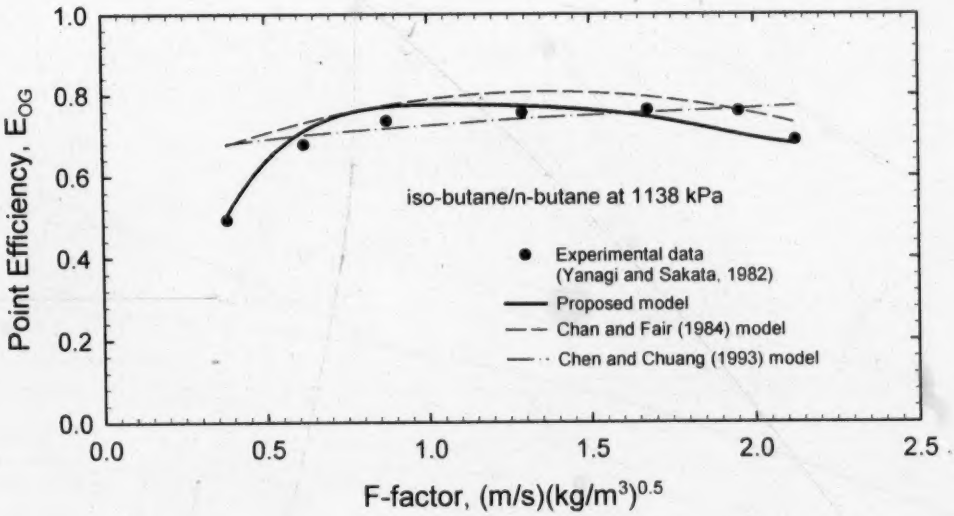

Figure 5-9

Comparison of measured and predicted point efficiencies for the iso-butane/n-butane system at 1138 kPa (Open hole area 8.3%)

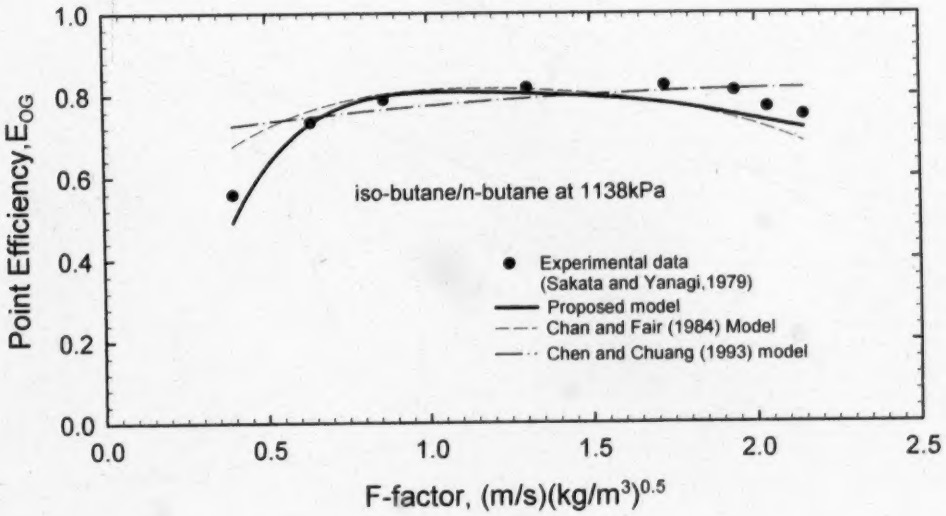

Figure 5-10

Comparison of measured and predicted point efficiencies for the iso-butane/n-butane system at 2068 kPa (Open hole area 8.3%)

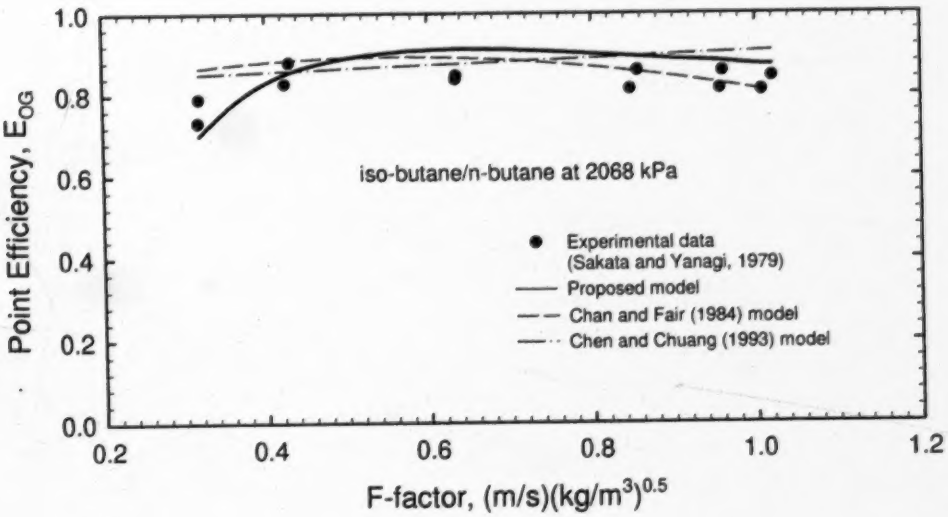

Figure 5-11

Comparison of measured and predicted point efficiencies for the iso-butane/n-butane system at 2758 kPa (Open hole area 8.3%)

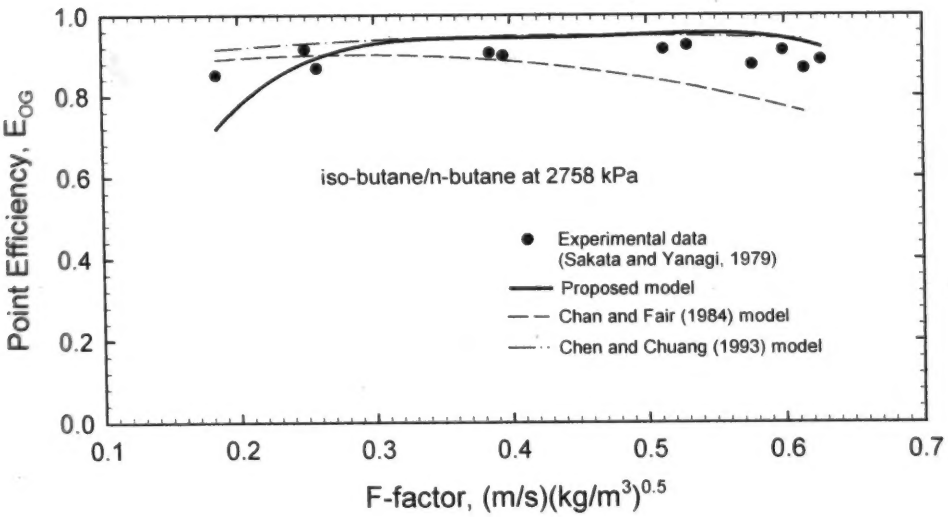

decrease in both fraction of small bubbles and bypassed jets results in gradual decrease of the point efficiency, E_{OG} as the F-factor approaches the weeping point. It also predicts the smooth transition of E_{OG} from froth to spray regime. Under high operating pressures (Figures 5-10 and 5-11), the breakage rate constant k is high enough to cause breakage of all large bubbles. This makes the fraction of small bubbles *FSB* unity and gives rise to high point efficiency under such operating condition. The fraction of bypassed gas is 0.8 at F-factor 2 (Figure 4-1). Beyond this point froth is dominated by spray and the model reduces to Zuiderweg's model for spray regime. Thus any error in predicting E_{OG} beyond F-factor 2 is inherited from Zuiderweg's model.

The prediction of Chan and Fair model is satisfactory for i-butane/n-butane system. However, it predicts higher efficiency than the measured data for cyclo-hexane/n-heptane at both pressure levels. This discrepency results from the N_G correlation of this model, which does not fit the FRI data of cyclo-hexane/n-heptane with 14% open hole area (Chan and Fair, 1984). In Chan and Fair model, N_G is a function of fractional approach of flooding u_s/u_{sf}. Here, u_{sf} is the flooding velocity, which directly depends on the tray spacing of distillation columns. This functionality of N_G is criticized by other authors as being unreasonable (Lockett, 1986) as it implies dependency of tray efficiency on tray spacing for fixed vapour and liquid loads. Another fundamental drawback of Chan and Fair model is that it gives two different expressions of interfacial area for N_G and N_L.

The prediction of Chen and Chuang model is satisfactory for all six sets of data. The interfacial area in this model is estimated from the bubble size distribution. Since the vapour/liquid dispersion in spray regime mostly consists of drops, the model is applicable only to froth regime. Although the model is shown to predict well beyond the froth regime, the results may be obtained through a wrong route.

Figure 5-12 compares the overall performance of the three models. The proposed model predicts within ±10% for all the systems and shows better performance than the two other models. The agreement between the experimental data and predictions of the new model proves the validity of the proposed approach.

5.6 DISCUSSION

Tray hydrodynamics is considered to be the key factor in determining the nature of two-phase mixture in distillation. The unique feature of the proposed model is that it is based on the analysis of tray hydrodynamics (Figures 5-1 to 5-4) that describes the real situation on a sieve tray. Here, froth is considered as a mixture of bubbles and continuous gas jets with liquid drops and splashes. The model includes both bubble and jet contribution to the total point efficiency. The bubble size distribution in froth is analyzed theoretically with the support of experimental data in literature. The often-reported bimodal distribution of bubbles in froth is explained as the result of incomplete break-up of formation bubbles in turbulent flow field. The fraction of small bubbles, *FSB*, is directly estimated by theoretical

Figure 5-12

Overall comparison of the proposed model with two other existing models

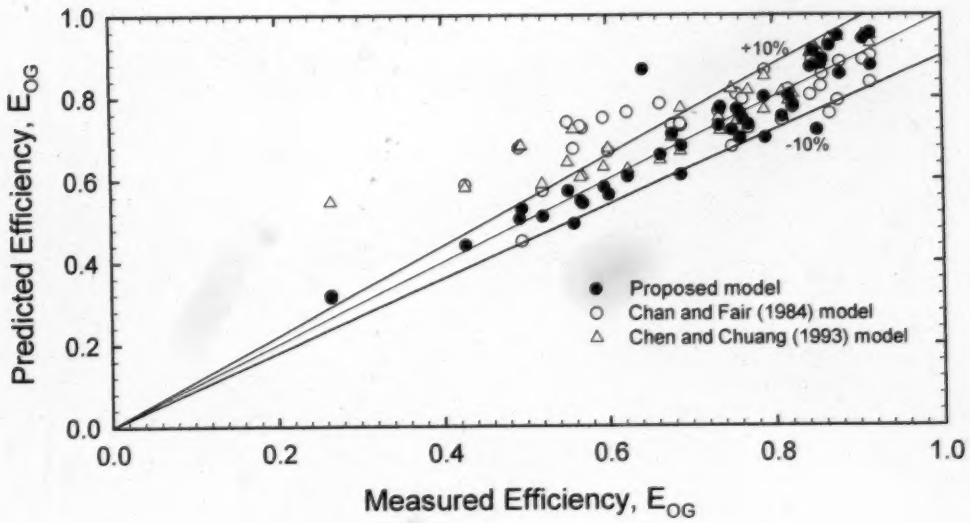

analysis of the rate of bubble breakage in froth. The single other similar effort to estimate *FSB* was done by Garcia and Fair (2000). Although their final model agreed with the database favourably, the study failed to identify the source of bimodal bubble size distribution observed in froth, which made their semi-theoretically obtained *FSB* expression rather arbitrary.

The proposed model divides the froth into two zones, namely bubbling and jetting zone. However, the calculation is much simpler than those of other similar models (Prado and Fair, 1990; Garcia and Fair, 2000). By considering the small bubbles saturated in froth, the model saves the calculation step required to estimate the contribution of small bubbles, E_{SB}, to the net efficiency, E_{OG}.

The model is developed for both froth and spray regimes. It includes f_j, the fraction of gas that forms continuous jets, as the determining factor of the regimes. For example, in froth regime $0< f_j <1$. As f_j increases with higher a gas load, transition to spray regime occurs gradually and f_j becomes unity as spray regime is reached. No drastic change in dispersion structure occurs during this transition, which justifies the smooth transition of FRI efficiency data from froth to spray regime. The approach of considering the effect of flow regimes on tray efficiency adopted in the proposed model is different from the two previous approaches of the existing models. One of the approaches is to apply the same efficiency model for both froth and spray regimes without considering the effect

of change of the dispersion structure (AIChE, 1958; Chan and fair, 1984; Chen and Chuang, 1993). The other approach is to use two completely different models for froth and spray regime (Zuiderweg, 1983). Since the dispersion structure in froth regime is just inverse to that of spray regime, using the same efficiency model for both regimes without considering the change in the dispersion structure is the incorrect way to estimate the tray efficiency. On the other hand, when two separate models are used for the two regimes difficulties arise in identifying the exact transition point. By including the fraction of jetting, the new model takes into account the difference in dispersion structure that exists between froth and spray regimes. Thus the model provides a logical solution to the dilemma of whether to use the same or separate models for both froth and spray regimes as well as explains the smooth transition between the regimes.

The effect of physical properties considered in the estimation of fraction of small bubbles *FSB* (equation 5.26) makes the model applicable to systems with wide range of physical properties. Moreover, the new model predicts well under different pressure levels, where physical properties of the same systems can vary significantly.

The model considers the jetting fraction of the dispersion as spray. Due to lack of definitive research conducted in the spray regime, this study resorts to the semi-empirical spray regime model of Zuiderweg (1983) to estimate the jetting

contribution. Thus the proposed model inherits the semi-empirical nature from Zuiderweg's model. More fundamental study of drop dynamics and point efficiency in spray regime will improve the correlation further.

Finally, although the new model covers the whole operating range of froth and spray regime, it is not applicable for extreme loads, where weeping, flooding or heavy entrainment might occur.

5.7 CONCLUSIONS

In this chapter a fundamental model to predict point efficiency has been proposed based on the hydrodynamics of an operating sieve tray. The new model predicts the FRI efficiency data of hydrocarbon systems within ±10%. It is also able to predict the trend of efficiency data from weeping to flooding point more closely than any other models. The model is based on the analysis of real froth, which makes it more fundamentally correct and more adoptable to the diversified conditions than any other existing models.

The model is equally applicable for the froth and spray regimes and should generally be applicable for the prediction of distillation tray efficiency. Further fundamental research on point efficiency in spray regime, however, would make the model more universal.

5.8 NOMENCLATURE

a	interfacial area per volume of two-phase mixture, m^2/m^3
a'	geometrical interfacial area per volume of gas, m^2/m^3
a^*	geometrical interfacial area per volume of liquid, m^2/m^3
A	dispersion gas flow area, m^2
b	weir length per unit bubbling area, m^{-1}
C	constant defined by equation (5.14b)
d_{32L}	sauter mean bubble diameter of large bubbles, m
d_{32S}	sauter mean bubble diameter of small bubbles, m
D_G	molecular diffusion coefficient for gas, m^2/s
D_H	orifice diameter, m
D_L	molecular diffusion coefficient for liquid, m^2/s
E_B	overall point efficiency for bubbling zone
E_j	overall point efficiency for jetting zone
E_{LB}	overall point efficiency for large bubbles
E_{OG}	overall point efficiency (gas composition basis)
E_{SB}	overall point efficiency for small bubbles
f_j	volume fraction of gas bypasses the froth bubbles as continuous jet
F	fraction of hole area per bubbling area
F_{bba}	vapour F-factor on bubbling area, $(kg/m^3)^{0.5}m/s$
FP	flow parameter, $\left(\frac{\rho_G}{\rho_L}\right)^{0.5}$ at total reflux

FSB	fraction of small bubbles
g	gravitational constant, 9.8 m/s^2
G	volumetric flow rate of gas, m^3/s
G_f	gas mass flow rate, kg/s
G_m	gas molar flow rate, kmol/s
h_f	froth height, m
h_L	clear liquid height, m
h_w	weir height, m
k	first order bubble breakage rate constant, s^{-1}
k_G	gas-phase mass transfer coefficient, m/s
k_{Gj}	k_G for jetting zone
k_{GLB}	k_G for large bubbles
k_L	liquid-phase mass transfer coefficient, m/s
k_{LLB}	k_L for large bubbles
k_{Lj}	k_L for jetting zone
K_{OGj}	K_{OG} for jetting zone
L_f	liquid mass flow rate, kg/s
N	the number of large bubbles
N_i	the number of large bubbles formed at the orifice at any instant
N_f	the number of unbroken large bubbles leaving the froth at any instant
$\overline{N_f}$	number of unbroken large bubbles remained from N_i at $t = \overline{\Delta t}$
N_G	number of gas-phase mass-transfer units

N_{GLB} N_G for large bubbles

N_L number of liquid-phase mass-transfer units

N_{LLB} N_L for large bubbles

N_{OG} number of overall gas-phase mass-transfer units

N_{OGLB} N_{OG} for large bubbles

$\overline{N_s}$ number of secondary bubbles formed from N_i at $t = \overline{\Delta t}$

p pitch of holes on sieve plate, m

Pe_G Peclet number, $D_B u_B / D_G$

Q_L liquid flow rate, m^3/s

Sh_∞ asymptotic Sherwood number, $k_G D_B / D_G$

t_G mean residence time of gas in dispersion, s

t_{GLB} mean residence time of large bubbles in dispersion, s

t_L mean residence time of liquid in dispersion, s

$\overline{\Delta t}$ the time when half of the total secondary bubbles are formed in froth from the initial N_i number of bubbles, s

u_H hole velocity, m/s

u_s superficial gas velocity based on net area conditions, m/s

U_{LB} rise velocity of large bubbles, m/s

W weir height, m

We_{cr} critical Weber number

Greek letters

α_e froth density defined by equation (5.18a)

μ_L liquid viscosity, Pa.s

ρ_G gas density, kg/m^3

ρ_L liquid density, kg/m^3

σ surface tension, N/m

5.9 LITERATURE CITED

AIChE Bubble Tray Design Manual; New York, 1958

Ashley, M. J., and G. G. Haselden, "Effectiveness of Vapor-Liquid Contacting on a Sieve Plate," Trans. Inst. Chem. Eng. **50**, 119-124, (1972).

Bennett, D. L., R. Agarwal and P. J. Cook, "New Pressure Drop Correlations for Sieve Tray Distillation Columns," AIChE J. **29**, 434-442, (1983).

Chan, H. and J. R. Fair, "Prediction of Point Efficiencies on Sieve Trays," Ind. Eng. Chem. Process Des. Dev. **23**, 814-819, (1984).

Chen, G. X. and K. T. Chuang, "Prediction of Point Efficiency for Sieve Tray in Distillation," Ind. Eng. Chem. Res. **32**(4), 701-708, (1993).

Fane, A. G., J. K. Lindsey and H. Sawistowski, "Operation of a Sieve Plate in the Spray Regime of Column Operation," Indian Chem. Engr. (Jan.) 45, (1977).

Garcia, J. Antonio and James, R. Fair, "A fundamental Model for the Prediction of Distillation Sieve Tray Efficiency. 1. Database Development," Ind. Eng. Chem. Res. **39**, 1809-1817, (2000).

Garcia, J. Antonio and James, R. Fair, "A fundamental Model for the Prediction of Distillation Sieve Tray Efficiency. 2. Model Development and Validation," Ind. Eng. Chem. Res. **39**, 1818-1825, (2000).

Hesketh, Robert P., Arthur W. Etchells, and T. W. Fraser Russell, "Bubble Breakage in Pipeline Flow," Chem Eng. Sci., **46**(1) 1-9, (1991).

Higbie, R., "The rate of Absorption of a Pure Gas into a Still Liquid during Short Periods of Exposure," Trans. Am. Inst. Chem. Eng. **31**, 365-388, (1935).

Hoek, P. J. and Zuiderweg, F. J., "Influence of Vapour Entrainment on Distillation Tray Efficiency at High Pressure," AIChE J., **28**(4) 535-539, (1982).

Hofer, H., "Influence of Gas-Phase Dispersion on Plate Column Efficiency," Ger. Chem. Eng. **6**, 113-118, (1983).

Kaltenbacher, E., "On the Effect of the Bubble Size Distribution and the Gas-Phase Diffusion on the Selectivity of Sieve Trays," Chem. Eng. Fund., **1**(1), 47-68, (1982).

Kawase, Y., and M. Moo-Young, "Mathematical Models for Design of Bioreactors: Applications of Kolmogoroff's Theory of Isotropic Turbulence," The Chem. Eng., **43**, B19-B36, (1990).

Klug, P. and A. Vogelpohl, "Bubble Formation with Superimposed Liquid Motion at Single-hole Plates and Sieve Plates," Ger. Chem. Eng. **6**, 311-317, (1983).

Lamb, H., "Hydrodynamics," 6th Edn. Cambridge University Press, Cambridge, (1932).

Lockett, M. J., R. D. Kirkpatrick and M. S. Uddin, "Froth Regime Point Efficiency for Gas-Film Controlled Mass Transfer on a Two-Dimensional Sieve Tray," Trans IChemE, **57**, 25-34, (1979).

Lockett, M. J. and T. Plaka, "Effect on Non-Uniform Bubbles in the Froth on the Correlation and Prediction of Point Efficiencies," Chem. Eng. Res. Des. **61**, 119-124, (1983).

Nicklin, D. J., "Two-Phase Bubble Flow," Chem. Eng. Sci. **17**, 693-702, (1962).

Porter, K. E., B. T. Davis and P. F. Y. Wong, "Mass Transfer and Bubble Sizes in Cellular Foams and Froths," Trans. Inst. Chem. Eng. **45,** T265-T273, (1967).

Prado, Miguel, Kim L. Johnson, and James R. Fair, "Bubble-to-Spray Transition on Sieve Trays," Chem. Eng. Prog. **83**(3), 32-40, (1987).

Prado, Miguel and James R. Fair, "Fundamental Model for the Prediction of Sieve Tray Efficiency," Ind. Eng. Chem. Res., **29**, 1031-1042, (1990).

Raper, J. A., N. T. Hai, W. V. Pinczewski and C. J. D. Fell, "Mass Transfer Efficiency on Sinulated Industrial Sieve Trays Operating in the Spray Regime," Inst. Chem. Engrs. Symp. Series No. 56, 2.2/57-2.2/74, (1979).

Raper, J. A., M. S. Kearney, J. M. Burgess and C. J. D. Fell, "The Structure of Industrial Sieve Tray Froths," Chem, Eng. Sci. **37**(4) 501-506, (1982).

Sakata, M. and Y. Yanagi, "Performance of a Commercial-Scale Sieve Tray," Inst. Chem. Eng. Symp. Ser. No.56, 3.2/21, (1979).

Stichlmair, J. Die Grundlagen des Ga-Flussig-Kontaktapparates Bodenkolonne; Verlag Chemie: Weinheim, (1978).

Valentas, K. J. and N. R. Amundson, "Breakage and Coalescence in Dispersed Phase Systems," Ind. Engng. Chem. Fundam 5, 533-544, (1966).

Valentas, K. J., O. Bilous and N. R. Amundson, "Analysis of Breakage in Dispersed Phase Systems," Ind. Engng. Chem. Fundam 5(2), 271-279, (1966).

Yanagi, Y. and M. Sakata, "Performance of a Commercial-Scale 14% Hole Area Sieve Tray," Ind. Eng. Chem Process Des. Dev. 21(4) 712-717, (1982).

Zaritzky N. And A. Calvelo, "Inefinal Mass Transfer Coefficient Within Single Bubbles. Theory and Experiment," Can. J. Chem. Eng. 57, 58-64, (1979).

Zuiderweg, F. J., "Sieve Trays: A View on the State of the Art," Chem. Eng. Sci. 37(10), 1441-1464, (1982).

CHAPTER 8
CONCLUSIONS

8.1 INTRODUCTION

The study has been carried out in two parts to investigate froth structure and mass transfer phenomenon on distillation sieve trays. The first part involves the investigation of surface tension gradient effect on froth structure and mass transfer efficiency of small-scale laboratory trays. A dimensionless correlation has been developed for gas hold-up on sieve trays for both pure and binary liquids using a 90 mm diameter simulator bubble column. A new point efficiency model is proposed based on this gas hold-up correlation and has been tested against efficiency data from an Oldershaw column.

The second part of the project deals with the study of froth structure and mass transfer on a large commercial tray. A new fundamental model for predicting sieve tray efficiency is developed based on a froth model proposed to characterize the froth on a commercial tray. In following sections, the achievements of the present study will be revisited briefly.

6.2 EFFECT OF SURFACE TENSION GRADIENT ON GAS HOLD-UP

A dimensionless correlation for gas hold-up in a shallow bubble column with sieve tray has been developed. The effect of surface tension gradient on froth stabilization in binary mixtures has been included successfully in the proposed correlation. For the first time, comprehensive data of gas hold-up with respect to concentration in four binary systems are presented. The often-reported enhancement of gas hold-up in aqueous alcohol mixtures has been observed experimentally. The proposed correlation is able to predict successfully the trend of gas hold-up enhancement with respect to concentration. The estimated values are found to be within ±7% of the measured values.

6.3 EFFECT OF SURFACE TENSION GRADIENT ON E_{OG} OF AN OLDERSHAW COLUMN

The effect of surface tension gradient on distillation tray efficiency has been investigated experimentally in an Oldershaw column. Six binary mixtures with wide range of physical properties are selected for this study. A point efficiency model is proposed, which takes into account the surface tension gradient effect that gives rise to froth stabilization in gas/liquid dispersions. The model satisfactorily predicts the trend and magnitude of point efficiency with respect to concentration for different systems, especially for the surface tension positive

systems where enhanced point efficiency accompanied by a sharp decline at the high concentration region is observed.

8.4 PREDICTING EFFICIENCY OF LARGE-SCALE INDUSTRIAL TRAYS

A new fundamental model for predicting the point efficiency of industrial sieve trays has been developed. The model is based on the hydrodynamics of an operating sieve tray represented by a proposed froth structure model. The froth model describes froth as a combination of bubbles and continuous jets that break the surface of the froth projecting liquid splashes and drops above. The efficiency model is developed for both froth and spray regimes. Fraction of by-passed or uninterrupted gas jet is considered as the determining factor for froth to spray transition. Turbulent break-up theory is used to estimate bubble size distribution in froth. The net efficiency is estimated by adding up the contributions of both bubbles and jets present in the dispersion. The model is tested against the efficiency data of *cyclo-hexane/n-heptane* and *i-butane/n-butane* mixtures published by Fractionation Research Inc. (FRI). The predicted efficiency is in good agreement with the experimental value and proves the validity of the new approach.

6.5 CONCLUSIONS

One gas hold-up correlation, and two efficiency models have been proposed in this study. The gas hold-up correlation successfully included surface tension gradient effect on froth stabilization. This correlation is the first attempt ever to predict the gas hold-up of binary mixtures with respect to concentration. The first efficiency model developed for small-scale distillation column is another pioneering work to include surface tension gradient effect in tray efficiency correlation.

The study of large-scale commercial tray performance leads to the development of a froth model and a point efficiency model. The froth model defines and characterizes the froth conclusively and explains the smooth transition between froth and spray regimes. The point efficiency model presents a fundamental method to estimate point efficiency of sieve trays in both froth and spray regimes. The most important contribution of this model is to provide logical solution to the dilemma of whether to use the same or separate efficiency models for both froth and spray regimes.

6.6 RECOMMENDATIONS FOR FUTURE WORK

The tray efficiency model developed in chapter 5 for industrial trays includes a semi-empirical spray regime model to estimate the contribution of gas jets in

gas/liquid dispersion. Further fundamental research to predict tray efficiency in spray regime will make the model more universal.

Studies of bubble size distribution in froth on sieve trays for systems other than air/water would provide better understanding of mass transfer phenomena in froth regime.

Publication of tray efficiency data in large diameter columns for different systems is needed to assess the range of applicability of the existing tray efficiency models.

APPENDIX A

OPERATING CONDITIONS AND EXPERIMENTAL RESULTS

A1. GAS HOLD-UP DATA IN AIR/LIQUID COLUMN (CHAPTER 2)

Column diameter: 90 mm

Hole diameter of the sieve tray: 3 mm

Air flow rate: 0.32 m/s

Clear liquid height: 11 mm

Table A1.1 Gas hold-up data for methanol/water and 2-propanol/water systems

Methanol/water		Methanol/2-propanol	
Mole fraction of methanol	**Gas hold-up**	**Mole fraction of 2-propanol**	**Gas hold-up**
0.0	0.63	0.0	0.63
0.06	0.79	0.05	0.89
0.2	0.83	0.15	0.78
0.37	0.81	0.3	0.75
0.6	0.78	0.5	0.73
0.8	0.76	0.68	0.74
0.9	0.745	0.8	0.73
1.0	0.74	1.0	0.69

Table A1.2 Gas hold-up data for ethylene glycol /water and methanol/2-propanol systems

Ethylene glycol/water		Methanol/2-propanol	
Mole fraction of ethylene glycol	**Gas hold-up**	**Mole fraction of methanol**	**Gas hold-up**
0.0	0.63	0.0	0.69
0.5	0.73	0.05	0.695
0.2	0.655	0.2	0.7
0.31	0.63	0.35	0.73
0.48	0.626	0.5	0.73
0.66	0.616	0.8	0.76
0.84	0.608	0.9	0.75
1.0	0.54	1.0	0.74

A2. POINT EFFICIENCY DATA IN OLDERSHAW COLUMN (CHAPTER 3)

Column Dimensions

Column diameter: 74.3 mm

Bubbling area: 3840 mm^2

Hole diameter: 0.889 mm

Open hole area: 317 mm^2

Operating Conditions

i) Total reflux

ii) Atmospheric pressure

iii) Constant gas load

Table A2.1 Efficiency data for methanol/water system (u_s=0.25m/s)

Mole fraction of Methanol, x	Point efficiency E_{OG}	Mole fraction of Methanol, x	Point efficiency E_{OG}
0.0750	0.3500	0.5008	0.8580
0.0867	0.4000	0.5203	0.8580
0.1098	0.4500	0.5968	0.8679
0.1503	0.5602	0.5800	0.8415
0.1642	0.5500	0.6200	0.8513
0.19	0.68	0.6700	0.8965
0.2035	0.7500	0.7400	0.9017
0.2437	0.7900	0.7700	0.8800
0.2873	0.8082	0.8000	0.8835
0.3000	0.8344	0.8527	0.8370
0.3122	0.8324	0.8900	0.8437
0.3395	0.8389	0.9000	0.7182
0.3554	0.8385	0.9300	0.6400
0.4704	0.8481	0.9607	0.6020

Table A2.2 Efficiency data for methanol/2-propanol system (u_s=0.25m/s)

Mole fraction of Methanol, x	Point efficiency E_{OG}	Mole fraction of Methanol, x	Point efficiency E_{OG}
0.9501	0.5700	0.5023	0.4100
0.9397	0.6390	0.4900	0.5100
0.9191	0.5500	0.5372	0.5400
0.8800	0.5300	0.4443	0.4741
0.8318	0.5295	0.4034	0.4090
0.7865	0.5400	0.3840	0.4956
0.7602	0.4900	0.3211	0.4515
0.6987	0.5200	0.2884	0.4146
0.6552	0.5415	0.2502	0.3302
0.6018	0.4800	0.2082	0.3080
0.5206	0.4979		

Table A2.3 Efficiency data for water/acetic acid system (u_s=0.29m/s)

Mole fraction of water, x	Point efficiency E_{OG}	Mole fraction of water, x	Point efficiency E_{OG}
0.9668	0.3089	0.7168	0.3522
0.9353	0.3355	0.7075	0.2928
0.9072	0.3851	0.7074	0.2954
0.8944	0.4356	0.6552	0.3900
0.8885	0.4253	0.5888	0.3634
0.8720	0.3436	0.5331	0.3124
0.8636	0.3518	0.5171	0.2995
0.8453	0.4275	0.4595	0.3500
0.8404	0.3757	0.3950	0.2889
0.8164	0.3805	0.2947	0.1972
0.7427	0.3893	0.2613	0.2991
0.7394	0.3206	0.2101	0.2500

Table A2.4 Efficiency data for n-heptane/tolune system (u_s=0.25m/s)

Mole fraction of n-heptane, x	Point efficiency E_{OG}	Mole fraction of n-heaptane, x	Point efficiency E_{OG}
0.9201	0.3850	0.4960	0.6600
0.9172	0.5044	0.4578	0.7296
0.9400	0.4400	0.4183	0.7177
0.9600	0.4000	0.4127	0.6270
0.8744	0.5828	0.3767	0.6820
0.8694	0.5112	0.3766	0.5802
0.8206	0.6219	0.3675	0.7472
0.8098	0.6500	0.3220	0.6073
0.7500	0.5830	0.3023	0.7139
0.7464	0.6786	0.2675	0.5450
0.7022	0.7260	0.2621	0.6229
0.6812	0.6600	0.2500	0.5720
0.6400	0.6600	0.1968	0.6000
0.6288	0.7052	0.1501	0.5200
0.5912	0.6961	0.1461	0.4800
0.5877	0.6590	0.1044	0.5080
0.4913	0.7488	0.1027	0.4500

Table A2.5 Efficiency data for cyclo-hexane/n-heptane system (u_s=0.29m/s)

Mole fraction of cyclo-hexane, x	Point efficiency E_{OG}	Mole fraction of cyclo-hexane, x	Point efficiency E_{OG}
0.9347	0.5841	0.5772	0.4803
0.9281	0.5131	0.5044	0.5297
0.9162	0.5794	0.4903	0.4696
0.9039	0.5557	0.4524	0.4467
0.8886	0.5694	0.4107	0.5205
0.8606	0.5480	0.3862	0.4400
0.8574	0.5854	0.3825	0.4593
0.8177	0.5917	0.3297	0.4513
0.8164	0.4602	0.3176	0.4294
0.7736	0.5108	0.2977	0.4048
0.7470	0.4678	0.2610	0.4589
0.7465	0.5212	0.2416	0.4104
0.7319	0.5576	0.2138	0.3727
0.6552	0.5372	0.2085	0.4864
0.6462	0.4043		

Table A2.6 Efficiency data for benzene/n-heptane system (u_s=0.29m/s)

Mole fraction of benzene, x	Point efficiency E_{OG}	Mole fraction of benzene, x	Point efficiency E_{OG}
0.9547	0.5635	0.6054	0.5434
0.9530	0.4465	0.5938	0.4710
0.9172	0.5500	0.5473	0.5020
0.9056	0.5600	0.5188	0.4773
0.8800	0.4600	0.4851	0.5766
0.8490	0.5682	0.4796	0.5078
0.8402	0.5135	0.4022	0.5494
0.8197	0.4530	0.3739	0.4379
0.8078	0.5800	0.3672	0.4458
0.7767	0.5673	0.3351	0.5395
0.7087	0.6238	0.2954	0.4559
0.7049	0.5498	0.2071	0.5258
0.6725	0.5673	0.2083	0.4447
0.6174	0.6364		

APPENDIX B

FRI DATA FOR SIEVE TRAY EFFICIENCIES

B1. EFFICIENCY DATA FOR CYCLO-HEXANE/N-HEPTANE

Column Dimensions

Column diameter: 1.22m

Hole diameter: 0.0127m

Tray spacing: 0.61m

Weir height: 0.0508m

Weir length: 0.94m

Active area: 0.859 m^2

Net area: 0.991 m^2

Table B1.1 Sieve tray efficiencies for cyclo-hexane/n-heptane at 34 kPa operating pressure and open hole area 14% (Yanagi and Sakata, 1982)

Liquid mass flow rate L_f (kg/hr)	Vapour mass flow rate G_f (kg/hr)	Point efficiency E_{OG}
4022.0000	4852.0000	0.5200
6017.0000	6759.0000	0.5664
7792.0000	8239.0000	0.5951
8851.0000	9085.0000	0.5509
10171.0000	10433.0000	0.3695

Table B1.2 Sieve tray efficiencies for cyclo-hexane/n-heptane at 165 kPa operating pressure and open hole area 14% (Yanagi and Sakata, 1982)

Liquid mass flow rate L_f (kg/hr)	Vapour mass flow rate G_f (kg/hr)	Point efficiency E_{OG}
2433.0000	2490.0000	0.2647
5022.0000	5124.0000	0.4267
7306.0000	8152.0000	0.5690
9536.0000	10391.0000	0.6243
14305.0000	14555.0000	0.6639
18900.0000	21196.0000	0.6882
21590.0000	22867.0000	0.6009
23763.0000	26250.0000	0.4950

B2. EFFICIENCY DATA FOR I-BUTANE/N-BUTANE

Column Dimensions:

Column diameter: 1.22m

Hole diameter: 0.0127m

Tray spacing: 0.61m

Weir height: 0.0508m

Weir length: 0.94m

Active area: 0.859m^2

Net area: 0.991 m^2

Table B2.1 Sieve tray efficiencies for i-butane/n-butane at 1138 kPa operating pressure and open hole area 14% (Yanagi and Sakata, 1982)

Liquid mass flow rate L_f (kg/hr)	Vapour mass flow rate G_f (kg/hr)	Point efficiency E_{OG}
6290.0000	6468.0000	0.4921
10254.0000	10258.0000	0.6783
14470.0000	14505.0000	0.7363
21456.0000	21332.0000	0.7565
27823.0000	27785.0000	0.7632
32408.0000	32380.0000	0.7598
35311.0000	35284.0000	0.6890

Table B2.2 Sieve tray efficiencies for i-butane/n-butane at 1138 kPa operating pressure and open hole area 8.3% (Sakata and Yanagi, 1979)

Liquid mass flow rate L_f (kg/hr)	Vapour mass flow rate G_f (kg/hr)	Point efficiency E_{OG}
6424.0000	6440.0000	0.5580
10428.0000	10359.0000	0.7345
14100.0000	14139.0000	0.7888
21376.0000	21270.0000	0.8177
28200.0000	28377.0000	0.8229
31670.0000	31828.0000	0.8100
33351.0000	33452.0000	0.7700
35028.0000	35256.0000	0.7500

Table B2.3 Sieve tray efficiencies for i-butane/n-butane at 2068 kPa operating pressure and open hole area 8.3% (Sakata and Yanagi, 1979)

Liquid mass flow rate L_f (kg/hr)	Vapour mass flow rate G_f (kg/hr)	Point efficiency E_{OG}
7446.0000	7388.0000	0.7898
10108.0000	10086.0000	0.8790
14823.0000	14925.0000	0.8466
20021.0000	20100.0000	0.8582
22576.0000	22483.0000	0.8567
23815.0000	24069.0000	0.8440
25122.0000	25224.0000	0.6436
7258.0000	7216.0000	0.7314
9662.0000	9703.0000	0.8270
1448.0000	14555.0000	0.8380
19329.0000	19467.0000	0.8130
21866.0000	21958.0000	0.8135
23035.0000	23112.0000	0.8098

Table B2.4 Sieve tray efficiencies for i-butane/n-butane at 2758 kPa operating pressure and open hole area 8.3% (Sakata and Yanagi, 1979)

Liquid mass flow rate L_f (kg/hr)	Vapour mass flow rate G_f (kg/hr)	Point efficiency E_{OG}
7560.0000	07408.0000	0.8682
11377.0000	11486.0000	0.8991
15241.0000	15451.0000	0.9245
17274.0000	17446.0000	0.9124
18169.0000	18133.0000	0.8883
19104.0000	19230.0000	0.8095
5169.0000	5039.0000	0.8513
6967.0000	6917.0000	0.9158
10688.0000	10815.0000	0.9066
14230.0000	14360.0000	0.9154
15946.0000	16164.0000	0.8764
16559.0000	17238.0000	0.8668